Doctoral Dissertation

Study on the thermal comfort of naturally ventilated gymnasiums in hot-humid regions of China

中国高温多湿地域における体育館の自然通風時の温熱快適性に関する研究

Xiaodan Huang

黄暁丹

Academic advisor: Professor Qingyuan Zhang (張晴原 教授)

Graduate School of Urban Innovation

Yokohama National University

March, 2021

Contents

Abstract

As a public building for exercise, entertainment and sport, gymnasiums play an important role in people's daily life. In regions with hot-humid climate, indoor thermal comfort in gymnasiums is directly related to the human health as well as energy consumption. However, little can be found in the systematic evaluation system reported for thermal comfort of the athletes in gymnasium in hot-humid climate regions, therefore there is a need to develop a thermal comfort model for evaluating thermal comfort of athletes partaking sports in these environments. In addition, as the gymnasiums in subtropical region with hot-humid climate are naturally ventilated during non-competition periods, athletes exercising indoor often feel uncomfortable especially in summer. In order to provide thermally comfortable and healthy environment for the athletes in gymnasium, the design on architectural form, are found to be an effective solution on improving indoor thermal comfort of naturally ventilated gymnasiums. Therefore, in this study, a field survey on thermal sensation of athletes in basketball games has been carried out in naturally ventilated gymnasiums in Guangzhou, China. The thermal environment and human physiology have been analysed and a predicted thermal sensation (PTS) model, which has been developed by this study to estimate the thermal sensation under high-intensive sport activities in gymnasiums in regions with a high temperature and high humidity, has been evaluated and validated. Furthermore, through numerical simulation of gymnasium forms by the way of orthogonal experiment method, the significance of gymnasium form affecting indoor thermal comfort has been given, and the optimal architectural forms of naturally ventilated gymnasium at hot-humid climate are determined.

This dissertation has been divided into six chapters. Chapter 1 is the introduction which includes the study background, literature review, purpose and the structure of the study. Chapter 2 deals with the comparative analysis of thermal comfort models, presenting the relationship between the PMV model and the SET* model in the imaginary standard environment. Chapter 3 is the field study on the thermal sensation under high-intensive

exercise in naturally ventilated gymnasiums in hot-humid regions of China. In this chapter, a field survey on the thermal sensation of athletes under basketball exercise was carried out in three naturally ventilated gymnasiums in Guangzhou, China. The indoor thermal environment of gymnasiums, human physiology including metabolic rate, blood pressure and skin temperature, and thermal sensation vote (TSV) of athletes during basketball exercise have been analysed. Chapter 4 presents the establishment of the Predicted Thermal Sensation (PTS) model. In this chapter, the influences of thermal parameters on TSV have been analysed and the Predicted Thermal Sensation (PTS) model for estimating the thermal sensation under high-intensive exercises in naturally ventilated gymnasiums in hot-humid regions of China has been developed and validated. Chapter 5 analyzes the optimization of gymnasium form for thermal comfort at hot-humid climate by orthogonal experiment. It presents the influence of gymnasium forms on indoor thermal comfort and proposes the optimum gymnasium form at hot-humid climate by simulation and orthogonal experiment method. Finally, Chapter 6 summarizes the main conclusions of this study and puts forward the suggestions for the future study.

This study provides the researchers with a new method to assess the indoor thermal environment and the thermal comfort of athletes under high-intensive exercises in naturally ventilated gymnasiums in hot-humid regions. Furthermore, it provides a new insight in optimizing the architectural form of gymnasiums for achieving the indoor thermal comfort at hot-humid climate.

Chapter 1

Introduction

1.1 Background

The study of indoor thermal comfort is an important branch in the science of human settlements. Moreover, the study of indoor thermal comfort in gymnasiums is becoming significantly important as an organic component of human settlements. With the arrival of the era of national fitness, gymnasium is not only limited to the competitive games, but also a place for human fitness. Therefore, it puts forward higher requirement for the gymnasium besides firmness, beauty and practicality. Thermal comfort becomes more and more essential in gymnasium design. However, due to the large space of gymnasium buildings and the high intensity of human activities, it is difficult to achieve indoor thermal comfort, especially for the gymnasium located in hot-humid regions. In this case, "What's the main influential factors on thermal comfort of gymnasium" and "how to improve the thermal comfort for the athletes exercising in gymnasiums" are the problems worthy of study.

1.1.1 Weather condition in hot-humid regions of China

The hot-humid regions, taking Guangzhou (China) as an example, belongs to the subtropical monsoon climate. Due to its location which is near the tropic of cancer, much solar radiation is obtained since the sun passes through the zenith of Guangzhou twice a year. In spring and early summer, the cold air from the north meets the moist and warm air stream landing from the sea, resulting in rain and humidity. In summer and autumn, however, it is easy to be affected by coastal typhoon, which leads to wind disaster and local rainstorm. Thus the climate of Guangzhou can be summarized by "hot, humid, windy and rainy".

Fig.1-1 shows the climate histogram of Guangzhou[1)], in which the highest average temperature (28.9°C) appears in July and the lowest (14.2°C) in January. The months with the highest humidity level of 80% are April, June and August. Above all, the period with high temperature and humidity is long in Guangzhou.

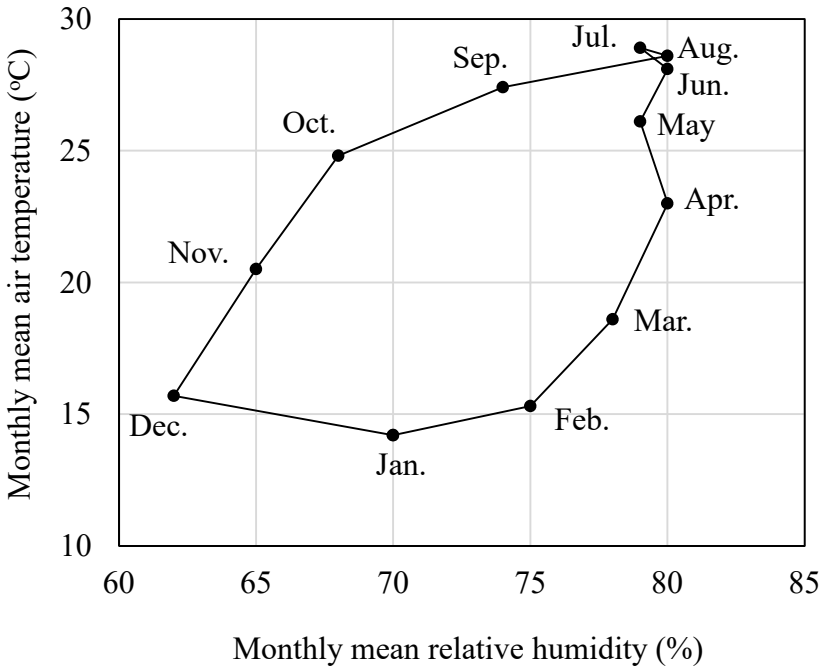

Fig.1-1 Climograph of Guangzhou, China

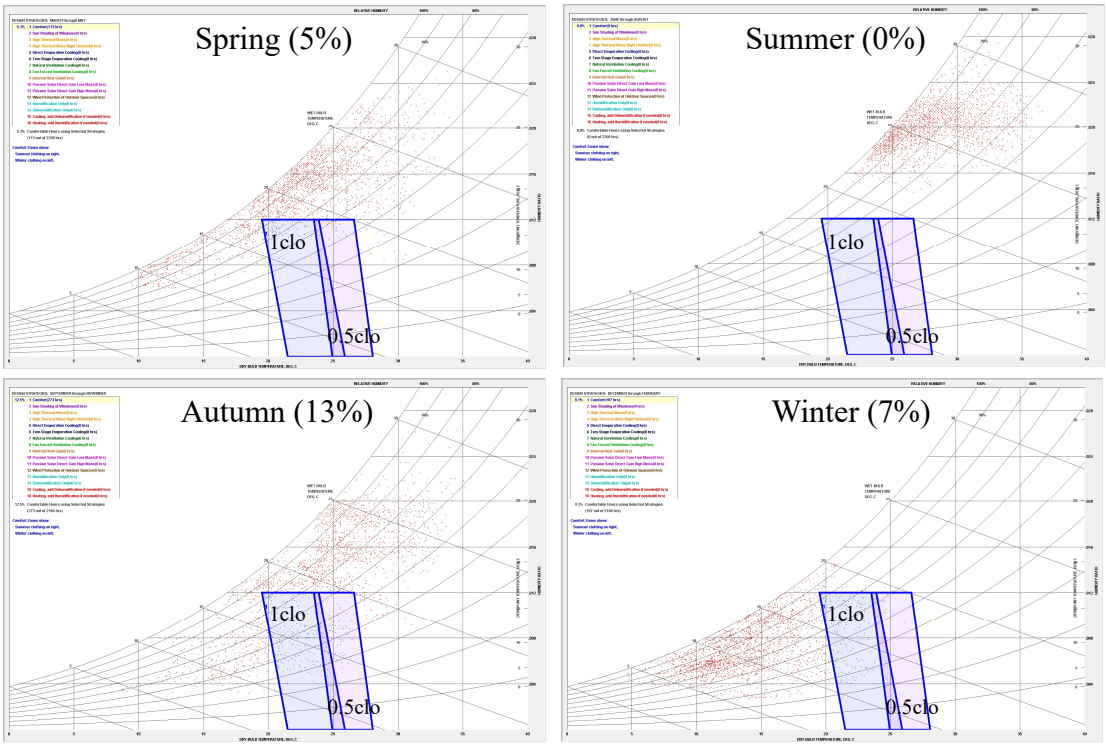

Fig.1-2 Psychrometric chart of four seasons in Guangzhou, China

(weather data from Energyplus)

Fig.1-2 shows the psychrometric chart of four seasons in Guangzhou (the blue line frames represent the thermal comfort zones for clothing insulation in 0.5clo and 1clo respectively, and the red scatter points represent the data points of the thermal environment in that season). Without any measures taken, the thermal comfort of Guangzhou is poor in most of the year, especially in hot summer (no data points fall into the thermal comfort zones).

1.1.2 Gymnasium situation

With the improvement of people's life quality, the indoor thermal comfort of gymnasium buildings has been gradually improved, with more and more researchers taking indoor thermal comfort into consideration in gymnasium construction. However, there are still a large number of gymnasiums that only pursue the architectural form and function in the stage of initial design, ignoring the indoor thermal environment and thermal comfort, resulting in large consumption of building energy during use and the poor indoor air quality even diseases such as the SARS occurred in 2003 and the COVID-19 appeared in 2020.

The four gymnasiums in Fig.1-3 are all located in the hot-humid regions of China. They reflect some problems, more or less, relanvent to the indoor environment and thermal comfort of gymnasium. Fig.1-3(a) is the Tangxia Zhen Gymnasium in Dongguan, Guangdong Province. Due to the excessive emphasis on architectural shape, a large number of glass curtain walls are settled, resulting in high temperature indoor and huge energy consumption. Fig.1-3(b) shows the enclosed facades of Hong Kong Coliseum, leading to the less circulating of indoor air and the fast breeding of SARS virus. Fig.1-3(c) is a gymnasium in an university in Guangzhou and Fig.1-3 (d) is a sport centre in Tsuen Wan, Hong Kong. The importance of natural lighting is ignored in both gymnasiums in the case of sun shading and ventilation. As a result, the indoor natural light is insufficient and the cost of artificial lighting is increased. These gymnasiums are perfect in shape and function, but all neglect the importance of indoor environment, resulting in defects in use.

(a) Tangxia Zhen Gymnasium

(b) Hong Kong Coliseum

(c) A university gymnasium in Guangzhou

(d) Tsuen Wan Sport Centre

Fig.1-3 Gymnasium current situation in hot-humid regions

1.1.3 Research field on thermal comfort

In the aspect of thermal comfort model, some models covering all or parts of the factors have been suggested, such as the Predicted Mean Vote (PMV) model developed by Fanger[2] and the model of Standard Effective Temperature (SET) put forward by Gagge[3], which are based on the two-node model established from the human physiology. In addition, some models are in line with the thermal environment parameters, such as the Wet Bulb Globe Temperature (WBGT), the Equatorial Comfort Index (ECI) and Equivalent Temperature (EqT)[4)~6)]. However, these models are limited to a certain extend. For instance, the PMV model is mainly applicable to steady-state environments; the SET model could apply to naturally ventilated building, on condition that the human body has a low metabolic rate.

As for the research field of thermal comfort in sport building, a large number of studies have shown the rapid development of thermal comfort and the people's efforts on pursuing higher quality of life. However, it should be noted that most above studies are primarily appliable to residential buildings, office buildings and classrooms, with the occupants at low metabolic rates[7)~10)]. Very few studies focus on the thermal comfort for sport buildings where the athletes conduct sports and exercise. However, thermal comfort study in exercising environment, as we all know, is one of the necessary topics for human beings to pursue health and high quality of life as well.

In terms of the research field of metabolic activity, which is one of the key parameters in existing thermal comfort theory. Most of the above studies were conducted in the climate chambers rather than in actual fields[11)~14)], which are less realistic when it comes to surroundings, behaviors and expectations of subjects, and are not necessarily suitable for real environment. So far, there has been no field study on thermal comfort under high-intensive exercise in naturally ventilated gymnasiums.

1.2 Literature review

1.2.1 Development of thermal comfort model

In the early 20th century, ASHRAE (American Society of Heating, Refrigerating and Air-Conditioning Engineers) established a climate laboratory on studying the effects of indoor thermal environment on human thermal comfort. The laboratory began to work in Pittsburgh in 1919. After amounts of experiments and analyse, the index of Equivalent Temperature (EqT) was obtained by Dufton[15)] and described in equation by Bedford[6)]. Since the index was concise in use at that time, it didn’t take into account humidity, which is an important factor on thermal comfort when the temperature is high.

From 1920s to 1950s, Yaglau and Houghton developed the index of Effective Temperature (ET)[16)] basing on the Equivalent Temperature, which represented by a set of equal comfort lines drawn on the psychrometric chart. It is defined as the temperature

of a still, saturated atmosphere, which would produce the same effect as the atmosphere in question. It thus combines the effect of dry air temperature and humidity. It became the most widely used index for the next 50 years. However, due to its overestimating on the effect of humidity[17], it is now superseded.

In the 1960s and 1970s, with the establishment of special laboratory for the study of thermal sensation, the scope of influencing factors of thermal comfort is not only limited to the air temperature, but also the relative humidity and air velocity. ASHRAE have invested a lot and achieved important results in this field. ASHRAE Standard 55[18] is one of the most important and acknowledged material in the research of thermal comfort. With the emergence of latest studies, the thermal comfort standard has been gradually developed from ASHRAE Standard 55-1974 to ASHRAE Standard 55-2017. At the same time, Professor Fanger from Denmark University of Technology put forward the famous thermal comfort evaluation indix-Predicted Mean Vote (PMV) [2], which is based on the comprehensive consideration of four environmental parameters (air temperature, relative humidity, air velocity and mean radiant temperature), and two human factors (metabolic rate and clothing insulation). The PMV model have been adopted by the ASHRAE Standard 55-2017[18], ASHRAE Handbook[19] and ISO Standard 7730[20], which are the worldwide thermal comfort standards.

In the 1980s and 1990s, the study on thermal comfort has developed to a new stage. The index of Standard Effective Temperature (SET) has been interpreted by Gagge et al.[3] as a sub-set of Effective Temperature under standardised conditions in 1986, which is one of the most common and widely applied thermal comfort models. In addition, human adaptation has been taken into consideration in this period. In 1998, deDear et al.[21] conducted field investigation on different climate regions of four continents and proposed the "adaptive model" considering that people are not passive recipients of environmental stimuli, but the active adapters. People's adaptation to the environment will make them gradually satisfied with the environment.

1.2.2 Thermal comfort in gymnasium design

Until the 1990s, with the rapid development of economy and the development of sports industry, people began to pay attention to the field of indoor environment of sports buildings, more and more researchers explored and achieved findings in this field.

Bouyer et al.[22] analyzed the thermal comfort of Stade de France in France and Ataturk Olympic Stadium in Istanbul by the index of Physiological Equivalent Temperature (PET) and developed the thermal comfort zone for the semi outdoor gymnasium. Ucuncu et al.[23] studied the thermal comfort of gymnasiums in tropical region and found the influencing factors of indoor thermal comfort, including solar radiation, air temperature and air velocity. Furthermore, simulations had been done by adaptive model and computational fluid dynamics to put forward the design strategy for the gymnasium in tropical region. Szucs et al.[24] evaluated the thermal comfort of gymnasium from the perspective of methodology and analyzed the influence of roof shape on thermal comfort through wind tunnel test. In China, Ji et al.[25] conducted the field investigation on the occupants with badminton exercise in gymnasiums and put forwarded the concept of clothing coverage rate on the basis of Fanger's model. Qian et al.[26] simulated the air distribution in the gymnasium competition hall under typical summer conditions without spectators by Airpak software and optimized the indoor thermal environment for the multi-functional gymnasiums. Li et al.[27] carried out a simulation study on a gymnasium with asymmetric overhanging eaves, and proposed that the asymmetric cornice shape could improve the wind speed of the venue and inhance the indoor ventilation rate, then further proposed the ventilation strategy for the gymnasiums during competitions.

1.2.3 Thermal comfort of athlete in metabolic acitvity

Early studies have shown that intensity level had a significant effect on thermal comfort. In 1957, Yaglou and Minard[28] developed WBGT index to evaluate the effect of heat on a person during total exposure over the working day. It provided reference limit for persons in five levels of intensity, which is a very early study of thermal comfort that

takes labor intensity into account. In 1967, Fanger[29] found that the sweat evaporation rate increases as the metabolic rate of subjects increases by experimental studies. Gagge et al.[30] in 1969 indicated that the human thermal sensation is strongly influenced by a wide range of activity levels of the subjects. Gonzales[31] in 1981 conducted field experiments at different exercise intensities and found subjects' comfort temperature diminished with the rising of the activity level. Humphreys and Nicol[32] noted that the PMV model is only valid to activities less than 1.4 met and produced errors with the metabolic rate above 1.8met. These studies contribute greatly to the thermal comfort research in terms of metabolic intensity. In recent years, Ji et al.[33] investigated 31 college-aged subjects riding a spinning bike (3.5met) in a chamber and found that the metabolic rate during transition affected thermal comfort significantly. Li et al.[34] conducted experimental research on strenuous exercise (3.5~5.0met) and indicated that the heart rate and wrist skin temperature can be utilized for evaluating thermal sensation. Xiao et al.[35] monitored the subjective sensation and physiology with high physical activity under different ambient temperature and found the significant effect of ambient temperature on objective response.

1.3 Purpose of the study

- Provide a theoretical reference for the evaluation of thermal comfort in gymnasiums in hot-humid regions

Due to the characteristics of hot-humid climate and the particularity of indoor thermal environment in gymnasiums, the current thermal comfort standards can not accurately predict and evaluate such kind of indoor thermal comfort. Meanwhile, with the development of human living standards, people's requirements for indoor thermal environment and thermal comfort are much higher, which requires in-depth study of indoor thermal comfort relied on the actual situation.

- Fill in the blank of thermal comfort study in the sport field

The experimental data show that the environmental adaptability of human body in exercising state is stronger than that in sedentary state. In addition, with the consumption of physical fitness, the exchanges of air and heat between body and environment are increased, which causing that the thermal response of human in exercise state is quite different from that in sedentary state. However, less thermal comfort models can be used to predict the state of exercise. Therefore, it is necessary to study the thermal comfort for athletes so as to better predict the thermal comfort in sports field.

- Realize the unity of building energy conservation and architectural form based on the thermal comfort

The purpose of gymnasium construction is to avoid bad weather, adjust indoor microclimate and create comfortable and healthy sports environment. However, many gymnasium designs only focus on the building function and architectural form, relying too much on the equipment in the regulation of indoor environment. It causes, on one hand, the gradual loss of natural regulation mechanism and ability. On the other hand, it aggravates energy consumption and pollution. The study on the thermal comfort of gymnasium aims to save energy under the premise of obtaining indoor thermal comfort, at the same time, it provides architects with appropriate passive design strategy in the initial design stage, effectively considers and analyzes the architectural form and indoor environment, and realizes the unity of human thermal comfort, building energy conservation and architectural form.

1.4 Structure of the study

The structure of the study is shown in Fig.1-4.

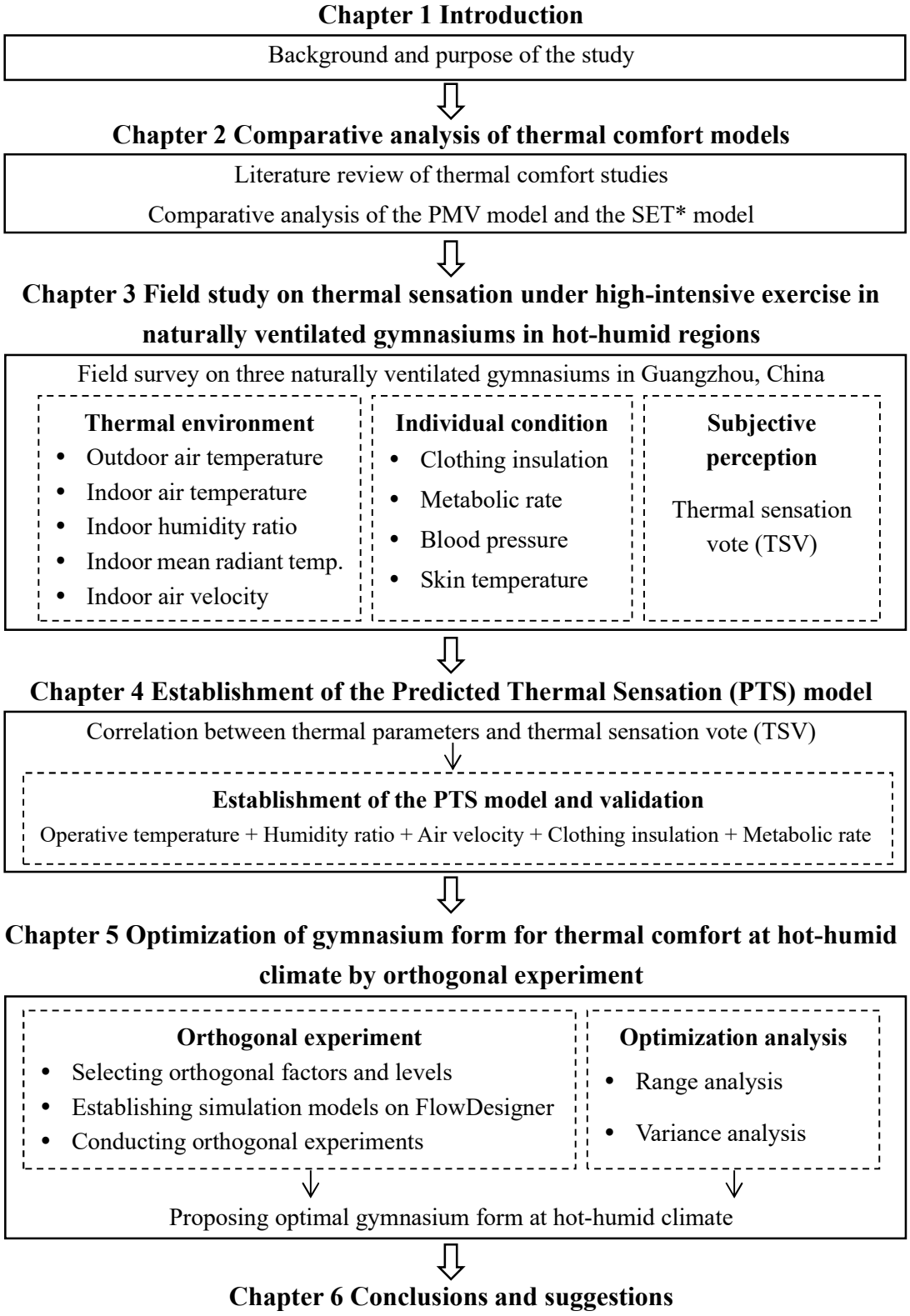

Fig.1-4 Structure of the study

Chapter 2

Comparative analysis of thermal comfort models

2.1 Introduction

The thermal comfort, affecting the human health, perception, and especially the energy consumption of buildings, plays a pivotal role on the aspect of the environmental quality. Since the energy consumption in buildings has been increased obviously, the regulation, prediction and evaluation of the thermal comfort are essential for the sustainable development. Thus, an efficacious thermal comfort model is necessary not only for the thermal environment assessment, but also for the social sustainability.

The Predicted Mean Vote (PMV) developed by Fanger[1)] and the Standard Effective Temperature (SET*) developed by Gagge et al.[2)] are the most common and widely applied thermal comfort models, which have been adopted by the ASHRAE Standard 55[3)] , ASHRAE Handbook[4)] and ISO Standard 7730[5)] that are the worldwide thermal comfort standards. The former is based on the heat balance equation and suitable for the evaluation in a steady-state environment. The latter is in line with the two-node model, which is more complicated and considers a quantity of factors.

The PMV model and the SET* model have been widely accepted and utilized in the research of thermal comfort. In terms of the PMV model, Cheung et al.[6)] used the ASHRAE Standard to assess the PMV accuracy, which was found to vary strongly in disparate architectural forms, ventilation methods and climate zones. Broday et al.[7)] conducted a comparative analysis between thermal sensation votes and the predicted mean vote (PMV), and they found that the PMV overestimated the actual thermal sensation. Kim et al.[8)] developed adaptive PMV models, which enhanced the accuracy against the original PMV model. In the aspect of the SET* model, Fang et al.[9)] carried out field surveys on the university campus and outlined a strong relationship between SET* and operative temperature. Li et al.[10)] investigated human thermal response to evaluate the influence of humidity on thermal comfort by the SET* model. Ji et al.[11)] conducted tests on the relationship between the metabolic rate and thermal comfort, with the finding that the SET* model was fit for the thermal sensation estimation at the high

metabolic rate. In addition, some studies involve both PMV and SET*. Gagge et al.[2] indicated the relationship between the air temperature, SET* and PMV for a special work environment. Gao et al.[12] presented comparisons between modified PMV models and modified SET* models on thermal sensation prediction in naturally ventilated buildings, and the latter was found to be more accurate for thermal sensation prediction. Ye et al.[13] proposed an instrument for measuring the PMV and SET* in an imaginary condition, which included an equivalent temperature sensor, a relative humidity sensor and a temperature sensor. These studies primarily focus on the wide range of application of the PMV model and the SET* model. Despite the application of them, their relationship in the theoretical condition is essential to be studied in consideration of few studies in this field from the previous researches.

This chapter aims to present a comparative analysis between the PMV model and the SET* model in the imaginary standard environment. The relationship between them and the effect of thermal parameters on them are preformed. Moreover, some noticeable problems in the correspondence between PMV and SET* are pointed out. It provides researchers with an innovative perspective to figure out the internal theoretical relationship between PMV and SET* models. Meanwhile, a clear direction and guidance for applying the models are presented.

2.2 Research methods

2.2.1 General concept of thermal comfort

The thermal comfort is defined as “The condition of mind that expresses satisfaction with the thermal environment and is assessed by subjective evaluation” in ASHRAE Standard. This definition underlines that regulation of the thermal comfort is a cognitive process, including many factors affected by physical, physiological and psychological. The conscious mind appears to reach conclusions about thermal comfort from direct temperature and moisture sensations from skin, deep body temperature and efforts necessary to regulate body temperatures[14]. Thermal comfort is also influenced by

conscious or unconscious human behaviors, such as changing clothing, posture and activity, regulating a window, and controlling the fan or the air conditioner.

2.2.2 Thermal comfort models

The study of thermal comfort model can be traced back to the 18th century on thermal tolerance evaluation[15], after which such research has been performed constantly. In the 1970s, Fanger[1] proposed a formulation based on the thermal balance equation--Predict Mean Votes (PMV), which is the most popular thermal comfort model in the world. In addition to the PMV model, the two-node model appearing in the 1970s is widely accepted either, which deems the human body as two-layer structure of core and skin[16]. Based on the two-node model, Gagge's model[2]--Standard Effective Temperature (SET*) -- has been applied widely until now. Furthermore, the Standard Effective Temperature (SET*) is the most representative model adopted by ASHRAE Standard 55[3]. In this section, the theory and application of the PMV model and the SET* model are described.

2.2.2.1 Predict Mean Votes (PMV)

The PMV model is calculated by the Fanger's equation for heat exchange of the human body[1]. People could achieve thermal comfort indoors under certain environmental conditions. Thus, the PMV model, calculated by four thermal environmental parameters (air temperature, relative humidity, air velocity and mean radiant temperature) and two personal parameters (the metabolic rate and clothing insulation), could be employed to evaluate the human thermal comfort[1]. The formulation of that model is presented as follow:

$$\begin{aligned}\mathrm{PMV} = {} & \left[0.303 * e^{(-0.036*M)} + 0.028\right] \\ & * \{(M-W) - 3.05 * [5.73 - 0.007 * (M-W) - P_a] \\ & * 0.42 * [(M-W) - 58.15] - 0.0173 * M * (5.87 - P_a) - 0.0014 * M \\ & * (34 - T_a) - 3.96 * 10^{-8} * f_{cl} * [(T_{cl}+273)^4 - (T_r+273)^4] - f_{cl} * h_c \\ & * (T_{cl} - T_a) \end{aligned} \quad (2\text{-}1)$$

where M is the metabolic rate in W/m^2; W is the rate of mechanical work in W/m^2; P_a is the water vapor pressure in ambient air in kPa; T_a is the air temperature in ^{o}C; f_{cl} is the ratio of the clothed surface area to the nude surface area; T_{cl} is the mean temperature of clothing in ^{o}C; T_r is the mean radiant temperature in ^{o}C; h_c is the convective heat transfer coefficient in W/(m^2 * ^{o}C).

The mean temperature of clothing T_{cl}, the convective heat transfer coefficient h_c and the ratio of the clothed surface area f_{cl} can be acquired by Equations (2-2), (2-3) and (2-4), respectively.

$$T_{cl} = 35.7 - 0.0275 * (M - W) - I_{cl} * \{(M - W)$$
$$-3.05 * [5.73 - 0.007 * (M - W) - P_a]$$
$$-0.42 * [(M - W) - 58.15] - 0.0173 * M * (5.87 - P_a) - 0.0014 * M \quad (2\text{-}2)$$

$$h_c = \begin{cases} 2.38 * (T_{cl} - T_a)^{0.25} & for \quad 2.38 * (T_{cl} - T_a)^{0.25} > 12.1 * \sqrt{v} \\ 12.1 * \sqrt{v} & for \quad 2.38 * (T_{cl} - T_a)^{0.25} < 12.1 * \sqrt{v} \end{cases} \quad (2\text{-}3)$$

$$f_{cl} = \begin{cases} 1.0 + 0.2 I_{cl} & for \quad I_{cl} < 0.5 clo \\ 1.05 + 0.1 I_{cl} & for \quad I_{cl} > 0.5 clo \end{cases} \quad (2\text{-}4)$$

where I_{cl} is the clothing insulation in clo; v is the air velocity in m/s.

The PMV model adopts the 7-point scale in ARSHER Standard 55[3], as shown in Table 2-1. In general, the PMV value of 0 is defined as a neutral environment, and the PMV value between -0.5 and +0.5 is considered to be the thermal comfort range. In the previous researches[17)~19)], the PMV values are found to differ greatly from the actual thermal sensation when the PMV is above +2 (warm) owing to the increase of the evaporative heat dissipation of sweat, indicating the limited accuracy of PMV to some extent. In addition, the PMV model is limited for predicting the thermal comfort in the

uniform and steady-state environments instead of the dynamic environments[20].

Table 2-1 Scale of the PMV model

-3	-2	-1	0	+1	+2	+3
Cold	Cool	Slightly cool	Neutral	Slightly warm	Warm	Hot

2.2.2.2 Standard Effective Temperature (SET*)

SET* is an index reflecting the human heat stress based on the two-node model that can be used to predict thermal comfort at dynamic environments[16] compared with the PMV model. Two-node model considers a human body as two concentric thermal compartments that represent the core and skin of the body. Metabolic heat is generated at the core thermal compartment. A small portion of that heat is dissipated by respiration, and the remainder is transferred to the environment through the skin surface, as shown in Fig.2-1.

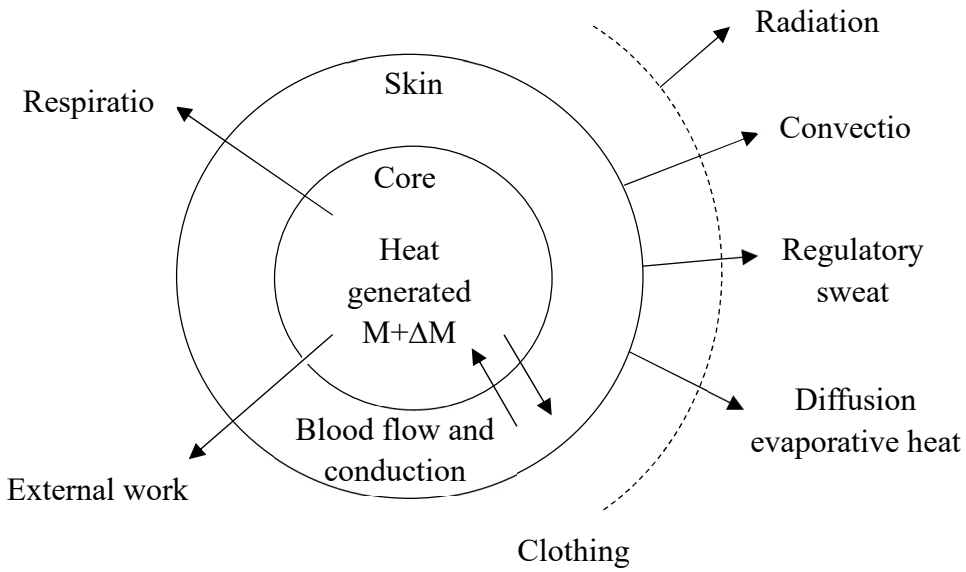

where M is metabolic rate in W/m^2; ΔM is metabolic level required for shivering in W/m^2.

Fig.2-1 Thermal interaction between the human body and environment based on the two-node model[16]

The fundamental equation of the two-node model is shown in Equation (2-5):

$$\mathrm{M} - \mathrm{W} = Q_{sk} + C_{res} + E_{res} + S \tag{2-5}$$

where Q_{sk} is the total heat loss from skin in W/m^2; C_{res} is the convective heat loss from respiration in W/m^2; E_{res} is the evaporative heat loss from respiration in W/m^2; S is the heat storage in W/m^2.

Based on the two-node model, the values of the skin temperature (Tsk) and skin wetness (w), which are obtained by inputting six parameters (air temperature, relative humidity, air velocity, mean radiant temperature, clothing insulation and the metabolic rate) into the two-node model, are used for the SET* calculation. The formulation of the SET* model is presented in Equation (2-6):

$$\begin{aligned} & h * \left(T_{sk} - T_{op}\right) + \mathrm{w} * h_e * (P_{sk} - P_o) \\ & = h' * (T'_{sk} - SET^*) + w * h'_e * (P_{sk} - 0.5 P_{SET*}) \end{aligned} \tag{2-6}$$

where h represents the sensible heat transfer coefficient in W/ (m^2 * ^{o}C); T_{sk} is the mean skin temperature in ^{o}C; T_{op} is the operative temperature in ^{o}C; w is the skin wetness. h_e is the evaporative heat transfer coefficient in W/(m^2 * kPa); P_{sk} is the saturation vapor pressure at the skin surface in kPa; P_o is the vapor pressure at actual environment in kPa; P_{SET*} is the saturation vapor pressure at the ambient temperature that equals SET* in kPa.

SET* is defined as the air temperature of an imaginary environment at 50% relative humidity, in which the skin temperature and skin wetness from the skin of an imaginary occupant with a certain clothing and activity are the same as those from a person in the actual environment[3)~4)]. However, it is found from the verification[16)] that it is hard to achieve the equal skin temperature and skin wetness for the human in two environments in a high metabolic rate (above 1 met), since the heat dissipation of the skin is largely different. Therefore, the SET model is indicated to be only suitable for evaluating the

thermal comfort at a low metabolic rate, which should be revised in the case of a high metabolic rate.

2.2.3 Selection of thermal parameters

In this part, the thermal parameters related to the PMV, SET* and their levels are selected for the analysis of PMV and SET* in the imaginary environments. In previous research, six thermal parameters, namely the air temperature (T_a), mean radiant temperature (T_r), relative humidity (φ), air velocity (v), the metabolic rate (M) and clothing insulation (I_{cl}), are found to be the main influential factors in the PMV and SET* calculations. Due to the high correlation between the air temperature and mean radiant temperature, they can be replaced by the operative temperature (T_{op})[4]. In terms of the levels, the operative temperature encompasses 16 levels from 10°C to 40°C; relative humidity contains 7 levels from 30% to 90%; air velocity ranges from 0.1 m/s to 0.5 m/s; the metabolic rate is divided into 3 levels (1met, 1.5met and 2met) and clothing insulation is split into 0.5clo for summer wearing and 1clo for winter wearing. Table 2-2 shows the information of selected factors and levels in this study.

2.2.4 Data analysis

In the present study, each level of parameters and the calculated values of PMV and SET* combine as a data sample, e.g. sample 1 for T_{op}: 10oC, φ: 30%, v: 0.1m/s, M: 1met, Icl: 0.5clo, PMV: -6.2 and SET*: 8.5. Finally, 3360 samples are collected in total.

2.3 Results and discussion

In this section, the relationship between PMV and SET*, the frequency distribution of PMV and SET*, the effect of influential factors on PMV and SET*, and the thermal comfort zones are analyzed.

Table 2-2 Information of selected thermal parameters and their levels

Factor / Level	T_{op} (°C)	φ (%)	v (m/s)	M (met)	I_{cl} (clo)
1	10	30	0.1	1	0.5
2	12	40	0.2	1.5	1
3	14	50	0.3	2	
4	16	60	0.4		
5	18	70	0.5		
6	20	80			
7	22	90			
8	24				
9	26				
10	28				
11	30				
12	32				
13	34				
14	36				
15	38				
16	40				

2.3.1 The relationship between PMV and SET*

2.3.1.1 PMV as a function of SET*

The variation of PMV with SET* has been shown in Fig.2-2. Through linear regression, the regression equations of PMV for 0.5clo (summer), 1clo (winter) and total (a whole year) are presented in Equations (2-7) to (2-9). Since the PMV between -3 and 3 makes sense, Table 2-3 outlines the correspondence between SET*and PMV.

PMV for 0.5clo: $PMV = -0.003SET^{*2} + 0.457SET^{*} - 8.942$ $(-3 \leq PMV \leq 3)$ (2-7)

PMV for 1clo: $PMV = -0.002SET^{*2} + 0.366SET^{*} - 7.837$ $(-3 \leq PMV \leq 3)$ (2-8)

PMV for total: $PMV = -0.003SET^{*2} + 0.430SET^{*} - 8.626$ $(-3 \leq PMV \leq 3)$ (2-9)

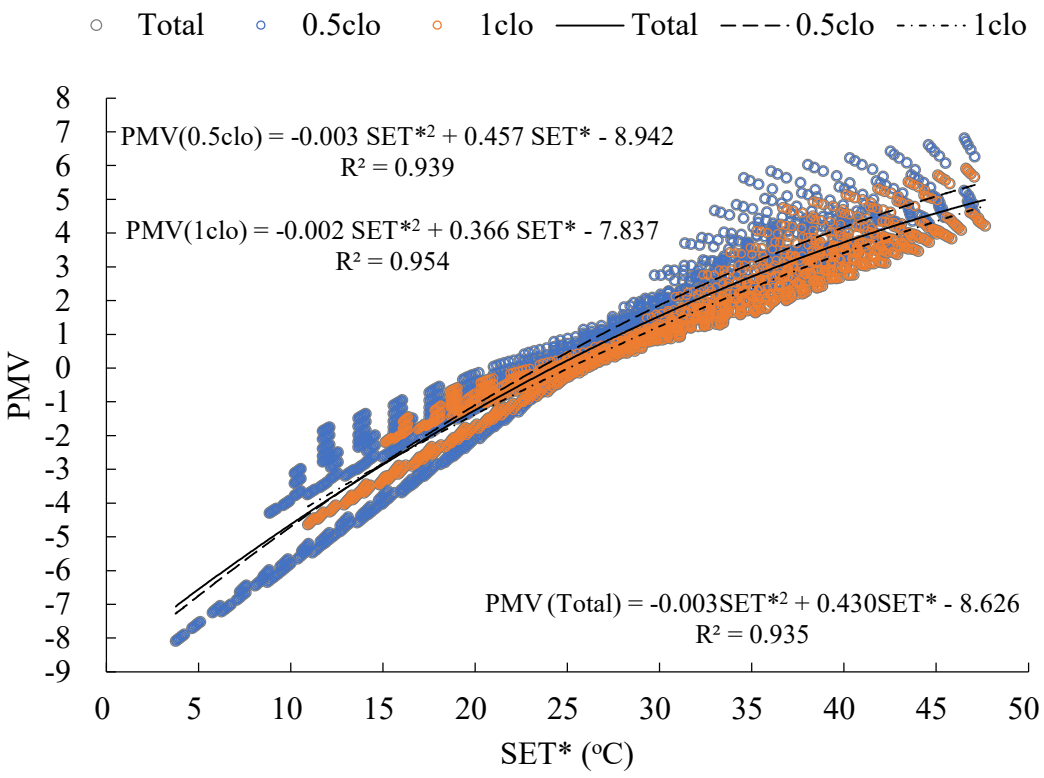

Fig.2-2 The variation of PMV with SET*

It can be seen from the above results that the linear fitting of SET* and PMV shows a curve relationship and a positive correlation. As SET* values go up, PMV values increase. Moreover, the slope of PMV for 0.5clo is the largest, signifying that the growth of PMV value is faster in summer wearing than that in winter wearing. In addition, the SET* values couldn't be calculated by equations if the PMV value is greater than 7. Although there is less research significance when the PMV value is greater than 3, this problem is still inevitable.

Table 2-3 The correspondence between SET* and PMV

SET* (°C)	PMV(0.5clo)	PMV(1clo)	PMV(Total)
15	-2.8	-2.8	-2.9
18	-1.7	-1.9	-1.9
21	-0.7	-1.0	-0.9
24	0.3	-0.2	0.0
27	1.2	0.6	0.8
30	2.1	1.3	1.6
33	2.9	2.1	2.3

2.3.1.2 SET* as a function of PMV

Fig.2-3 shows the variation of SET* with PMV. Through linear regression, Equations (2-10) to (2-12) present the regression equations of SET* for 0.5clo, 1clo and total. As the PMV between -3 and +3 makes sense, the correspondence between PMV and SET* is outlined in Table 2-4.

The result shows a curve relationship and a positive correlation between SET* and PMV. The SET* values mount with a bump in PMV values. Moreover, the slope of SET* for 1clo is the largest, which represents the faster growth of SET* value in winter wearing in comparison with that in summer wearing. In addition, it should be mentioned that the results in this section are more reasonable than those in section 2.3.1.1, because each PMV value can calculate the corresponding SET* value by equations under the premise that the SET* is greater than 0. Hence, for the sake of research preciseness, results in section 2.3.1.2 are adopted in the following analysis of PMV and SET*.

SET* for 0.5clo: $SET^*=0.104PMV^2+3.238PMV+23.581 \quad (-3\leq PMV\leq 3)$ (2-10)

SET* for 1clo: $SET^*=0.059PMV^2+3.833PMV+25.505 \quad (-3\leq PMV\leq 3)$ (2-11)

SET* for total: $SET^*=0.092PMV^2+3.469PMV+24.653$ $(-3\leq PMV\leq 3)$ (2-12)

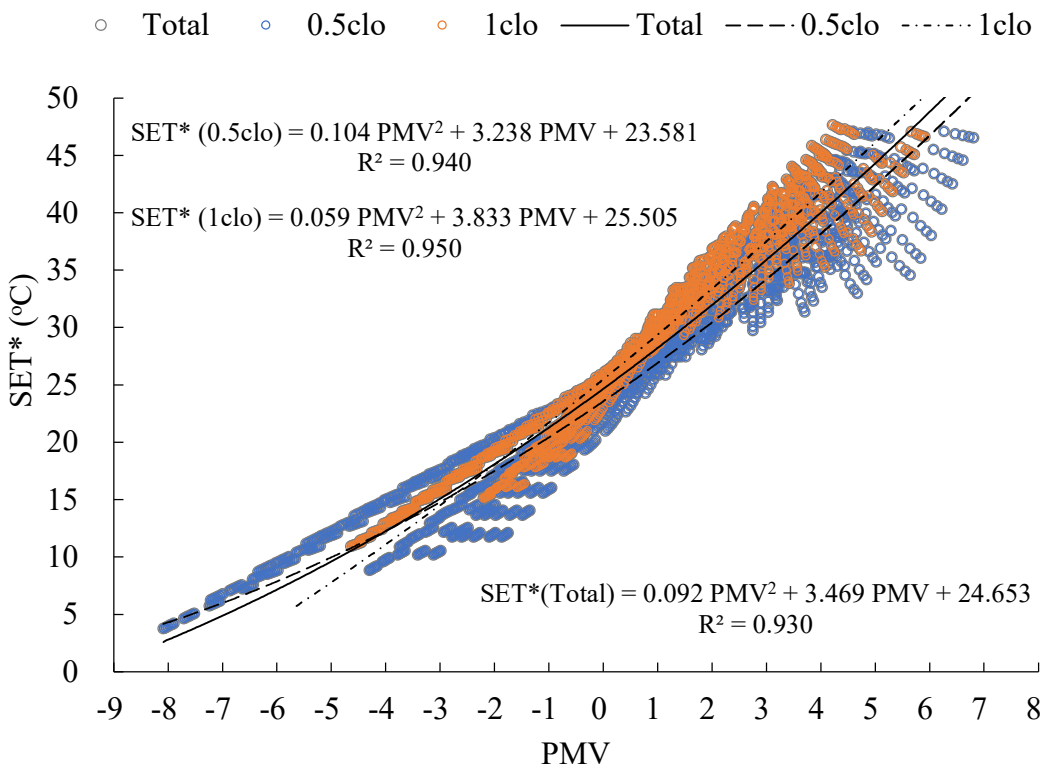

Fig.2-3 The variation of SET* with PMV

Table 2-4 The correspondence between PMV and SET*

PMV	SET*(0.5clo) (ºC)	SET*(1clo) (ºC)	SET*(Total) (ºC)
-3	14.8	14.5	15.1
-2	17.5	18.1	18.1
-1	20.4	21.7	21.3
0	23.6	25.5	24.7
1	26.9	29.4	28.2
2	30.5	33.4	32.0
3	34.2	37.5	35.9

2.3.2 Frequency distribution of PMV and SET*

Fig.2-4 shows the frequency distribution of PMV and SET*, where the legend presents the correspondence between PMV and SET* (Total) shown in Table 2-4. The frequency distribution illustrates that each scale of PMV and SET* occupies different amounts of samples, which are the most in the scale of x≥3 (35.9) and the least in (15.1) -3≤x<-2 (18.1). Furthermore, the frequency of PMV and SET* in the scale of (32)2≤x<3(35.9) is the most similar, with only 0.1% difference. On the contrary, they show the maximum difference (2.6%) in the scale of (21.3) -1≤x<0 (24.7).

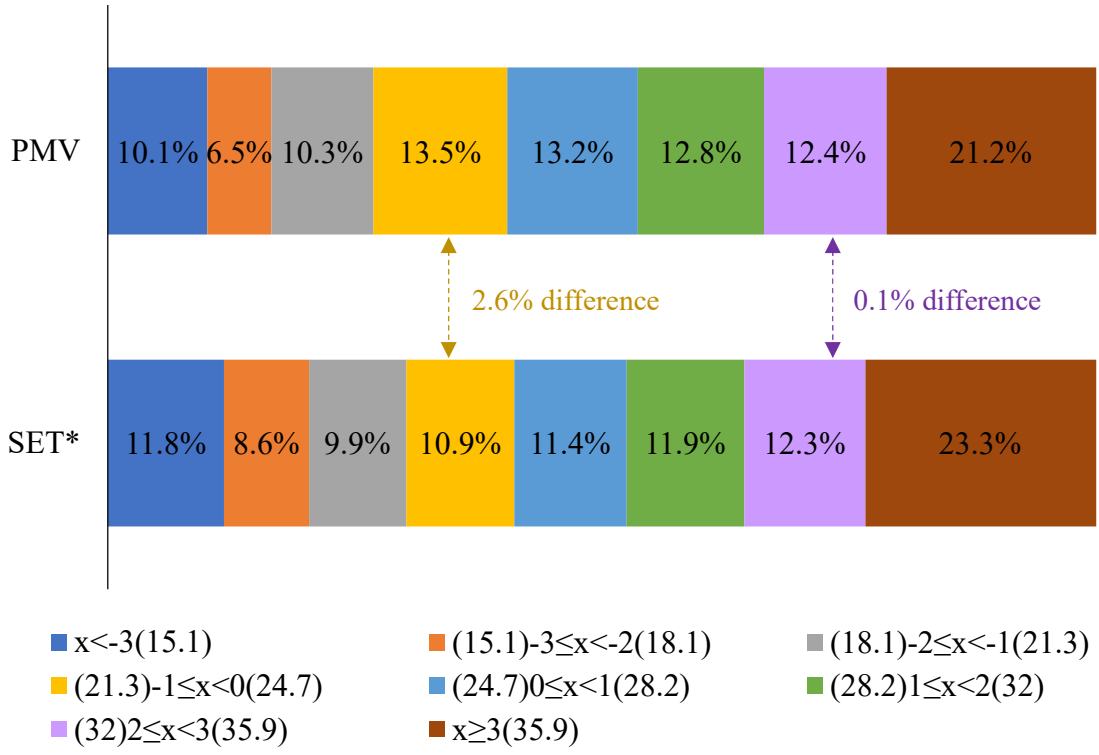

Fig.2-4 Frequency distribution of PMV and SET*

The results reveal that the correspondence between PMV and SET* is meaningful simply to the calculation results, rather than parameters involved in the calculation. For example, the thermal parameters involved in the calculation are 32ºC, 30%, 0.1 m/s, 0.5clo and 1 met in the operative temperature, relative humidity, air velocity, clothing insulation and the metabolic rate, respectively. Then, the calculated result for PMV is 2 and the one for SET* is 30.4ºC, which are not in the same scale in spite of the identical

thermal parameters. Therefore, it can merely be matched from the calculation results in the correspondence between PMV and SET*.

2.3.3 Analyses of thermal parameters

In the context of different thermal parameters (relative humidity, air velocity, the metabolic rate and clothing insulation), the change of thermal comfort value with operative temperature is shown in Fig.2-5 to Fig.2-8. To reflect the relationship between thermal comfort and thermal parameters more explicitly and intuitively, the values of thermal parameters are adopted as maximum and minimum ones in this study. Relative humidity is 30% and 90%; air velocity is 0.1 m/s and 0.5 m/s; the metabolic rate is 1met and 2met; clothing insulation is 0.5clo and 1clo. Furthermore, the PMV values are converted to SET* values by Equations (2-7) and (2-8) for unified comparison.

In Fig.2-5, the values of PMV and SET* rise with the increase of operative temperature, which are chiefly affected by the air velocity and relative humidity at lower and higher operative temperatures, respectively. Moreover, the distinction of SET* values between 30% and 90% relative humidity increases from an operative temperature of 24°C. In addition, the values of PMV rise faster than those of SET* at high operative temperature (above 30°C).

In Fig.2-6, the values of PMV and SET* are larger than those in Fig.2-5. Nevertheless, the increasing rate drops with the augment of operative temperature, so that the values of PMV and SET* in the case of 1clo at 40°C are consistent with those in the case of 0.5clo at 40°C. Meanwhile, the values of PMV and SET* are mainly under the influence of the air velocity at lower operative temperatures and relative humidity at higher operative temperatures, which is the same as Fig.2-5. Furthermore, the difference of SET* affected by relative humidity increases from an operative temperature of 24°C. Besides, the difference between PMV and SET* is smaller than that in the case of 1met and 0.5clo.

As shown in Fig.2-7, with the increase of the metabolic rate, the air velocity at lower operative temperatures and relative humidity at higher operative temperatures exert a major influence on values of PMV, while relative humidity remains the only influencing factor for values of SET*. Moreover, the difference of SET* affected by relative humidity increases from an operative temperature of 16°C. In the aspect of the relationship between PMV and SET*, the value of PMV at low operative temperature (10°C~24°C) is larger than that of SET*, while the growth rate of PMV is slower than that of SET*. It is indicated that as the metabolic rate increases, the increasing rate of PMV falls with increasing operative temperature.

The values of PMV and SET* in Fig.2-8 are larger than those in Fig.2-7, but the increasing rate diminishes with the increase of operative temperature. Meanwhile, the same as Fig.2-7, the air velocity at lower operative temperatures and relative humidity at higher operative temperatures have a primary effect on values of PMV, while values of SET* are simply affected by relative humidity. Furthermore, the difference of SET* affected by relative humidity increases from an operative temperature of 10°C. Besides, the difference between PMV and SET* is smaller than that in the case of 2met and 0.5clo.

2.3.4 Analyses of thermal comfort zones

In ASHRAE Standard 55[3)], two methods for determining the thermal comfort zone in occupied space are proposed, namely the Graphic Comfort Zone Method and the Analytical Comfort Zone Method. The applicability of these methods is shown in Table 2-5. In general, the Graphic Comfort Zone Method is the most intuitive and commonly used but restricted by conditions. The Analytical Comfort Zone Method is wider in use conditions with the PMV calculation method ($-0.5 \leq PMV \leq 0.5$), which suits the calculation of a large amount of data. This section attempts to present the comfort zone by the Analytical Comfort Zone Method and the Graphic Comfort Zone Method in a graphical manner.

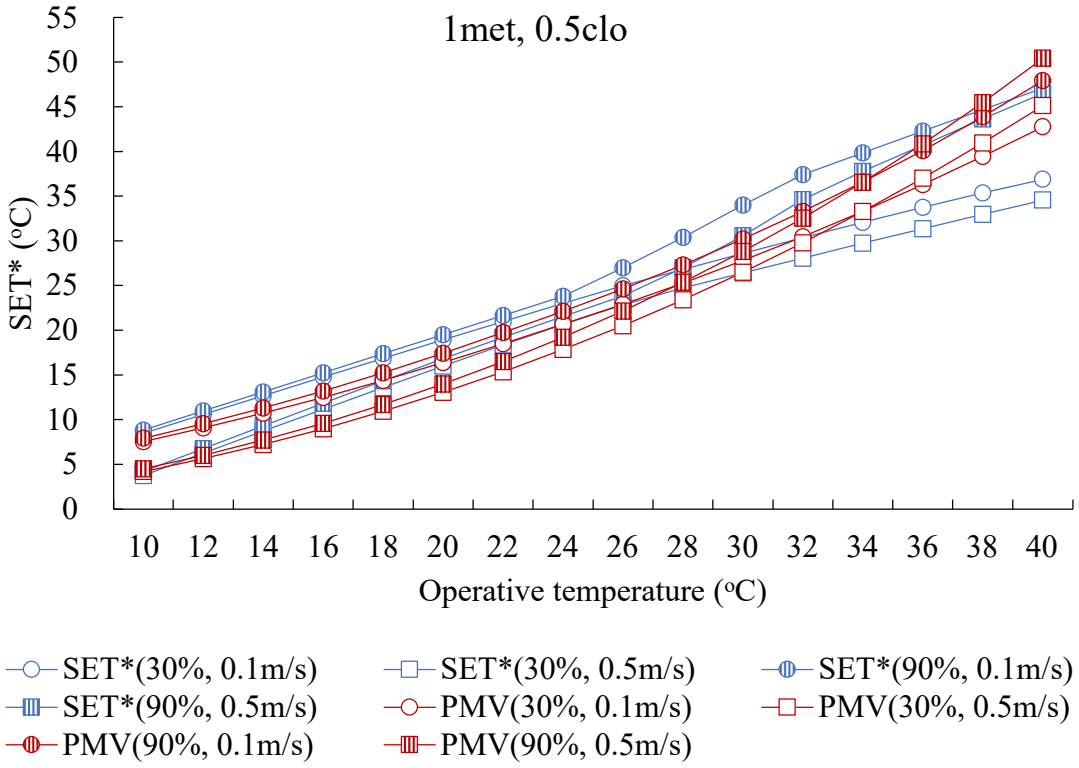

Fig.2-5 The variation of SET* and PMV with operative temperature at 1met and 0.5clo

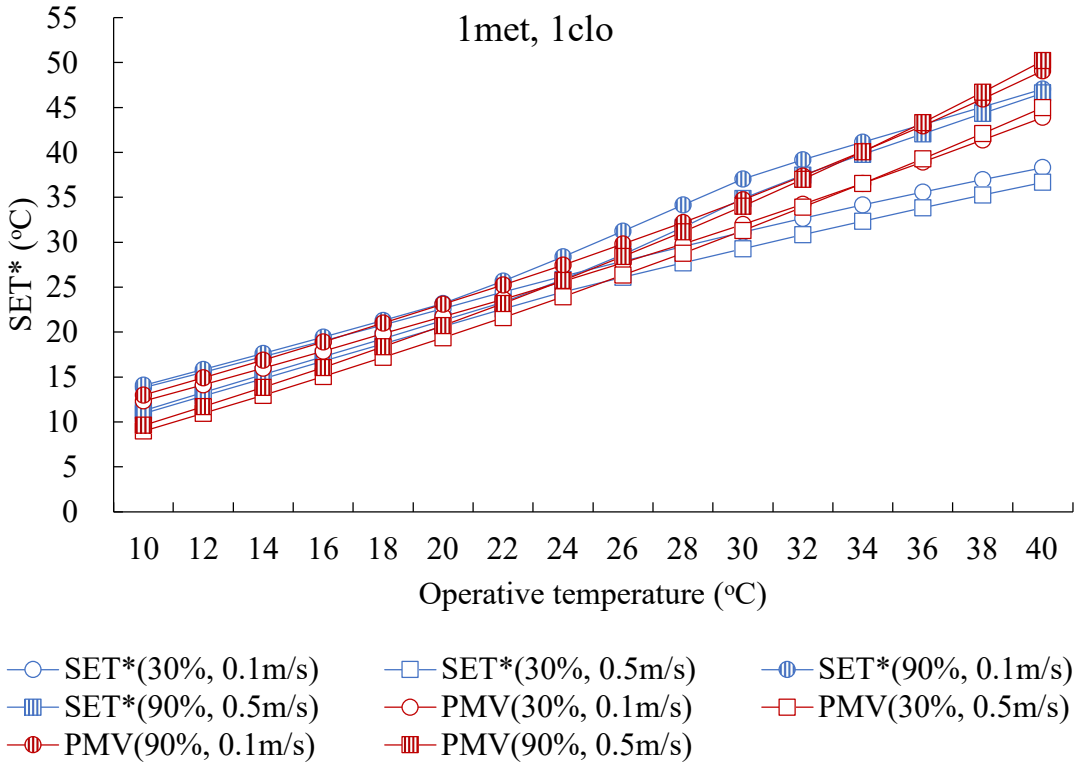

Fig.2-6 The variation of SET* and PMV with operative temperature at 1met and 1clo

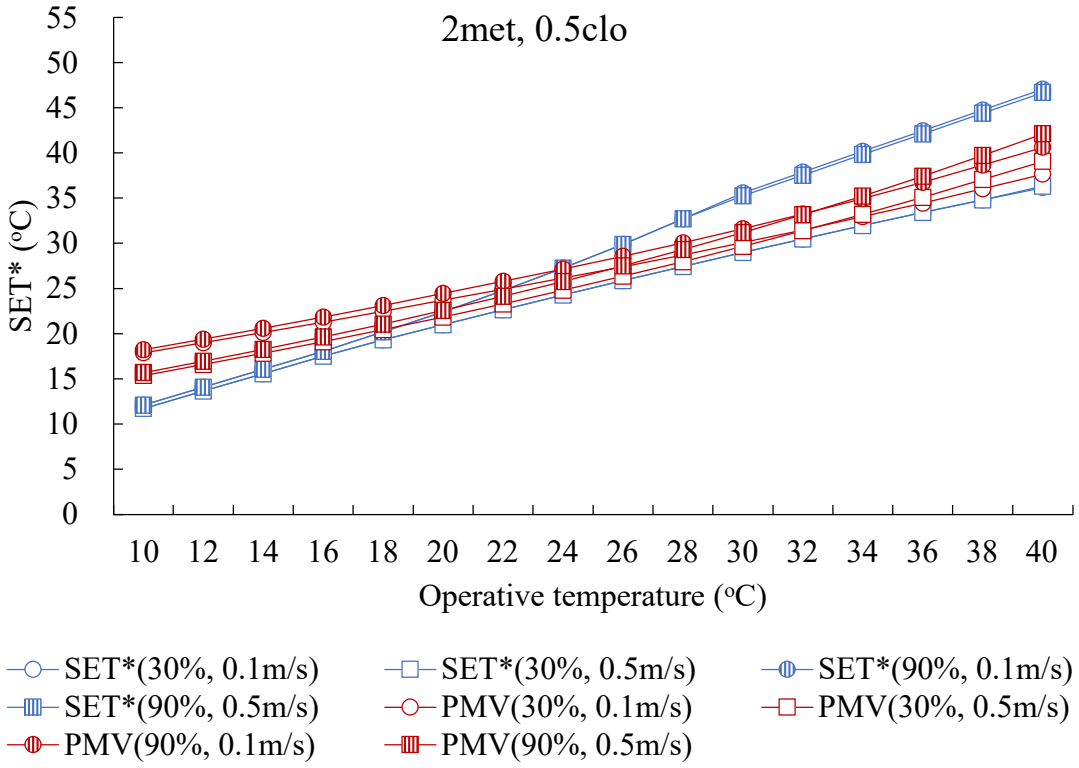

Fig.2-7 The variation of SET* and PMV with operative temperature at 2met and 0.5clo

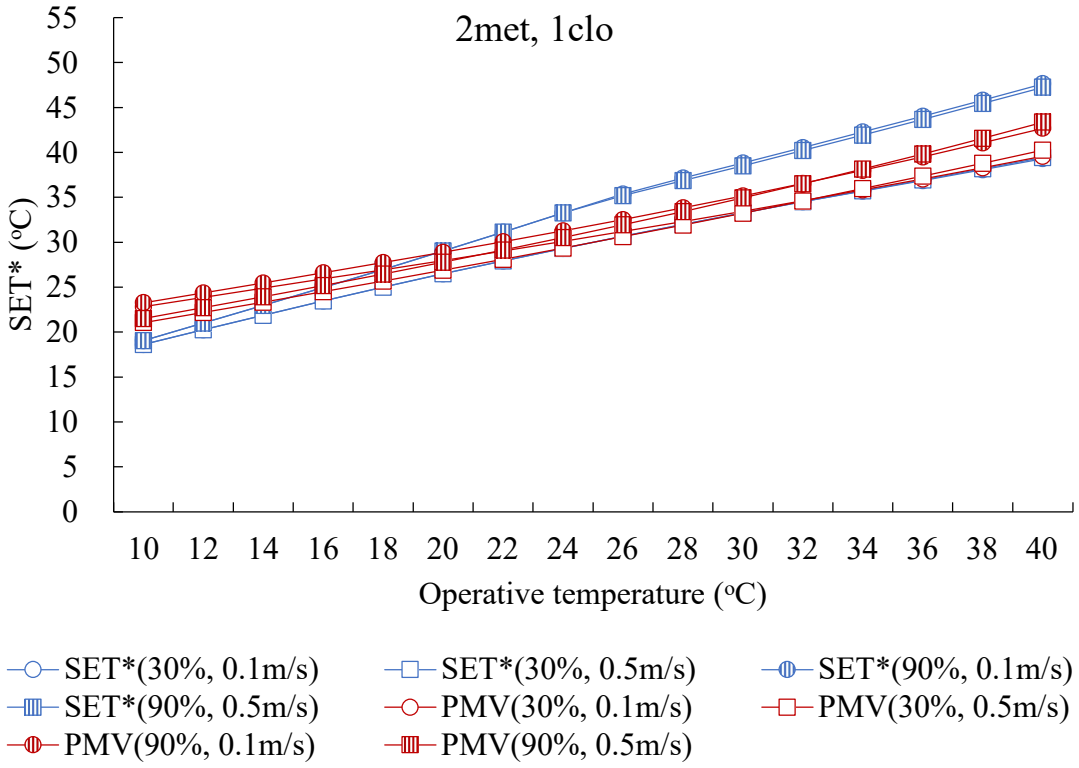

Fig.2-8 The variation of SET* and PMV with operative temperature at 2met and 1clo

Table 2-5 Applicability of methods for determining thermal comfort zone

Air speed (m/s)	Humidity ratio (kg·H_2O/kg dry air)	Metabolic rate (met)	Clothing insulation (clo)	Comfort Zone Method
<0.2	<0.012	1 to 1.3	0.5 to 1	Graphic Comfort Zone Method
<0.2	All	1 to 2	0 to 1.5	Analytical Comfort Zone Method

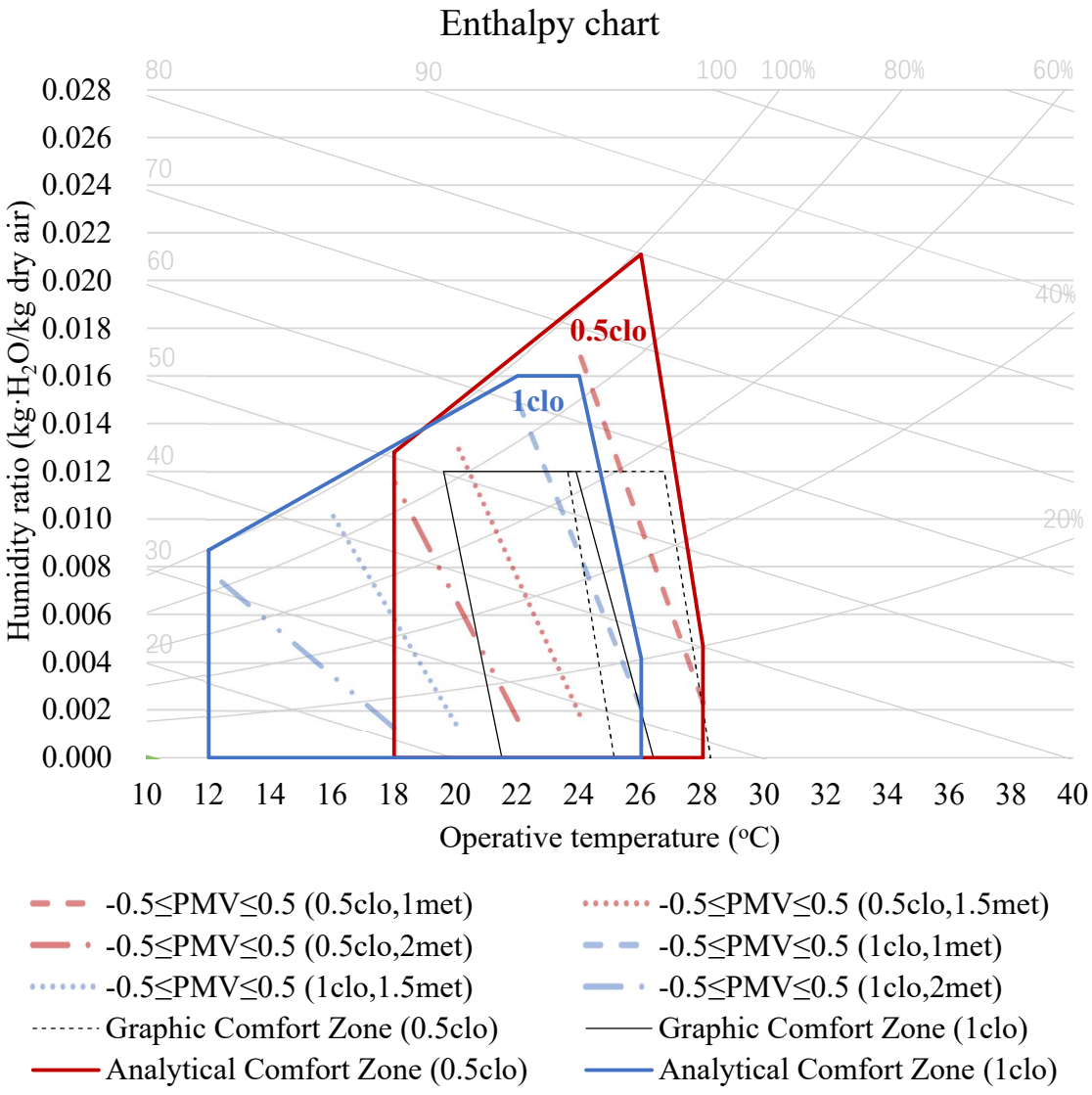

Fig.2-9 Thermal comfort zones by the Graphic Comfort Zone Method and the Analytical Comfort Zone Method

In Fig.2-9, the red circles and squares represent the PMV values between -0.5 and 0.5 calculated by the operative temperature from 10°C to 40°C, the relative humidity from 10% to 90%, the air velocity for 0.1m/s, the metabolic from 1met to 2met and the clothing insulation in 0.5clo and 1clo, respectively. The dashed line and the solid line are the comfort zones calculated by Analytical Comfort Zone Method for 0.5clo and 1clo, respectively. Compared with the comfort zones by Graphic Comfort Zone Method, the comfort zones by Analytical Comfort Zone Method are more extensive, mainly extending to the left and above due to the increase of the metabolic rate and relative humidity.

2.3.5 Comparison between SET* in this study and other studies

The previous study has witnessed some research achievement of the relationship between the comfort vote and SET* by the field investigations. Gonzalez et al.[21] studied the relationship between the predicted discomfort vote and SET* based on the physiological and physical theory. Gagge et al.[22] presented the relationship between the new effective temperature scale for sedentary clothed subjects, the thermal sensation, the physiological responses and health factors concerned. Moreover, Gagge et al.[2] indicated the relationship between the ambient temperature at saturation, SET* and the PMV for moderate exercise. After summarizing achievements from previous studies, ASHRAE[23] put forward the relationship between SET*, PMV, sensation and physiology in the sedentary environment. To analyze the relationship between the PMV and SET* in the imaginary standard condition and the practical condition, Table 2-6 sorts out values of SET*(0.5clo), SET*(1clo), SET*(Total) and SET*(ASHRAE) corresponding to the PMV.

The values of SET*(ASHRAE) are close to values of SET* in this study near the PMV of 0, and the difference of SET*(ASHRAE) and SET*(0.5clo), SET*(ASHRAE) and SET*(1clo), as well as SET*(ASHRAE) and SET*(Total), at the PMV of 0 is 0.3°C, 1.6°C and 0.8°C, respectively. With the increase of the PMV, SET*(ASHRAE) is greater than the SET* in this study and in keeping with the SET*(1clo) at the PMV of 3.

Moreover, SET*(ASHRAE) is much smaller than the SET* in this study at the PMV below 0, with the biggest gap appearing at the PMV of -3. In addition, the values of SET*(0.5clo) and SET*(1clo) show coincidence at the PMV of -3, and then the increasing rate of SET*(1clo) is faster than that of SET*(0.5clo) with the increase of the PMV, which reaches 3.3ºC in difference at the PMV of 3. The results in this section indicate that values of SET in the imaginary and practical condition are of difference due to disparate obtaining ways of the thermal comfort vote. The results suggest that the SET* can be referred in the comfort condition (PMV=0) and should be considered in other comfort conditions in line with the situation of the study.

Table 2-6 The comparison between SET*(0.5clo), SET*(1clo), SET*(Total) and SET*(ASHRAE) corresponding to the PMV

PMV	SET*(0.5clo) (ºC)	SET*(1clo) (ºC)	SET*(Total) (ºC)	SET* (ASHRAE) (ºC)
-3	14.8	14.5	15.1	10
-2	17.5	18.1	18.1	14.5
-1	20.4	21.7	21.3	17.5
0	23.6	25.5	24.7	23.9
1	26.9	29.4	28.2	30
2	30.5	33.4	32.0	34.5
3	34.2	37.5	35.9	37.5

2.4 Summary

In this chapter, a comparative analysis of PMV and SET* has been performed. The main findings are as follows:

1) The relationships between PMV and SET* in the case of 0.5clo (summer), 1clo (winter) and total (a whole year) have been obtained by the regression of 3360 samples in the imaginary standard condition.

2) The correspondence between PMV and SET* is only meaningful to the calculation results, instead of the thermal parameters involved in the calculation.

3) The values of PMV and SET* are principally affected by the air velocity at low operative temperatures and affected by the relative humidity at high operative temperatures in the sedentary condition. However, with the increase of the metabolic rate, the values of SET* are only affected by relative humidity.

4) The values of PMV and SET* increase with the increase of clothing insulation while the increasing rates lower. Moreover, the difference between PMV and SET* gets smaller with the increasing clothing insulation.

5) Compared with the comfort zones by Graphic Comfort Zone Method, the comfort zones by Analytical Comfort Zone Method are more extensive and mainly extend to the left and above thanks to the increase of the metabolic rate and relative humidity.

Chapter 3

Field study on the thermal sensation under high-intensive exercise in naturally ventilated gymnasiums in hot-humid regions

3.1 Introduction

As a public building for exercise, entertainment and sport, gymnasiums play a significant part in people's daily life. In the subtropical areas where climates are hot and humid, indoor thermal comfort in gymnasiums is relevant to energy consumption directly. Furthermore, the activities of athletes, like basketball playing, badminton playing and running, are quite different from other kinds of activities in other spaces, which are bound up with public health. A balance among health, energy consumption and thermal comfort in gymnasiums is of necessity to be found. Besides, it is vital to develop a thermal comfort model for athletes in gymnasiums in hot-humid regions.

Previous studies indicated that indoor thermal comfort was affected by the factors of indoor thermal environment and human physiology. Some models covering all or parts of the factors have been suggested, such as the Predicted Mean Vote (PMV) model developed by Fanger[1)] and the model of Standard Effective Temperature (SET) put forward by Gagge[2)], which are based on the two-node model established from the human physiology. In addition, some models are in line with the thermal environment parameters, such as the Wet Bulb Globe Temperature (WBGT), the Equatorial Comfort Index (ECI) and Equivalent Temperature (EqT) [3)~5)]. However, these models are limited to a certain extend. For instance, the PMV model is mainly applicable to steady-state environments; the SET model could apply to naturally ventilated building, on condition that the human body has a low metabolic rate.

Due to the development of thermal comfort research, thermal comfort of different regions and different types of buildings has been extensively explored. Takeing the hot-humid region as an example, Zhang et al.[6)] conducted a field survey in rural residences in Guangdong, China and analyzed the thermal comfort of various spaces of residences. Djamila et al.[7)] in Malaysia investigated 890 residences in residential buildings and the moderate temperature of 30 °C was confirmed by different methods. Buonocore et al.[8)] investigated the thermal performances in classrooms in Brazil, finding the occupants are

more thermal tolerant in hot climate. Some other studies have focused on thermal comfort studies of different types of buildings and people in hot-humid regions as well as other regions[9)~11)]. A large number of studies have shown the rapid development of thermal comfort research and people's efforts to pursue higher quality of life. It should be noted that most above studies are primarily appliable to residential buildings, office buildings and classrooms, with the occupants at low metabolic rates. Very few studies focused on the thermal comfort of sport players in sports buildings undertaking sports and exercises. However, thermal comfort study in the sport environment, as we all know, is necessary to pursue health and wellbeing and to attain a high quality of life for human subjects. Based on this background, this study undertake a research into the thermal comfort under high-intensive exercises in gymnasium.

Early studies have shown that intensity level could have a significant effect on the thermal comfort. In 1957, Yaglou and Minard[12)] developed WBGT index to evaluate the effect of heat on a person during total exposure over the working day. The study provided a reference limit for persons in five levels of intensity, which is a very early study of thermal comfort that takes labour intensity into account. In 1967, Fanger[13)] found that the sweat evaporation rate increases as the metabolic rate of subjects increases by experimental studies. Gagge et al.[14)] in 1969 indicated that the human thermal sensation is strongly influenced by a wide range of activity levels of subjects. Gonzales[15)] in 1981 conducted field experiments at different exercise intensities and found subjects' comfort temperature diminished with the rising of the activity level. Humphreys and Nicol[16)] noted that the PMV model is only valid to activities less than 1.4 met and produced errors with the metabolic rate above 1.8met. These studies contribute greatly to the thermal comfort research in terms of metabolic intensity. In recent years, Ji et al.[17)] investigated 31 college-aged subjects riding a spinning bike (3.5 met) in a chamber and found that the metabolic rate during transition could affect thermal comfort significantly. Li et al.[18)] conducted experimental research on strenuous exercise (3.5~5.0 met) and indicated that the heart rate and wrist skin temperature can be utilized for evaluating the thermal sensation. Researches from Henriques, Guéritée and Zhai et al. analysed the

relationship between themal comfort and different levels of intensity as well[19)~21)]. Metabolic activity is one of the key parameters in existing thermal comfort theory, however, most of the above studies were conducted in the climate chambers rather than in actual fields, which are less realistic when considering surroundings, behaviours and expectations of subjects. So far, there has been no field study on thermal comfort of athletes undertaking high-intensive exercise in a naturally ventilated gymnasium.

Through field investigation in three gymnasiums in hot-humid region of China (Guangzhou City), this chapter aims to analyse the indoor thermal environment (air temperature, humidity ratio, air velocity and mean radiant temperature), human physiology (metabolic rate, blood pressure and skin temperature) and thermal sensation of athletes under high-intensive exercise.

3.2 Methods

3.2.1 Selection of exercise type

In order to find out the most typical sport of high intensity in gymnasiums as the research object in this study, the facilities and 150 subjects (75 males and 75 females) in 10 gymnasiums in Guangzhou, China were investigated as a preliminary survey. In general, the high-intensive sports require an average metabolic rate higher than 230W/m^2, thus the following sports: basketball, badminton, football, volleyball, boxing and track and field were surveyed[22)]. The number of facilities in 10 gymnasiums for these sports and the sports preferences of 150 participants were sueveyed through questionnaires. Figure 3-1 presents the subjects' preferences for various sports and the proportion of facilities in these gymnasiums. It shows that most of subjects in gymnasiums prefer basketball playing, rather than badminton, football, volleyball, boxing and track and field, making it a reasonable choice for equating with the high intensive exercise in this study considering that basketball courts are set in all gymnasiums as the main facilities. On this basis, a field survey was conducted on thermal sensation of subjects in a basketball game in naturally ventilated gymnasiums in a hot and humid region.

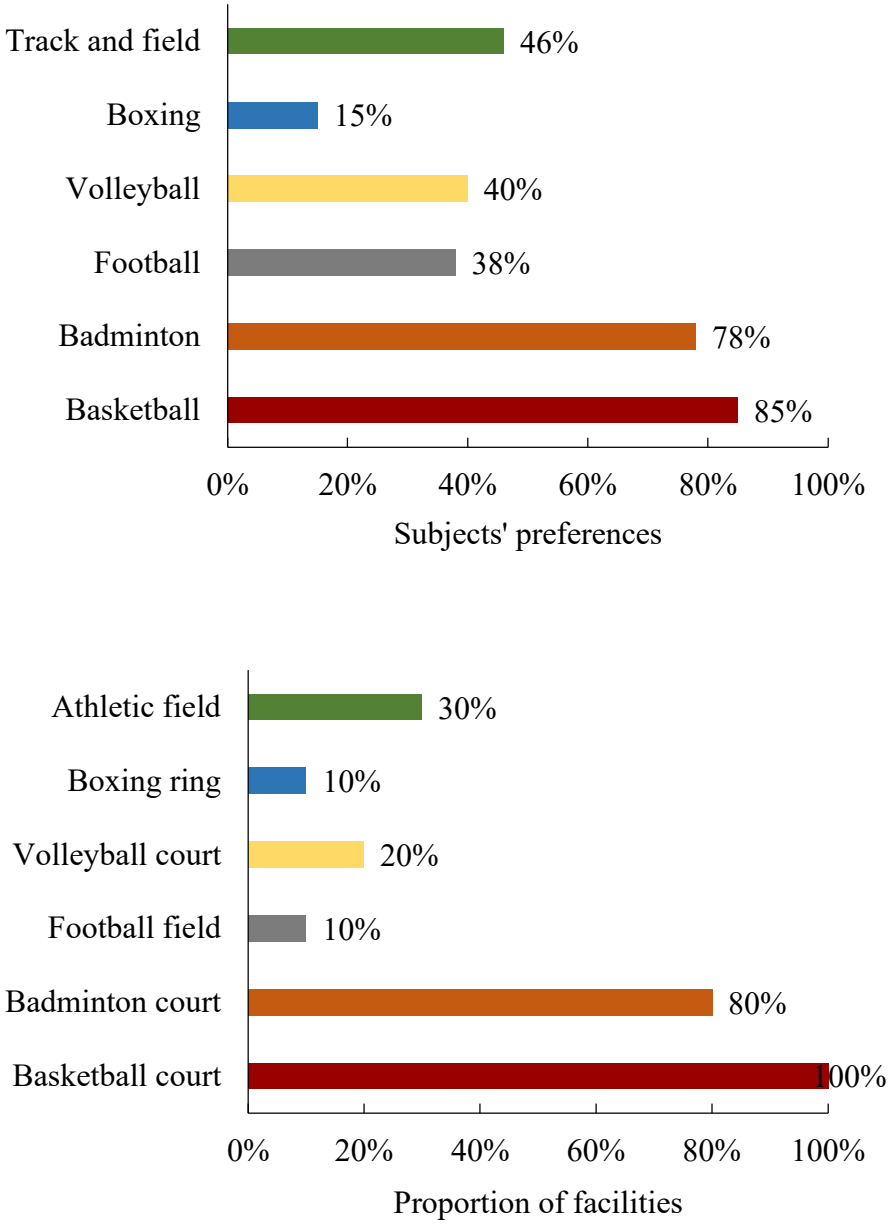

Fig.3-1 Subjects' preferences and proportion of facilities in investigated gymnasiums

3.2.2 Study sites

To investigate the thermal sensation of athletes in gymnasiums in hot-humid regions, three gymnasiums in Guangzhou (China), a typical city in the subtropical region of hot summer and warm winter climate with high humidity, was selected as the research location of this study. Fig.3-2 shows the location and climate histogram of Guangzhou[23)], in which the highest monthly average temperature (28.9°C) appears in July and the

lowest average temperature (14.2°C) in January. The months with the highest humidity level of 80% are April, June and August. Above all, long periods with high temperature and humidity is common in Guangzhou.

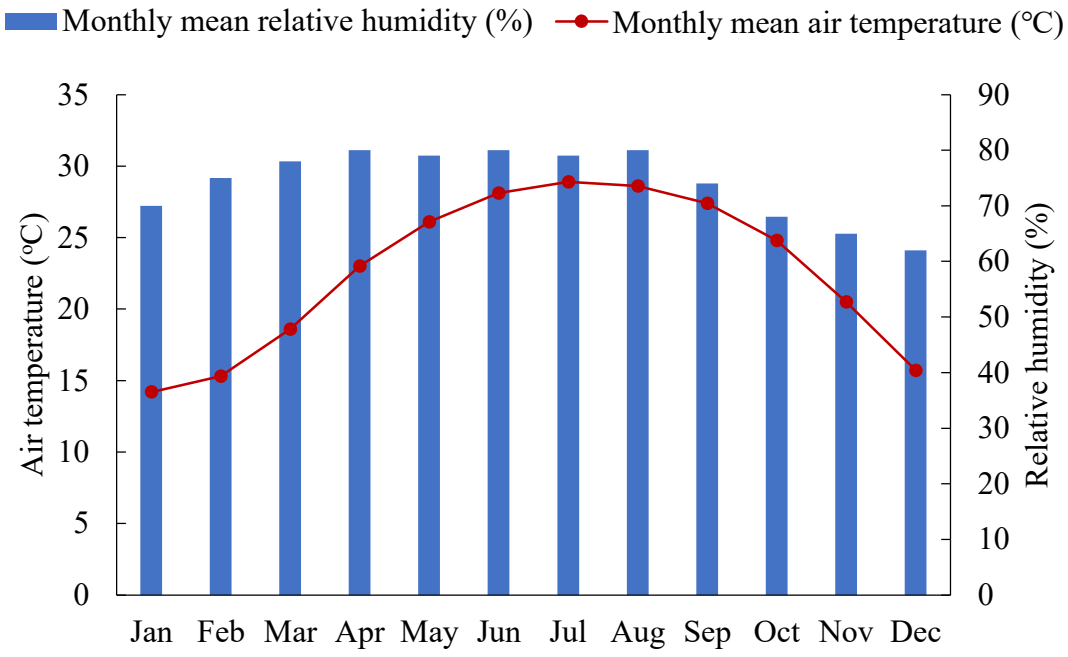

Fig.3-2 Location and climate histogram of Guangzhou, China[23)]

Exterior Interior


Gymnasium A


Gymnasium B


Gymnasium C

Fig.3-3 Exterior and interior views of the surveyed gymnasiums

Fig.3-3 presents the exterior and interior views of three gymnasiums located at the downtown area of Guangzhou (Gymnasiums A, B and C) surveyed in this study, which are all built with a reinforced concrete structure. Gymnasium A is a 5-storey building built in 2006. It has 6 basketball courts of 96m x 32m x 7.8m in length, width and height, on the ground floor. The construction of Gymnasium B was completed in 2009 and it has 4 basketball courts of 86m x 45.5m x 16m in length, width and height. The two-storey Gymnasium C was built in 2003 and it has 4 basketball courts of 65m x 46m x 15m in length, width and height, on the upper floor. The above three are all indoor gymnasiums that are naturally ventilated during the survey even though the air conditioning systems are installed in Gymnasium B and C.

3.2.3 Survey plan

Since the hot and humid indoor environment is the principal issue in this region, this field survey was carried out from August to October 2019. The survey time was between 9:00 and 18:00, which was divided into several periods of 60 minutes, e.g. 9:00-10:00, 10:00-11:00. The subjects could participate in the survey at any period.

The process of the field survey was split into three stages, as shown in Fig.3-4. In the first stage, subjects prepared for the survey for 10 minutes (sitting or standing); then, they kept playing basketball for 40 minutes; finally, subjects were given 10 minutes of rest. During the survey, data of thermal environment parameters, physiological parameters and thermal sensation of subjects were measured and analysed by instruments and questionnaires.

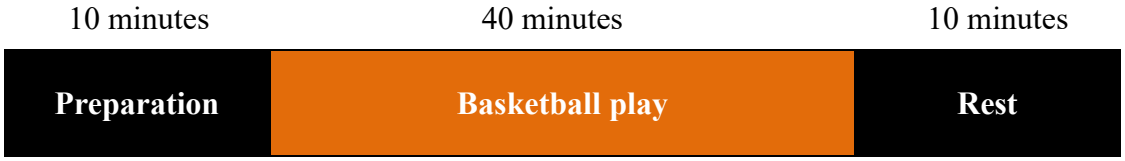

Fig.3-4 The process of field survey

The reason for allocating 40 minutes for the basketball game as this is the actual duration of a basketball match. However, in order to control the intensity of basketball exercise, the occupants in this study played basketball in practice rather than a competition, without role issues and competitive intensity. Furthermore, due to different intensities of individuals, a pre-test was performed to master the intensity level of playing basketball and was adjusted in a certain range of human metabolic rate. As for the 10 minutes of preparation and rest, the reason is that the physiological performance and the thermal sensation of subjects would be stabilized in 10 minutes. The results were confirmed in the pre-test of this study and some previous research findings.

3.2.4 Questionnaire survey

The information of subjects was surveyed by questionnaires, which includes:

1) Personal information, as shown in Table 3-1.

2) Personal situation, e.g. current clothing, illness and alcohol intake.

3) Thermal sensation vote (TSV) with the scale shown in Table 3-2.

Table 3-1 Information of subjects

	Male	Female
Number	18	18
Age (years old)	18-24	18-25
Height (cm)	170-183	150-172
Weight (kg)	50-85	42-60
BMI (kg/m^2)	17-25	19-20
Time of local living (year)	≥1	≥1
Exercise time per week (hour)	3-15	2-20

Table 3-2 Scale of thermal sensation vote

-3	-2	-1	0	+1	+2	+3
Extremely cold	Cold	Slightly cold	Comfortable	Slightly hot	Hot	Extremely hot

In the present study, a total of 36 college-aged subjects (18 males and 18 females) were surveyed. In order to minimize the influence of acclimation, all subjects have normal physical conditions, namely without illness or bad habits, and have lived in the local area for at least one year. In addition, they did not drink alcohol or consume irritating food at least one day before the survey.

During the survey, the subjects were required to fill out the first and second parts of questionnaires before each survey. The third part of questionnaire was answered by subjects every 10 min during the survey. To avoid interfering with basketball playing, the subjects only needed to verbally express the thermal sensation at the time.

3.2.5 Thermal environment measurement

The outdoor and indoor air temperatures, globe temperature, relative humidity and air velocity were recorded at 5-minute intervals in each survey. The measuring instruments is summarized in Table 3-3. Thanks to subjects playing on a half court, the physical measuring instruments (instrument No.1 and No.2) were arranged in three points around the half court at a height of 1.1m in line with the relevant standards[24], as shown in Fig.3-5. The outdoor instruments were placed in shaded locations near the gymnasiums at a height of 1.1m.

The humidity ratio instead of relative humidity was calculated and used, because it is a variable independent of the air temperature, which is more objective and accurate for the establishment of the predictive model in this study. Conversely, the saturated vapour pressure with air temperature at various air exchanges, makes the relative humidity a dependent variable related to the air temperature.

Table 3-3 Information of instruments

No.	Instrument	Model	Test content	Accuracy
1	Black-bulb thermometer	AZ-87786	Globe temperature	±0.3ºC
2	Hot-wire anemometer	TES-1341	Air temperature Relative humidity Air velocity	±0.4ºC ±1.0% ±0.03m/s
3	Infrared thermometer	IT-122	Skin temperature	±0.2ºC
4	Wearable motion detector	TomTom Spark 3	Heart rate	±5 bpm
5		Fu Hanlin-H166	Blood pressure	±6 mmHg

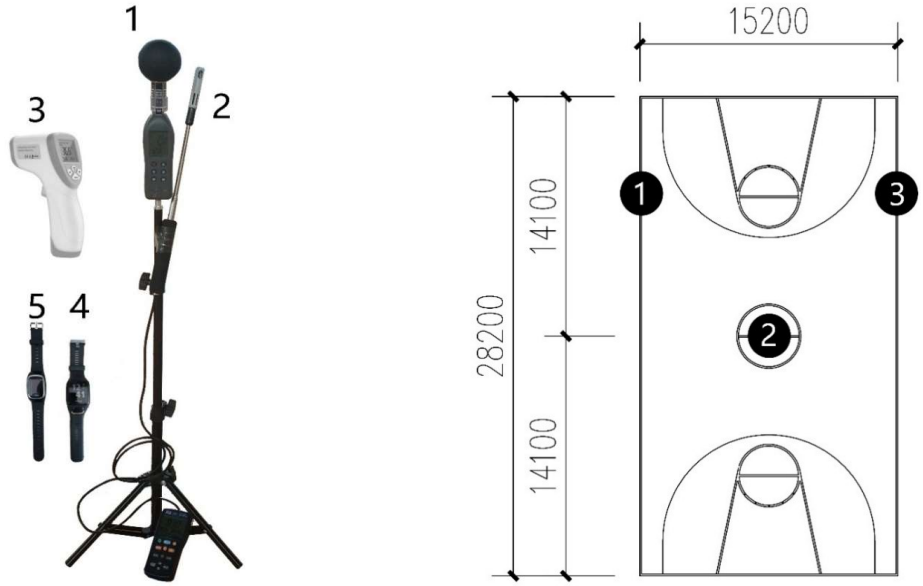

Fig.3-5 Instruments and the distribution in survey basketball court

(Points ① to ③ represent the locations of instruments No.1 and No.2)

The mean radiant temperature was calculated by the formula regarding the indoor globe temperature, air velocity and air temperature[25], as shown in Equation (3-1):

$$T_r = T_g + 2.37\sqrt{v}(T_g - T_a) \quad (3\text{-}1)$$

Where T_r is the mean radiant temperature in °C; T_g is the globe temperature in °C; v is the air velocity in m/s; T_a is the air temperature in °C.

3.2.6 Physiological data measurement

Collected immediately at the end of each surveyed stage (preparation, basketball play and rest), the mean skin temperatures of subjects were recorded by an infrared thermometer and calculated by the weighted mean skin temperature at four locations of the body (the chest, the arm, the thigh and the leg). The 4-point method was developed and validated by Rmanathan[26], and was used in this study due to less measurement points required, which can be measured with accuracy under hot ambient conditions[27]. The formula of mean skin temperature is shown below:

$$T_{sk} = 0.3T_{chest} + 0.3T_{arm} + 0.2T_{thigh} + 0.2T_{leg} \quad (3\text{-}2)$$

where T_{sk} is the mean skin temperature in °C; T_{chest} is the chest temperature in °C; T_{arm} is the forearm temperature in °C; T_{thigh} is the thigh temperature in °C; T_{leg} is the leg temperature in °C.

The blood pressures and heart rates of subjects were recorded at 5-minute intervals in each survey. For the sake of the most accurate data recording of subjects during the survey, the wearable motion detectors (Detectors for blood pressure is based on the principle of "Pulse Transmit Time, PTT") were introduced, as shown in Table 3-3 and Fig.3-5. The metabolic rates were obtained using the heart rate equation given by the ISO8996: 2004[22], as shown in Table 3-4.

3.2.7 Data analysis

In the present study, the average values of thermal environment parameters, physiological parameters and thermal sensation of subjects in each surveyed stage were used as a data sample. Finally, a total of 372 valid samples were collected, including 124

Table 3-4 Relationship between metabolic rate (W/m^2) and heart rate (bpm)

Age (years)	Weight (kg)				
	50kg	60kg	70kg	80kg	90kg
Women					
20	2.9×HR-150	3.4×HR-181	3.8×HR-210	4.2×HR-237	4.5×HR-263
30	2.8×HR-143	3.3×HR-173	3.7×HR-201	4.0×HR-228	4.4×HR-254
40	2.7×HR-136	3.1×HR-165	3.5×HR-192	3.9×HR-218	4.3×HR-244
50	2.6×HR-127	3.0×HR-155	3.4×HR-182	3.7×HR-207	4.1×HR-232
60	2.5×HR-117	2.9×HR-145	3.2×HR-170	3.6×HR-195	3.9×HR-219
Men					
20	3.7×HR-201	4.2×HR-238	4.7×HR-273	5.2×HR-307	5.6×HR-339
30	3.6×HR-197	4.1×HR-233	4.6×HR-268	5.1×HR-301	5.5×HR-333
40	3.5×HR-192	4.0×HR-228	4.5×HR-262	5.0×HR-295	5.4×HR-326
50	3.4×HR-186	4.0×HR-222	4.4×HR-256	4.9×HR-288	5.3×HR-319
60	3.4×HR-180	3.9×HR-215	4.5×HR-249	4.8×HR-280	5.2×HR-311

samples in each stage. Since the high-intensive exercise is the key point in this study, the 124 samples collected during the basketball game would be major object of this study.

The study was conducted according to the guidelines of human-research ethics in China[28)] and was approved by the management departments of measured gymnasiums. All participants signed an informed consent form before the start of the study.

3.3 Results

The values of thermal environment parameters, the data of subjects and the thermal sensation of subjects are presented. Moreover, the correlations among the thermal environment, human physiology and thermal sensation were analysed.

3.3.1 Values of thermal environment parameters

Fig.3-6 shows the maximum, minimum, average and standard deviation (SD) values of the surveyed thermal environment parameters.

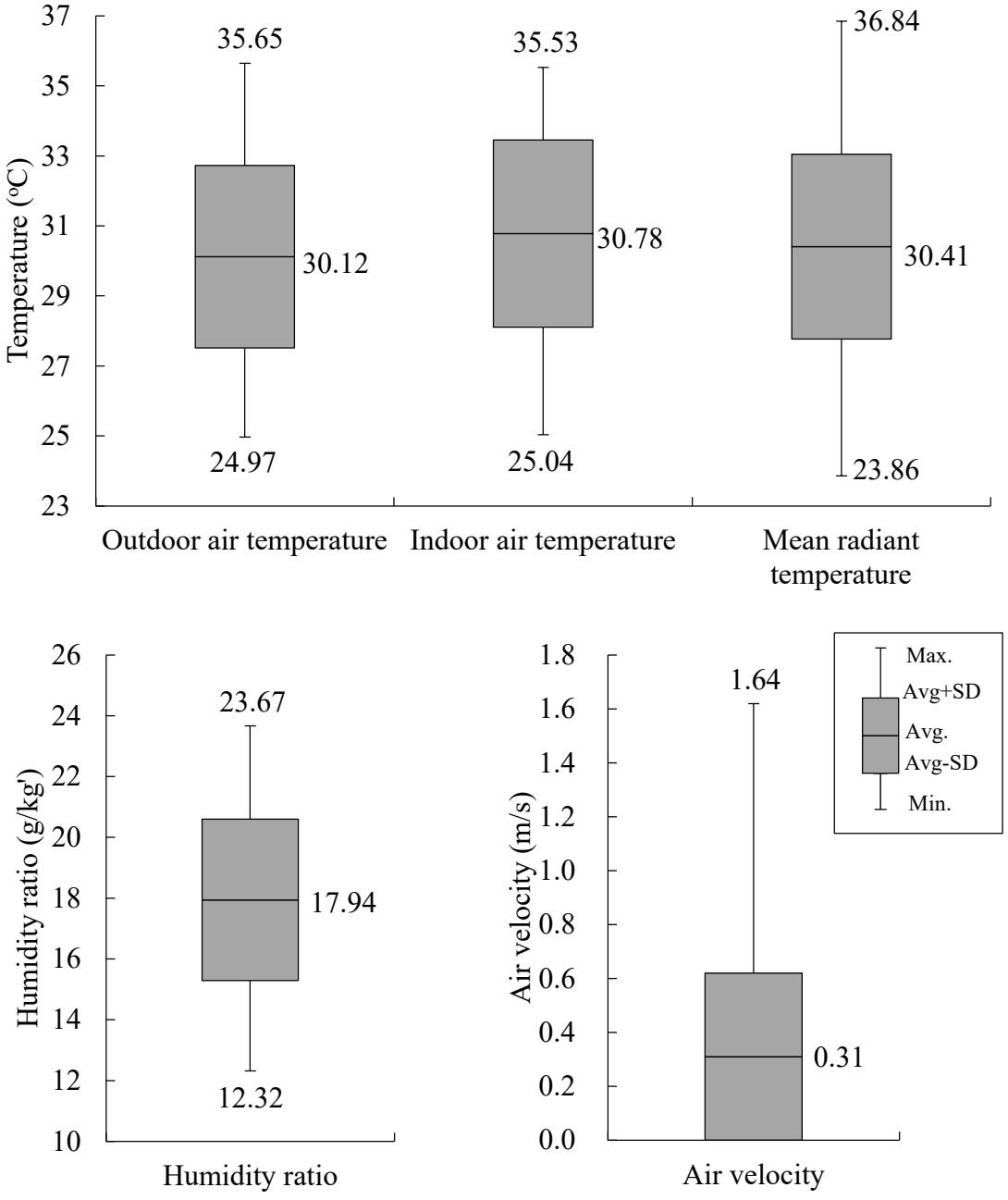

Fig.3-6 Summary of thermal environment parameters

During the survey, the outdoor air temperature ranged from 24.97°C to 35.65°C, while the indoor air temperature ranged from 25.04°C to 35.53°C. By comparison, the average

value of indoor air temperature (30.78°C) was 0.66°C higher than that of outdoor air temperature. Moreover, the mean radiant temperature scope was between 23.86°C and 36.84°C, which is wider than air temperature range. The humidity ratio changed from 12.32g/kg' to 23.67g/kg' and the average air velocity was 0.31m/s that meets the required wind speed for basketball games[29].

3.3.2 Conditons of subjects

3.3.2.1 Clothing insulation

During the field survey, the subjects were dressed in sportwear suitable for playing basketball. The clothing insulation values in this study, which were calculated from ASHRAE Standard 55-2017[30], was 0.22clo for males and 0.22clo / 0.29clo for females, as shown in Table 3-5.

Table 3-5 Clothing insulation of subjects (Unit: clo)

Clothing		Male	Female
Tops	Underwear	None	0.01
	T-shirt	0.08	0.08
Bottoms	Briefs	0.04	0.03
	Shorts or trousers	0.08	0.08 or 0.15
	Socks	0.02	0.02
Clothing insulation in total		0.22	0.22 or 0.29

3.3.2.2 Metabolic rate

As mentioned above, the metabolic rate was calculated using the formula of the heart rate as prescribed by the ISO8996: 2004[22]. Fig.3-7 shows the variation of maximum, minimum and average values in the metabolic rate of males and females. In the preparation stage, the metabolic rate of subjects declined to around 111W/m^2 (1.91met)

at the 10th min. During the early stage of playing basketball, the metabolic rate of subjects was raised apparently and kept steady for 40 minutes, with an average rate of 334W/m^2 (5.75met) for males and 274W/m^2 (4.72met) for females. However, males' metabolic rates were more fluctuated than females' in the aspect of maximum and minimum values. After 40 minutes' basketball game, the metabolic rate fell sharply to around 156W/m^2 (2.68met) in 10 minutes. The results indicate the sport intensity has a great influence on the metabolic rate.

3.3.2.3 Blood pressure

In Fig.3-8, the variation of average values in systolic blood pressure (SBP) and diastolic blood pressure (DBP) of male and female subjects is presented. During the survey, the SBP of subjects during the basketball game (the average is 124mmHg for males and 123mmHg for females) was slightly higher than that during preparation and rest, which is consistent with the trend in the metabolic rate of subjects. Besides, the DBP of subjects remained steady during the whole survey, with an average of 82mmHg and 81mmHg for males and females, respectively. Notably, the trend of blood pressure presented in this study resembles that shown in some previous research[31)~33)].

3.3.2.4 Skin temperature

As shown in fig.3-9, the average value of mean skin temperature was 37.13°C during preparation, which then declined slightly during basketball play (37.10°C for females and 37.02°C for males). The reason for the reduction lies mainly in the cooling by evaporation of sweat and the cutaneous vasoconstriction response to exercise[34)]. In the stage of rest, the mean skin temperature of subjects rose to 37.20°C and 37.30°C for females and males respectively. In terms of gender, the range of mean skin temperature for males was higher than that for females. Meanwhile, the average skin temperature of males were higher than those of females during preparation and rest, but lower during basketball play.

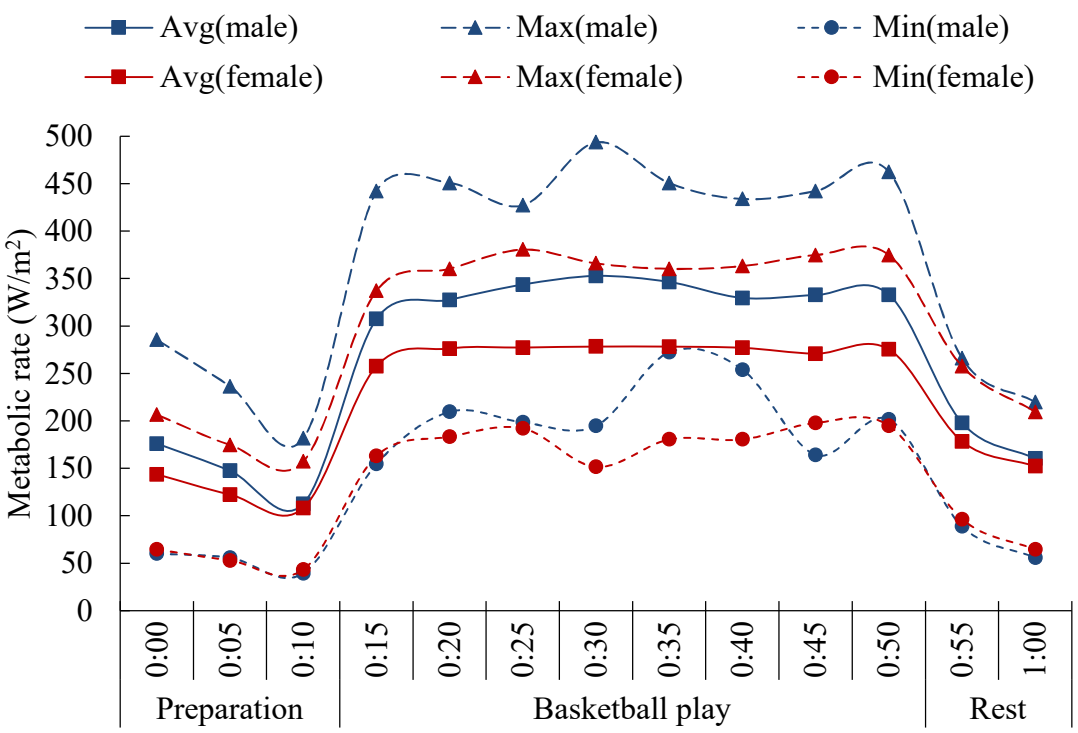

Fig.3-7 Variation in metabolic rate of subjects

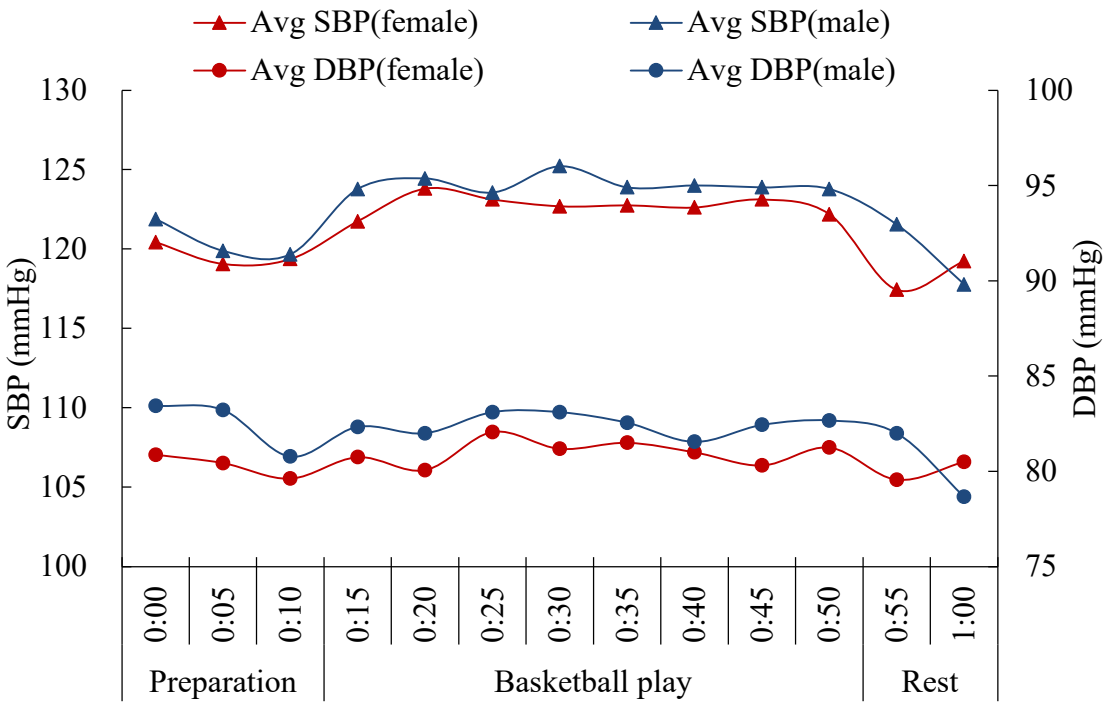

Fig.3-8 Variation in blood pressure of subjects

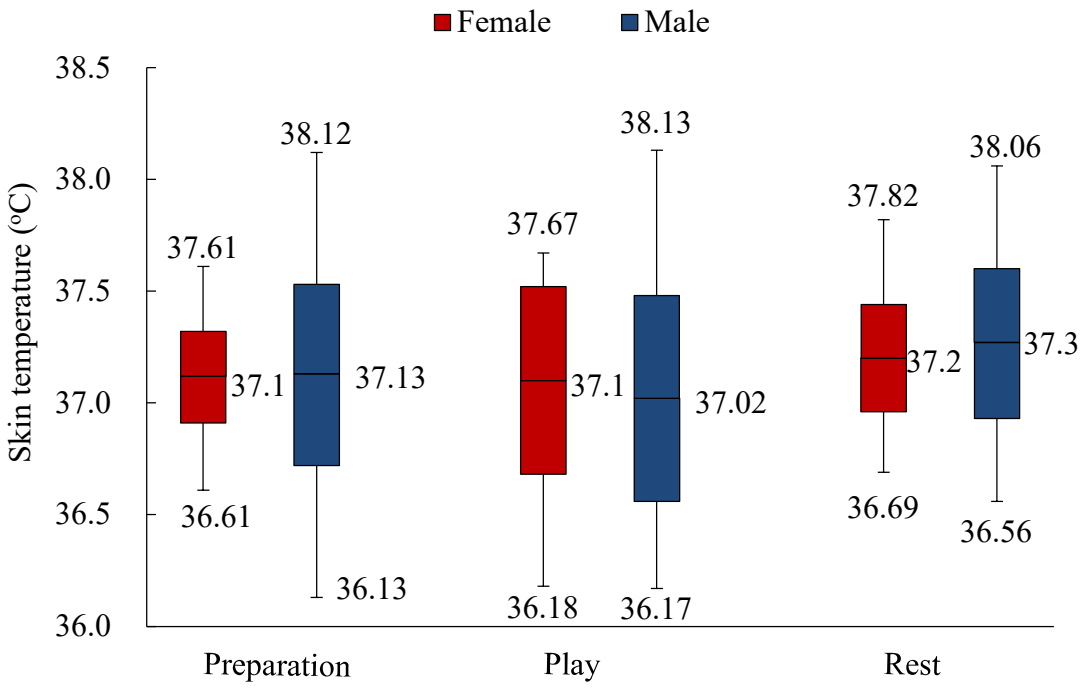

Fig.3-9 Variation of mean skin temperature of subjects

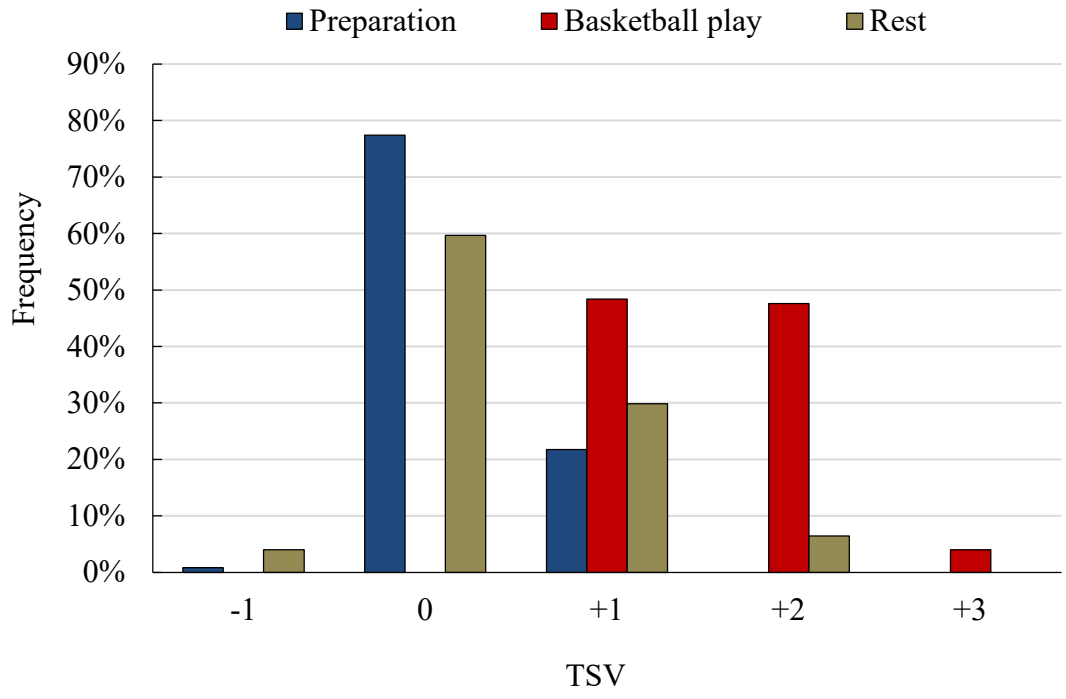

Fig. 3-10 Frequency distribution of the TSV in three survey stages

3.3.3 Thermal sensation vote (TSV)

Fig.3-10 shows the frequency distribution of the thermal sensation vote (TSV) during each stage of the survey, the scale of which is an interval. For example, 0 is $-1 < TSV \leq 0$, and +1 is $0 < TSV \leq +1$. Before the basketball play, the TSV was mainly in 0 (comfortable). During the basketball play, 48.4% of the TSV was in +1 (slightly hot) and 47.6% was in +2 (hot). The TSV was mainly in 0 (comfortable) and +1 (slightly hot) during rest. The results illustrate that the TSV during the basketball play differed widely to that during preparation and rest, mainly due to two aspects: thermal environment and human physiology. Thus, analysing the correlation between the TSV and thermal environment parameters and physiological parameters during basketball play is essential.

3.4 Discussion

3.4.1 Comparison between metabolic rate in this study and ASHRAE Standard

Compared with metabolic rates of basketball players in this study with those presented in ASHRAE Standard 55-2017, the metabolic rate in this research (152W/m^2 to 494W/m^2) has a wider range than the latter (290W/m^2 to 440W/m^2)[35]. Moreover, the metabolic rates of male and female subjects are disparate in this study (with an average of 267W/m^2 for females and 325W/m^2 for males), while it failed to be distinguished in ASHRAE Standard 55-2017. The reason for the differences mainly results from two factors: (1) The metabolic rates of activities defined in ASHRAE Standard are used for engineering purposes, which are the general met levels covering the amount of people and periods of time. (2) Although the metabolic rate can be assessed by the measurement of the heart rate, the measurement is still not accurate especially when the met level higher than 3 met (175W/m^2), and thus the values may have a certain error. In any case, these values should be properly referenced in the light of the specific research purpose.

3.4.2 Mean skin temperature during basketball activity

The mean skin temperature of players during basketball activities shows almost constant in this study. It is argued that the constant skin temperature during the sport activity is due to two opposing responses, thermoregulatory that cause a rise vasodilation and evaporative cooling that cause a fall in the skin temperature. Literature data, to the authors' knowledge, for the dynamic response of mean skin temperature of basketball player are hard to find. However, some studies similar to that have been found. Torii et al.[34] found a reduction in mean skin temperature less than 1°C due to bicycle cycling at the ambient temperature of 30°C and 40°C. Nakayama et al.[36] indicated the mean skin temperature remained unchanged during 100W pedalling of bicycle. Although the mean skin temperature remains constant during sport activities, the skin temperatures of different parts of the body would still fluctuate. The skin temperature falls at the beginning followed by a slight increase, which is the net result of the competition between the vasoconstrictor response and the vasodilator response[36)~38)]. As for the significance of fluctuation, the response is mainly influenced by the initial skin temperature related to the ambient temperature and the skin temperature of different body parts, e.g. hands, feet and the skin area of the muscles. The mean skin temperature rising after the basketball game in this study, as well as most literature data, is probably due to the reduction in the convective heat loss and the reduction in the vasoconstrictive tension caused by the sport activity to some extent, resulting in an increase of heat flow in the body.

3.5 Summary

In this chapter, a field survey on the thermal sensation under high-intensive exercise was carried out in three naturally ventilated gymnasiums in Guangzhou, China from August to October 2019. A total of 372 valid data regarding indoor thermal environments, physiological parameters and thermal sensations were collected. The main findings of this chapter are as follows:

1) The thermal environment parameters ranged from 24.97°C~35.65°C, 25.04°C~35.53°C, 23.86°C~36.84°C, 12.32g/kg' ~23.67g/kg' and 0m/s~1.64m/s in outdoor air temperature, indoor air temperature, mean radiant temperature, humidity ratio and air velocity, respectively.

2) The clothing insulations were 0.22clo and 0.22clo / 0.29clo for males and females, respectively. The metabolic rate of subjects during basketball play (the average is 334.24W/m^2 for males and 274.01W/m^2 for females) was higher than that during preperation and rest.

3) The blood pressure of subjects during the basketball game (the average is 124mmHg for males and 123mmHg for females) was slightly higher than that during preparation and rest, which is consistent with the trend in the metabolic rate of subjects.

4) The mean skin temperature was 37.13°C during preparation, then declined slightly during basketball play, which lies mainly in the cooling by evaporation of sweat and the cutaneous vasoconstriction response to exercise. Besides, the skin temperatures are different in terms of gender.

5) The thermal sensation of athletes during basketball play was highly differed to those during the preparation and rest state.

Chapter 4

Establishment of the Predicted Thermal Sensation (PTS) model

4.1 Introduction

In Chapter 3, the values of inoor thermal environemt, human physiology and thermal sensation of athletes under basketball exercise in gymnasiums in Guangzhou, China have been presented. The results indicate that the indoor thermal environment, human physiology and thermal sensation under high-intensive exercise state are quite different from those in the preparation and rest state. It is vital to develop a thermal comfort model for athletes exercising in gymnasiums in hot-humid areas. However, the current researches on this field mainly focus on the existing evaluation indices, which are limited to a certain extend. For instance, the PMV model[1)] is mainly applicable to steady-state environments; the SET model[2)] could apply to naturally ventilated building, on condition tha the human body has a low metabolic rate and the Wet Bulb Globe Temperature (WBGT) model is used for evaluating the stress extremum under the prolonged work[3)~6)]. Therefore, basing on the data of field survey in Chapter 3, this chapter aims to analyse the influences of thermal environment and human physiology on thermal sensation under exercise and to propose a predicted thermal sensation model applicable to athletes exercising in high-intensity in gymnasiums of hot-humid regions of China.

4.2 The influences of thermal parameters on the TSV

4.2.1 Relationship between indoor thermal environment and the TSV

The relationship between indoor thermal environment and the thermal sensation vote (TSV) during basketball play is shown in Fig.4-1. The varieties of air temperature, mean radiant temperature, humidity ratio and air velocity in disparate thermal sensation levels are presented in Fig.4-1(a) to Fig.4-1(d). Fig.4-1(a) to Fig.4-1(c) show that the thermal sensation levels increased with the rise in air temperature, the mean radiant temperature and the humidity ratio, indicating that the higher the air temperature, the mean radiant temperature and the humidity ratio, the hotter the body feels. Meanwhile, the trends of thermal sensaiton variation with air temperature and mean radiant temperature

were quite similar. On the contrary, the thermal sensation levels, in Fig.4-1(d), increased with the decline in the air velocity, indicating that the higher the wind speed, the colder the body feels.

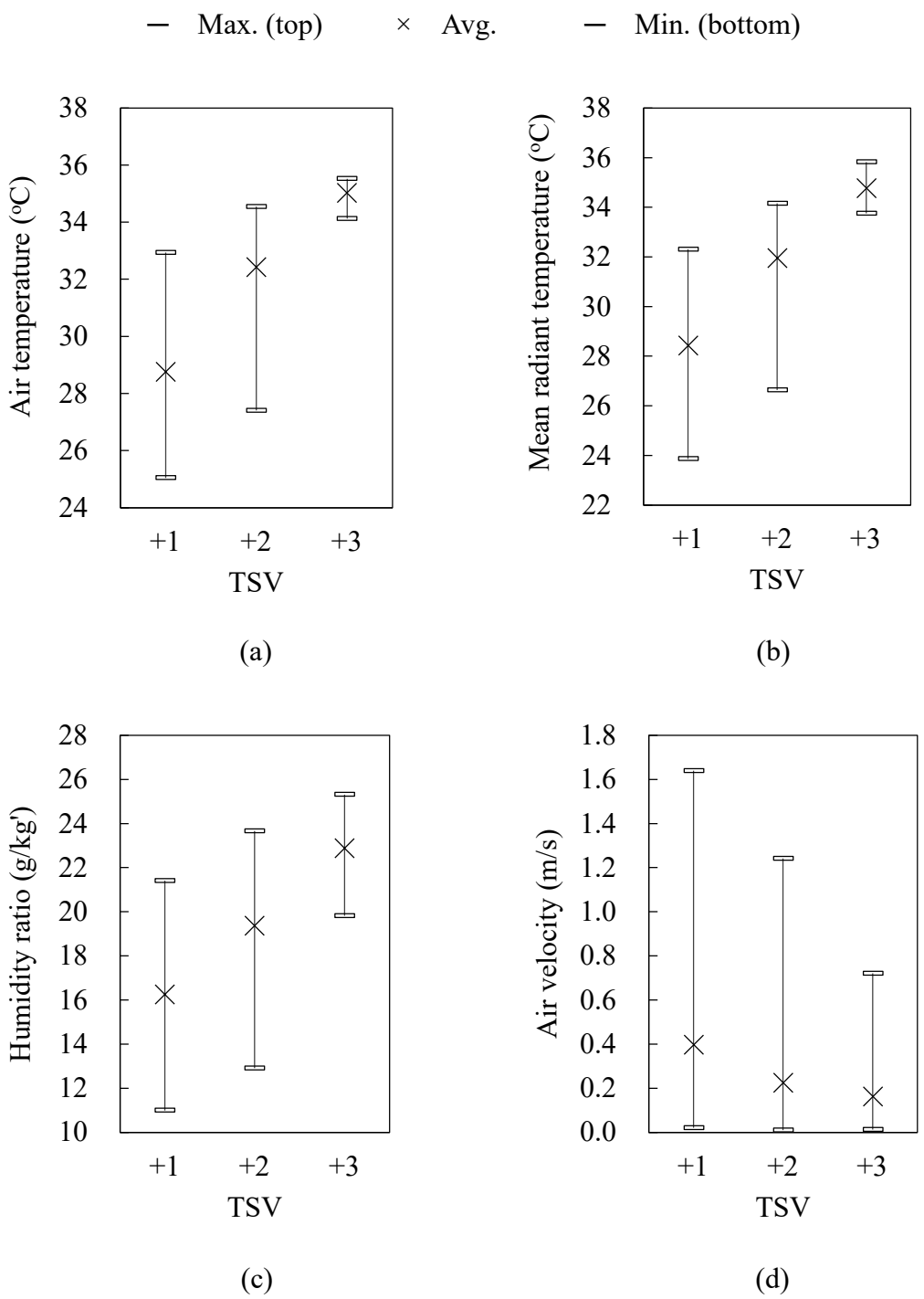

Fig.4-1 Relationship between indoor thermal environment and the TSV

4.2.2 Relationship between human physiology and the TSV

The relationship between human physiology and thermal sensation vote (TSV) during basketball play is shown in Fig.4-2.

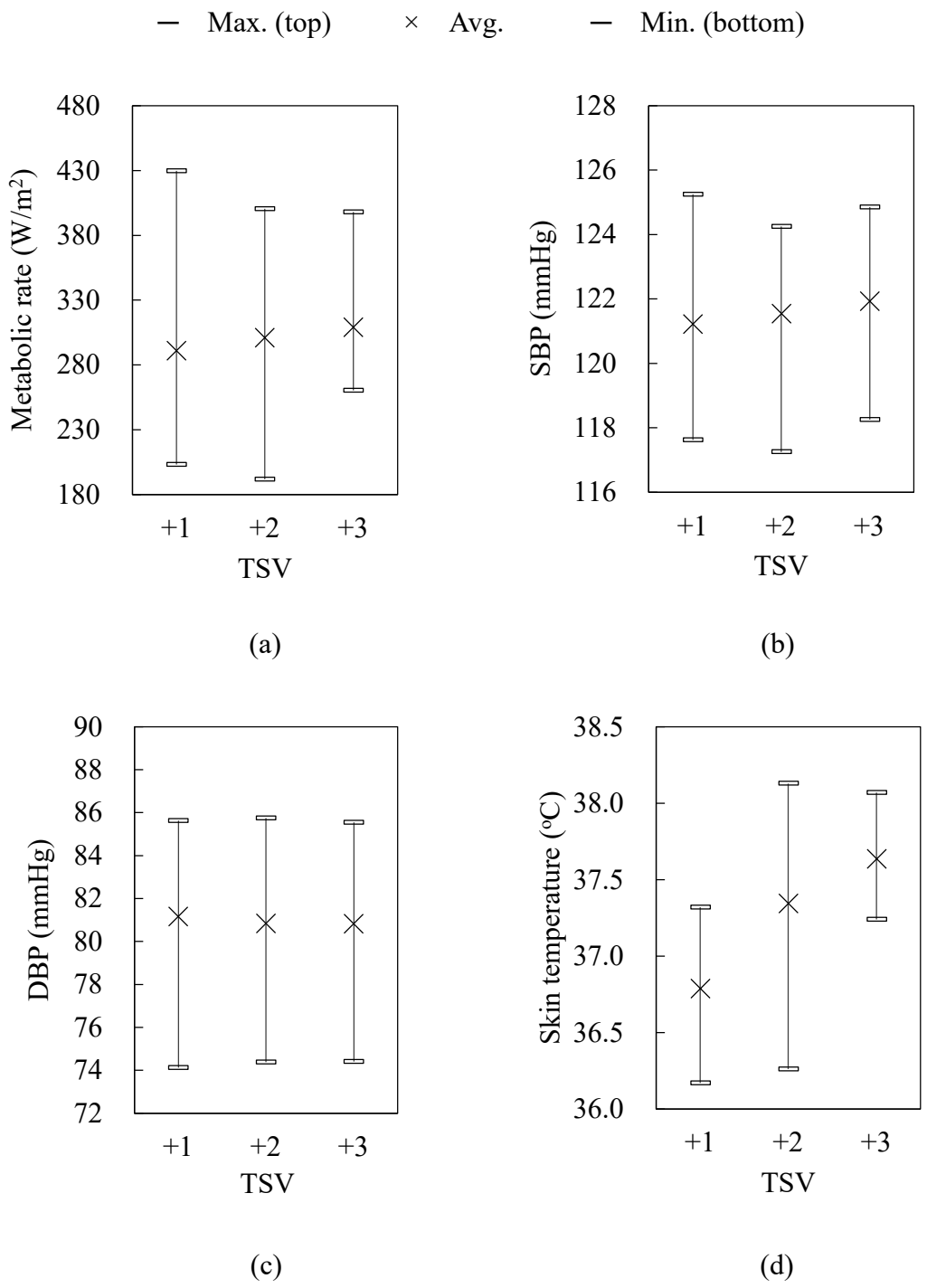

Fig.4-2 Relationship between human physiology and the TSV

Fig.4-2(a), Fig.4-2(b) and Fig.4-2(d) show that the average values of the metabolic rate, systolic blood pressure (SBP) and skin temperature were increased as the level of thermal sensation rose, indicating their positive correlations. Moreover, the increasing rates of average values in skin temperature were much higher than those in metabolic rate and SBP, illustrating the significant correlation between skin temperature and thermal sensation. Fig.4-2(c) presents that the average values of diastolic blood pressure (DBP) deseased a little as the thermal sensation rose, indicating that the variety of diastolic blood pressure (DBP) in disparate thermal sensation level is not significant.

4.2.3 Correlation among thermal environment, human physiology and the TSV

The R^2 and P values of correlations among thermal environment parameters, physiological parameters and the TSV during basketball play are summarized in Table 4-1. In total, 10 parameters including thermal sensation vote (TSV), air temperature (T_a), mean radiant temperature (T_r), humidity ratio (x), air velocity (v), clothing insulation (I_{cl}), metabolic rate (M), systolic blood pressure (SBP), diastolic blood pressure (DBP) and skin temperature (T_{sk}), from 124 samples were analysed. In these correlations, the air temperature (T_a) is highly related to the mean radiant temperature (T_r), with the R^2 value of 0.966 and P value of 0.243, indicating the close mutual effect of these two parameters. Associated with it, the TSV is correlated positively with the air temperature (T_a) and the mean radiant temperature (T_r), with the R^2 value being 0.761 and 0.742, respectively. As a physiological value formed by heat exchange between the human body and the surrounding, the skin temperature (T_{sk}) exertes an important influence in the correlation with the air temperature, the mean radiant temperature and the TSV, with the R^2 values of 0.708, 0.669 and 0.521, respectively. Furthermore, the humidity ratio (x) has a positive correlation with the air temperature and the mean radiant temperature, with the R^2 values of 0.579 and 0.570, respectively.

Table 4-1 The correlation among thermal environment parameters, physiological parameters and the TSV during basketball play

R^2 value P value	TSV	T_a	T_r	x	v	I_{cl}	M	SBP	DBP	T_{sk}
TSV		0.761 0.000	0.742 0.000	0.318 0.000	0.123 0.000	0.006 0.000	0.021 0.000	0.016 0.000	0.150 0.000	0.521 0.000
T_a	0.761 0.000		0.966 0.243	0.579 0.000	0.123 0.000	0.001 0.000	0.001 0.000	0.002 0.000	0.123 0.000	0.708 0.000
T_r	0.742 0.000	0.966 0.243		0.570 0.000	0.143 0.000	0.001 0.000	0.004 0.000	0.000 0.000	0.128 0.000	0.669 0.000
x	0.318 0.000	0.579 0.000	0.570 0.000		0.163 0.000	0.011 0.000	0.027 0.000	0.005 0.000	0.018 0.000	0.470 0.000
v	0.123 0.000	0.123 0.000	0.143 0.000	0.163 0.000		0.028 0.005	0.002 0.000	0.003 0.000	0.011 0.000	0.050 0.000
I_{cl}	0.006 0.000	0.001 0.000	0.001 0.000	0.011 0.000	0.028 0.005		0.017 0.000	0.196 0.000	0.029 0.000	0.009 0.000
M	0.021 0.000	0.001 0.000	0.004 0.000	0.027 0.000	0.002 0.000	0.017 0.000		0.051 0.000	0.028 0.000	0.004 0.000
SBP	0.016 0.000	0.002 0.000	0.000 0.000	0.005 0.000	0.003 0.000	0.196 0.000	0.051 0.000		0.053 0.000	0.002 0.000
DBP	0.150 0.000	0.123 0.000	0.128 0.000	0.018 0.000	0.011 0.000	0.029 0.000	0.028 0.000	0.053 0.000		0.243 0.000
T_{sk}	0.521 0.000	0.708 0.000	0.669 0.000	0.470 0.000	0.050 0.000	0.009 0.000	0.004 0.000	0.002 0.000	0.243 0.000	

Where the TSV is the thermal sensation vote; T_a is the air temperature in °C; T_r is the mean radiant temperature in °C; x is the humidity ratio in g/kg'; v is the air velocity in m/s; I_{cl} is the clothing insulation in clo; M is the metabolic rate in W/m^2; SBP is the systolic blood pressure in mmHg; DBP is the diastolic blood pressure in mmHg; T_{sk} is the skin temperature in °C.

4.3 The Predicted Thermal Sensation (PTS) model and validation

4.3.1 Establishment of the PTS model

From the above analysis, we know that the thermal sensation is influenced by the thermal environment and human physiology. Considering the closed relationship between the air temperature and mean radiant temperature, the operative temperature (T_{op}) could be an alternative[7]. As an indirect variable in the thermal comfort, the skin temperature is thus unnecessary to be perceived as a parameter when an estimation model is used. Therefore, a Predicted Thermal Sensation (PTS) model in relation to thermal sensation and the key factors of thermal comfort (the operative temperature, humidity ratio, air velocity, clothing insulation and metabolic rate) was developed in this study to estimate the thermal sensation of athletes in the gymnasium. The derivation process is shown below. Firstly, a multiple linear regression model is created as Equation (4-1):

$$PTS = c_0 + c_1 \cdot T_{op} + c_2 \cdot x + c_3 \cdot v + c_4 \cdot M + c_5 \cdot I_{cl} \quad (4\text{-}1)$$

where PTS is the Predicted Thermal Sensation whose values range from -3 to 3 as the TSV does; C_0 to C_5 are the partial regression coefficients; T_{op} is the operative temperature in °C; x is the humidity ratio in g/kg'; v is the air velocity in m/s; M is the metabolic rate in W/m^2; I_{cl} is the clothing insulation in clo.

Assuming that c_0 to c_5 are constants decided by the least square method in Excel[8], then the Predicted Thermal Sensation (PTS) is established, as shown in Equation (4-2):

$$PTS = -5.127 + 0.201T_{op} + 0.001x - 0.045v + 0.002M - 1.184I_{cl} \quad (4\text{-}2)$$

where PTS is the Predicted Thermal Sensation whose values range from -3 to 3 as the TSV does; T_{op} is the operative temperature in °C; x is the humidity ratio in g/kg'; v is the air velocity in m/s; M is the metabolic rate in W/m^2; I_{cl} is the clothing insulation in clo.

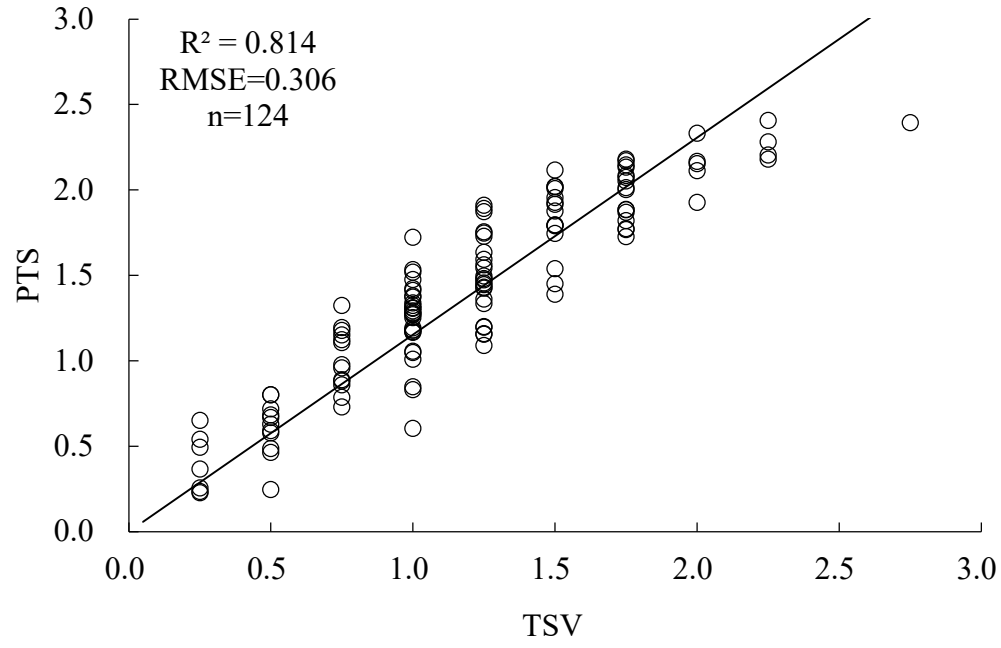

Fig.4-3 The correlation between the TSV and the PTS

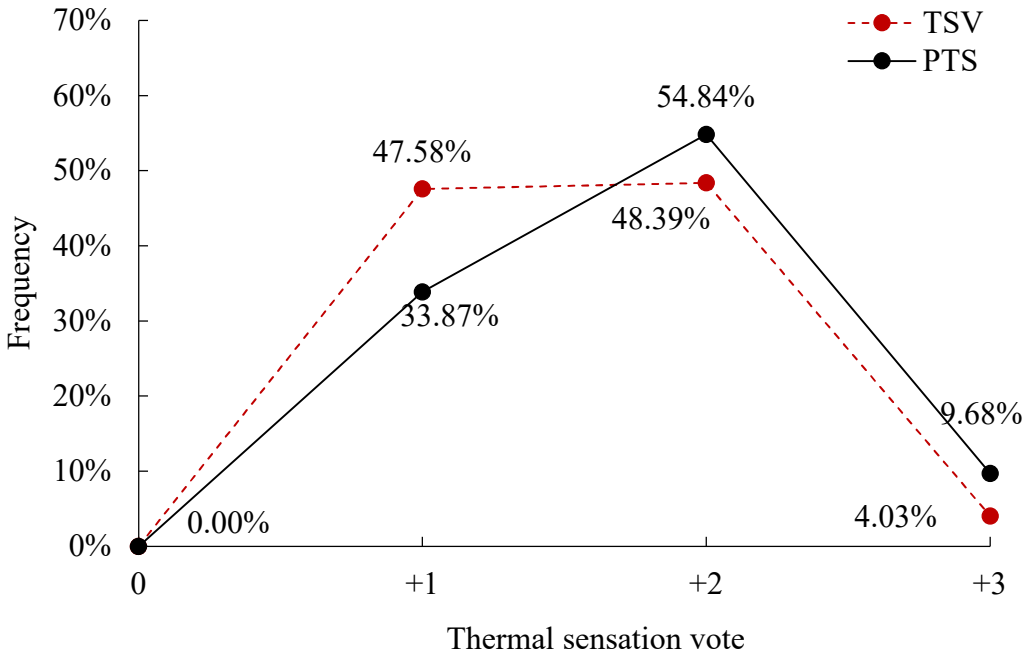

Fig.4-4 The frequency distribution of the TSV and the PTS

The correlation between PTS and the TSV is shown in Fig.4-3, with the R^2 value of 0.814 and the RMSE (Root Mean Squared Error) of 0.306. The frequency distribution of TSV and PTS values is shown in Fig.4-4. It shows that the proportion of PTS values in +2 and +3 (54.84% and 9.68%, respectively) are slightly higher than that of TSV values (48.39% and 4.03%, respectively). While the frequency of PTS values in +1 is lower than that of TSV values. Despite the small differences in proportions, the trend between TSV and PTS remains the same. Therefore, since the PTS model was based on the basketball activity in gymnasiums in Guangzhou, it could be used to estimate the thermal sensation of athletes undertaking high-intensive sport activities in the gymnasium in hot-humid regions of China.

4.3.2 Validation of the PTS model

To verify the applicability of the PTS model, a field survey was conducted using the same method in other two naturally ventilated gymnasiums in Guangzhou China, from summer to winter in 2016, with subjects partaking in basketball game with high intensity. The measured air temperature varied from 15.24°C to 36.93°C and the humidity ratio varied from 8.18g/kg' to 23.59g/kg'. The average metabolic rate of subjects was 304.13W/m^2 (5.23met), the clothing insulations were 0.22clo to 0.29clo and the TSV was between -1.67 and +2.

Fig.4-5 illustrates the correlation between the measured TSV and the PTS calculated by Equation (4) for validation. The R^2 value is 0.804 and the RMSE is 0.534. Although the frequencies between TSV and PTS, as shown in Fig.4-6, are different at each scale point, they do not affect the consistency of the tendencies. Therefore, to some extent, it signifies the reasonable validation of the PTS model. As the data in winter have been taken into consideration, we can conclude that the PTS model developed by this study is valid for the precise evaluation of the thermal sensation under high-intensive sport activities in gymnasiums for the whole year in the future.

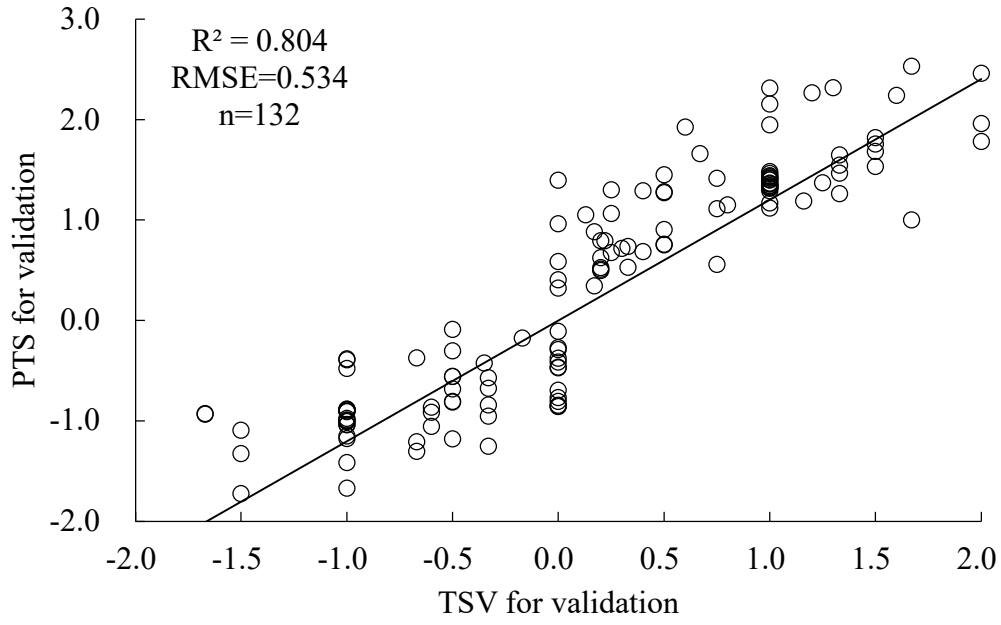

Fig.4-5 The correlation between the TSV and the PTS for validation

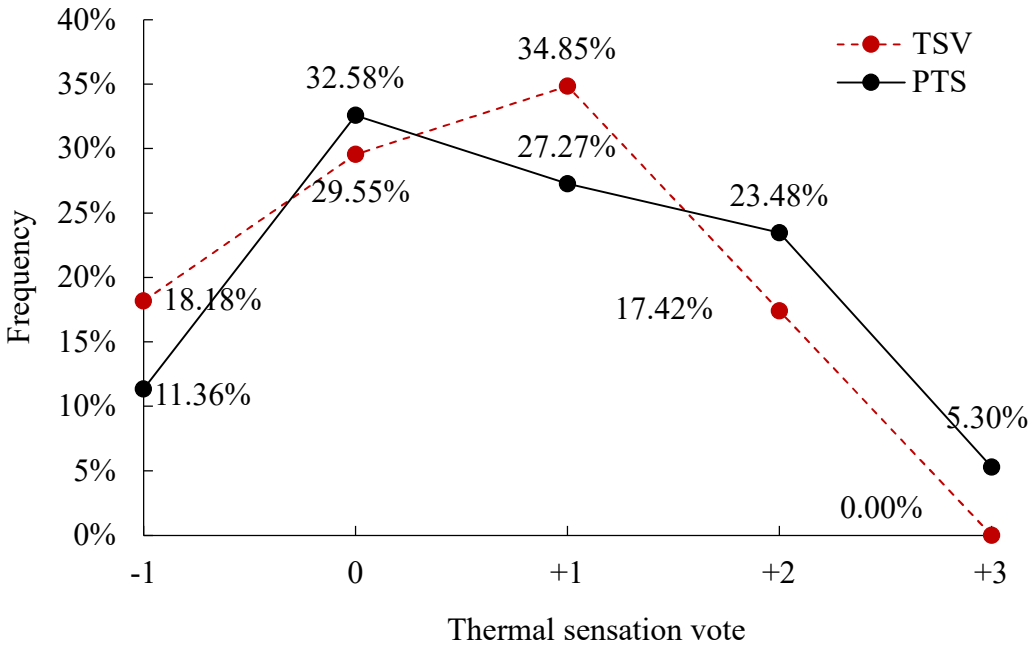

Fig.4-6 The frequency distribution of the TSV and the PTS for validation

4.4 Discussion

4.4.1 The PTS model versus other evaluation models

Currently, an abundance of indices is available for thermal comfort evaluation. In terms of the purpose, some indices are to avoid excess by setting exposure limits, such as WBGT, TSI and HIS[9)~11)]; some define comfort by drawing up the comfort zones, e.g. PMV, SET, T_{op} and EqT[1),2),7),12)]. In this section, the indices of T_{op}, SET and WBGT, which are widely used and could be applied to the natural ventilated environment, and these are chosen to compare with the PTS model developed in this study.

Table 4-2 and Fig.4-7 show the correlation between these models and the TSV. Although T_{op}, SET and WBGT are related positively to the TSV, the R^2 values (0.761, 0.687 and 0.627, respectively) are not as good as the R^2 value in the PTS model (0.814). While the SET model could be used in the natural ventilated environment, intensive sport activity would confine the model's accuracy on account of the two-node model it based. With the focus on environmental factors other than physiological parameters, WBGT and T_{op} indices are limited to the application under different intensive sport activities. In general, the current evaluation models are widely used but have poor precision. To some extent, the PTS model could provide a reference for predicting the thermal comfort of athletes under the high-intensive exercise in naturally ventilated gymnasiums in the hot-humid environment.

Table 4-2 The comparison among the PTS, T_{op}, SET and WBGT

Model	Equation	R^2	RMSE
PTS	y = 1.154x	0.814	0.306
T_{op}	y = 4.477 x + 25.309	0.761	5.531
SET	y = 4.764 x + 26.402	0.687	5.659
WBGT	y = 3.882 x + 22.013	0.627	5.157

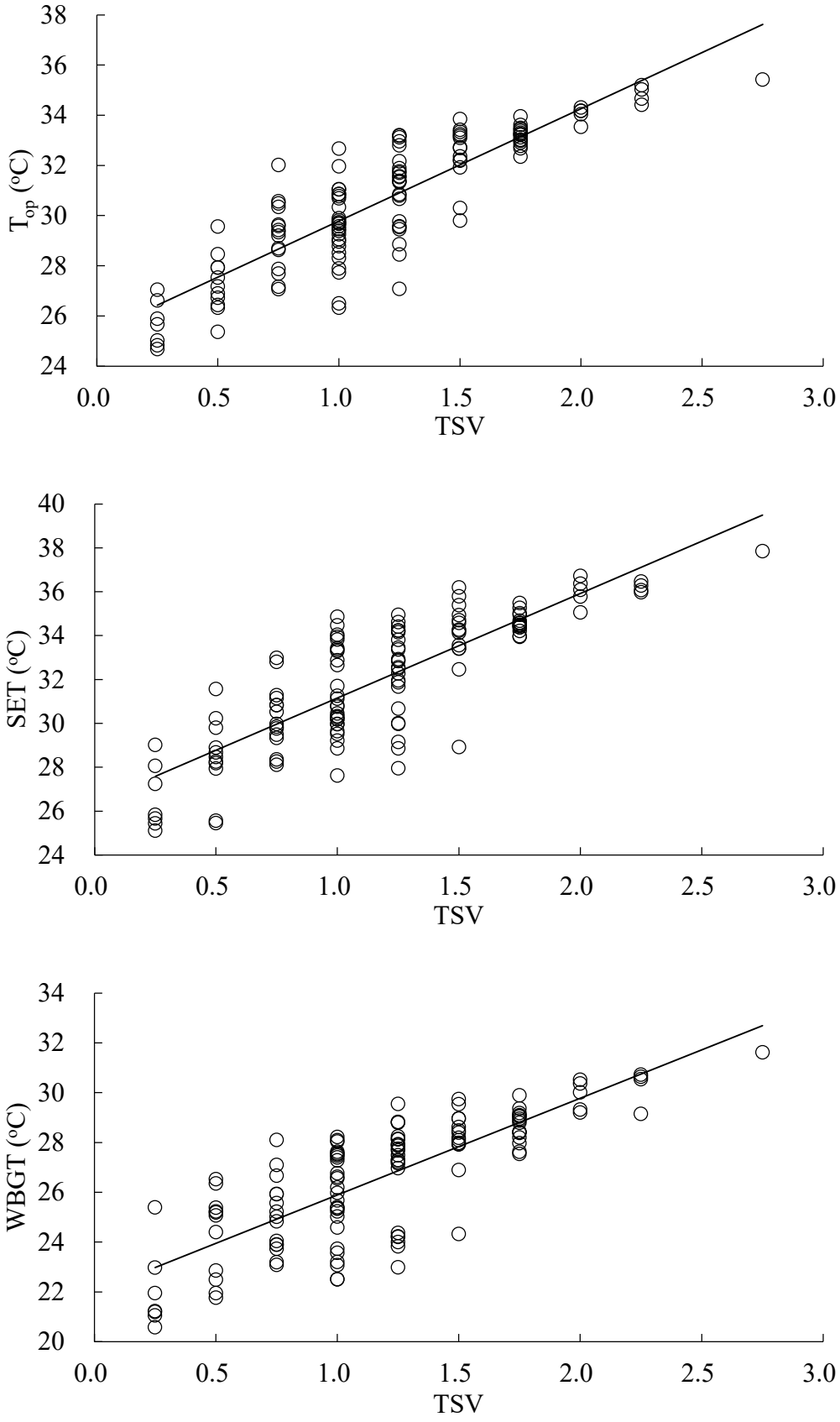

Fig.4-7 The correlation between current models and the TSV

4.4.2 Importance of thermal parameters in the PTS model

In the PTS model, six thermal parameters, the operative temperature (T_{op}), humidity ratio (x), air velocity (v), metabolic rate (M) and clothing insulation (I_{cl}) have been presented. Throught the method of standardization in Excel, the PTS model has been standardized in Equation (4-3):

$$PTS = 0.866T_{op} + 0.047x - 0.020v + 0.183M + 0.008I_{cl} \quad (4\text{-}3)$$

where PTS is the Predicted Thermal Sensation; T_{op} is the operative temperature in °C; x is the humidity ratio in g/kg'; v is the air velocity in m/s; M is the metabolic rate in W/m^2; I_{cl} is the clothing insulation in clo.

In this formula, the coefficient value of each thermal parameter represents the importance of this parameter. By calculating the proportions of these coefficients, it can be obtained that the operative temperature accounts for 76.9%, the metabolic rate accounts for 16.3%, the humidity ratio accounts for 4.2%, the air velocity accounts for 1.8% and the clothing insulation accounts for 0.8%. Therefore, among the thermal parameters, the operative temperature has the greatest influence on the PTS model, followed by the metabolic rate, humidity ratio and air velocity. The least impact on the PTS model is the clothing insluation. It can also be inferred that the best way to improve the PTS is to adjust the operative temperature.

4.4.3 Application of the PTS model

According to the present study, the thermal response of a subject during high-intensive sport activity is significantly different to the response when undertaking low to moderate intensive sport activity. The findings in this study indicate that the architects should take into consideration the thermal sensation of athletes so as to design the buildings rationally. Instead of the existing integrated thermal comfort models, which are used for estimating thermal comfort of occupants in low metabolic rate, the PTS model

developed in this study provides the architects with a new method to assess the indoor environment and thermal comfort.

In the future design of gymnasiums in related climate regions, the optimum ranges of thermal environment, e.g. air temperature, relative humidity and air velocity, can be decided based on the comfort zone estimated by the PTS model (-1 < PTS < 1) under natural ventilation, which would bring a comfortable environment to people who partake in sports in the sport ground. In addition, the design parameters of active equipment such as air conditioners can be referenced according to the limits of the comfort zone when the competition is to be held in gymnasium. Compared with the Chinese standard for sports building design[13)], the thermal parameters corresponding to the PTS comfort range are higher than those prescribed in the Chinese standard, illustrating more energy saving and better comfort efficiency. The reason for the difference lies in the fact that the audiences who are at low metabolic rate have been taken into account in the Chinese standard, and the types and regions of gymnasiums are relatively broad. The PTS model is specifically adopted for athletes and hot-humid regions and is more accurate and targeted to a certain extent. As a result, based on the PTS model, passive and active devices could work better for regulating the indoor environment, enhancing the thermal comfort of occupants and saving energy in gymnasiums.

4.5 Summary

In this chapter, the influences of thermal environment and human physiology on thermal sensation under exercise state have been analyzed. In addition, accroding to the data of field survey in Chapter 3, the Predicted Thermal Sensation (PTS) model has been developed, which is applicable to estimate the thermal comfort under high-intensive sport activity in gymnasiums in hot-humid regions of China. The main findings are shown below:

1) The TSV rose with the rise in the air temperature, mean radiant temperature and humidity ratio, while decreases with an increase in air velocity.

2) When considering the physiological parameters, the average values of the metabolic rate, systolic blood pressure and skin temperature are positively correlated with the TSV.

3) The PTS model, as shown in Equation (4-2), was developed based on the field survey. Furthermore, the rationality and accuracy of this model have been validated. This model can provide a theoretical reference for the study of thermal comfort under high-intensive sport activities in gymnasiums in hot-humid regions of China.

Chapter 5

Optimization of gymnasium form for thermal comfort at hot-humid climate by orthogonal experiment

5.1 Introduction

As a public space for sports, exercises and entertainments, gymnasiums play an important role in people's daily life. In the subtropical areas, the thermal comfort of occupants exercising in gymnasiums is related to the utilization rate of gymnasiums, energy consumption and human health. In hot and humid climate, occupants prefer to pursuit thermal comfort by air conditioners when doing sports. However, although the air conditioners provide comfortable environment for occupants directly, this would increase energy consumption and carbon dioxide emissions. Moreover, human adaptive ability to the natural environment would be weaken, as well as their health, while exercising in such places for a long time[1)]. Therefore, the study on the thermal comfort in naturally ventilated gymnasium at hot and humid climate has been significantly regarded nowadays[2)].

People could achieve thermal comfort mainly from two aspects by two methods: One is individual adjustment, such as the activity level, clothing and psychological expectation[3)~4)]; the other is thermal environment regulating, such as the indoor air temperature, relative humidity and air velocity[5)~6)]. Although occupants could adjust themselves on achieving thermal comfort, the regulating on thermal environment could be more effective and comprehensive[7)]. Furthermore, in the aspect of architectural design, improving the thermal environment by adjusting the architectural forms is one of the most effective methods to achieve thermal comfort.

In the research of the correlation between the architectural form and the thermal comfort, Barbosa[8)] estimated the thermal acceptance levels in naturally ventilated office buildings with double skin façade (DSF) in Brazilian with various climates and underlined the complexity of the DSF technology application to buildings. Yang et al.[9)] investigated the adaptive thermal comfort and climate responsive strategies in dry-hot and dry-cold areas in China and found that the architecture with a semi-basement could satisfy the thermal comfort efficiently, followed by night ventilation in summer. Li[10)] simulated the wind

pressure in a gymnasium in hot and humid area in China to analyze the influences of interface form on natural ventilation and found that the form of asymmetric interface could improve the ventilation capacity. Huang et al.[11] analyzed the top and side interface forms of gymnasiums in Guangzhou, China and found that the double skin roof and openable side interface could enhance the human thermal comfort. Although the researches correlated between the architectural form and the thermal comfort can be found, most of them are focused on dwelling, school and office buildings[12)~14)], rare focused on the gymnasium building which played a distinctive role on thermal comfort for the features of large space, specific function and certain group of people. In addition, few researches study multi-factor by orthogonal experiment method, most of them, however, focus on single influential factor of building form, rarely conduct comprehensive and integrated analysis on multi-factor, which has a more practical and meaningful for the research of thermal comfort.

This study aims to improve the indoor thermal comfort of naturally ventilated gymnasiums at hot and humid climate through comprehensive architectural form optimization. Basing on the field investigation in 15 gymnasiums in Guangzhou China, which is a typical city in subtropical region with hot and humid climate[15)], an initial model of gymnasium was established to analyze the indoor thermal comfort and explore the optimizing orientation. An orthogonal experiment with variety of factors and levels chosen by analyzing the field investigation was then conducted and simulated with the FlowDesigner software. Based on the simulation results, the significant factors of architectural form on thermal comfort were identified. Furthermore, the optimal combination of architectural forms of gymnasium was suggested to provide reference for the gymnasiums design at hot and humid climate.

5.2 Methodology

In order to analyze the thermal comfort with multiple factors and the optimization of architectural form in gymnasiums, a hybrid method that combines the orthogonal

experiment and computer simulation is conducted in this study shown in Fig.5-1.

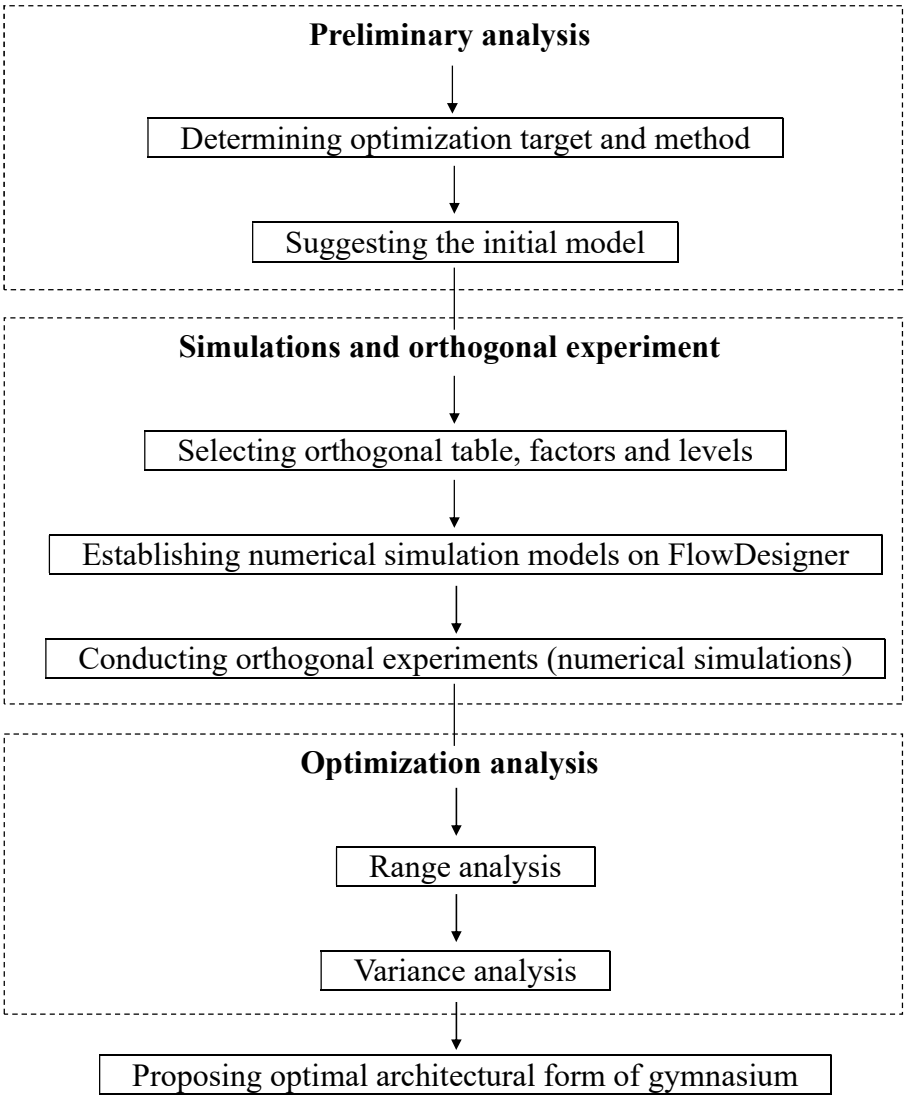

Fig.5-1 Flow chart of the hybrid method for simulation and optimization

5.2.1 Simulation tool and its validation

The first step aims to consider a suitable tool for thermal environment simulation. In order to achieve accurate calculation, simulation tools have been developed by researchers and engineers, such as Ecotect, TRNSYS, PHOENICS, Fluent, FlowDesigner. Considering the dynamic thermal environment, e.g. air temperature, relative humidity, air velocity, and the thermal comfort are the main factors in this study, FlowDesigner, a common commercial thermal environment dynamic simulation

software, which is friendly used and verified in many studied[16)~18)], is used in this study for the thermal and fluid simulations of gymnasiums.

In order to verify the accuracy of the results from the FlowDesigner, the thermal environment between simulation and that from field measurements are compared in Fig.5-2. The field measurement was conducted in a gymnasium in Guangzhou, China, between 28th July and 10th August 2016. The values of the indoor air temperature, indoor relative humidity and indoor air velocity were measured in the competition field of gymnasium at 30-min interval, from 9:00 to 18:00. The gymnasium was simulated using the FlowDesigner with the weather data for the simulation is obtained from The United States National Climatic Data Center[19)], which provides global historical weather and climate data from observations.

Fig.5-2 shows the variations of indoor air temperature, relative humidity and air velocity in measurement and simulation. The variation tendencies of air temperature in measurement and simulation, as shown in Fig.5-2(a), are consistent with each other, as well as the tendency of relative humidity, as shown in Fig.5-2(b). While the variation of air velocity between measurement and simulation are less consistent due to the modeling errors and complex wind environment, as shown in Fig.5-2(c), the average values of measurement and simulation are 0.31m/s and 0.43m/s respectively, as shown in Fig.5-2(d), which shows little difference. Therefore, the software of FlowDesigner is feasible for simulation in this study.

5.2.2 Selection of thermal comfort model

Since the thermal comfort is the main issue discussed in this study, a thermal comfort model would be selected. The thermal comfort models such as PMV, SET, WBGT are widely used around the world, however, none of them is proper to evaluate the thermal comfort for moving subjects such as athletes[5),6),20)]. For example, PMV is limited to the steady state environment, SET could be applied in the naturally ventilated environment,

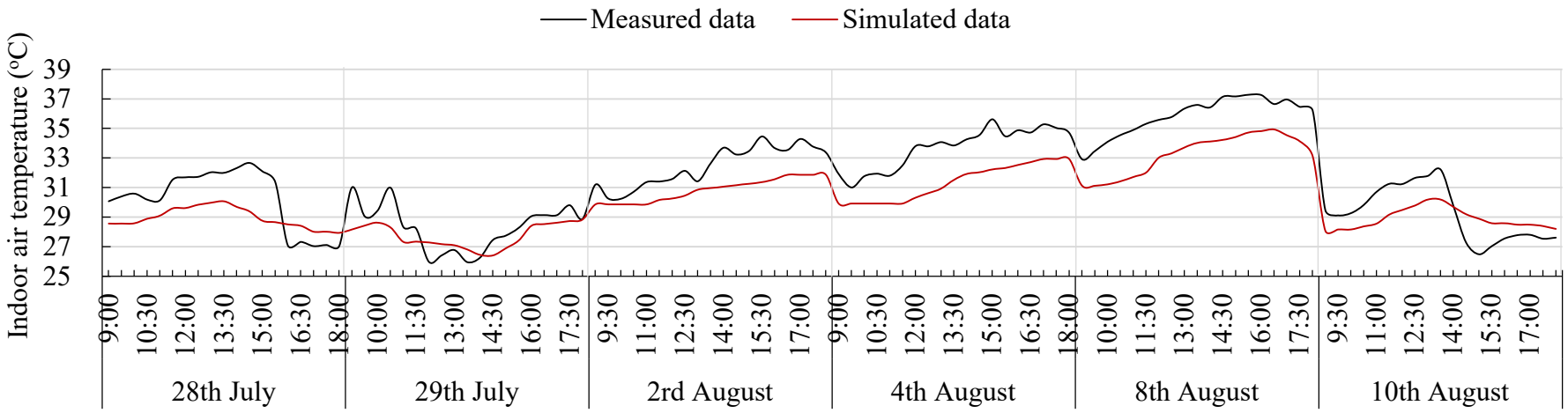

(a) Variation of indoor air temperature

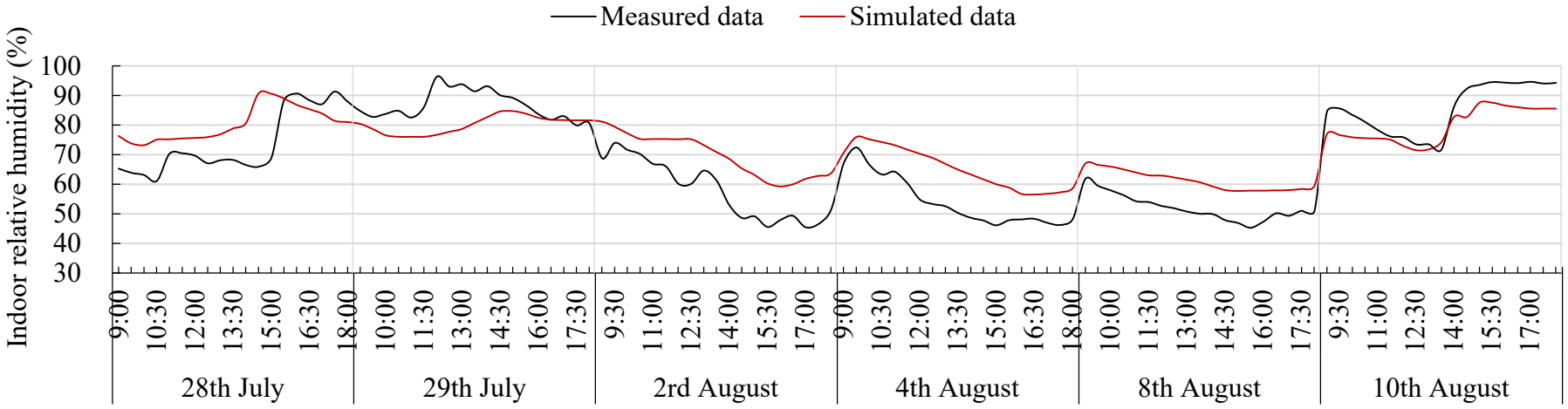

(b) Variation of indoor relative humidity

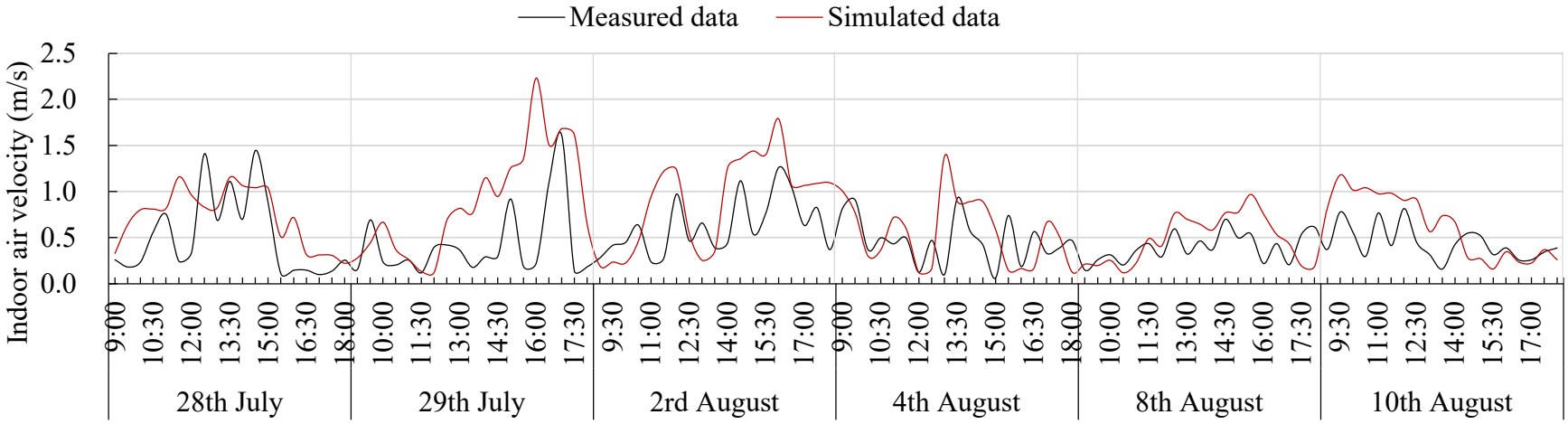

(c) Variation of indoor air velocity

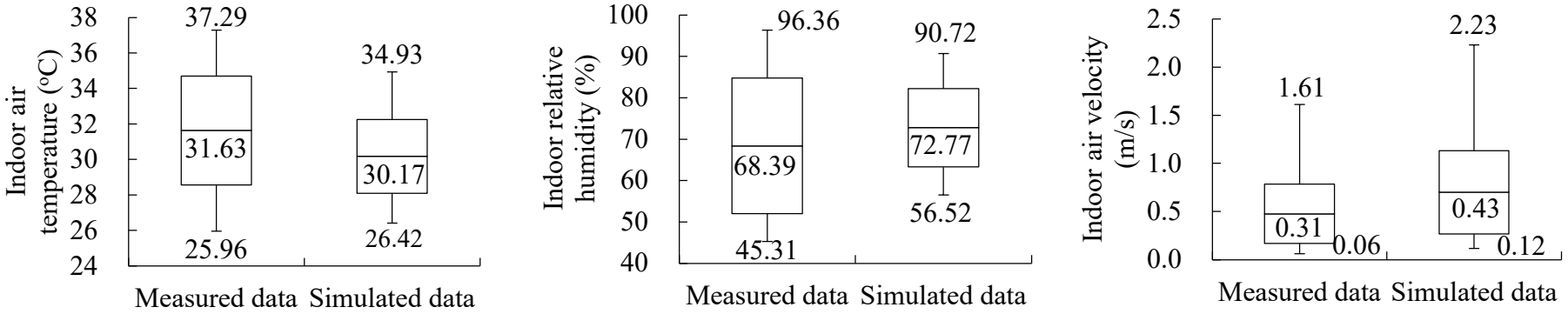

(d) Variation of indoor air velocity

Fig.5-2 Comparison of the thermal environment variations between measurement and simulation

however, it could only be used for the people in low metabolic rate. Due to the research object in this study is the thermal comfort in the state of exercise in naturally ventilated gymnasiums, the Predicted Thermal Sensation (PTS) model proposed in Chapter 4, which is available for accurately estimating the thermal sensation under high-intensive exercise in gymnasiums of hot-humid regions of China, has been chosen. The PTS model is formulated in Equation (4-2) and the scale is shown in Table 5-1.

$$\mathrm{PTS} = -5.127 + 0.201\mathrm{T_{op}} + 0.001\mathrm{x} - 0.045\mathrm{v} + 0.002\mathrm{M} - 1.184\mathrm{I_{cl}} \quad (4\text{-}2)$$

where PTS is the Predicted Thermal Sensation; T_{op} is the operative temperature in °C; x is the humidity ratio in g/kg'; v is the air velocity in m/s; M is the metabolic rate in W/m^2; I_{cl} is the clothing insulation in clo.

Table 5-1 Scale of PTS model

-3	-2	-1	0	+1	+2	+3
Extremely cold	Cold	Slightly cold	Comfortable	Slightly hot	Hot	Extremely hot

5.2.3 Principles of orthogonal experiment

Orthogonal experiment is a systematic and statistical method for achieving the optimization of multiple factors with different levels of values[21]. These standard arrays provide the way of conducting the minimal number of experiments which could give the full information of all the factors that affect the performance parameter. The orthogonal table is the foundation of the orthogonal experiment, as shown in Equation (5-1).

$$\mathrm{L_n(m^k)} \quad (5\text{-}1)$$

Where L is the symbol of the orthogonal table; n is the number of trials arranged in the orthogonal experiment; m is the number of levels; k is the number of factors.

5.2.3.3 Range analysis

As the appropriate analysis methods for the orthogonal experiment, two method are introduced, range analysis and variance analysis. Range analysis aims to detect the levels of different influential factors on indices, as shown in Equation (5-2). In this analysis, the larger value of R_j, the greater importance of the factor.

$$R_j = \max(k_{ji}) - \min(k_{ji}) \quad (5\text{-}2)$$

Where R_j is the range of values between the maximum and minimum values of k_{ji}. k_{ji} is the average value of the sum of the experimental results at all levels (i,i=1,2,3) of each factor (j, j=A, B, C, D, E, F).

5.2.3.4 Variance analysis

For further analysis, the variance analysis can be used to determine the influences from experimental conditions, errors and the significant of factors. In the variance analysis, the sum of the squared deviation (SS), the degree of freedom (df) and the variance of the factor or error (V) are expressed as Equation (5-3) and (5-4). The F value is compared to a critical value of a significant level, which is normally set at 0.05. The impact of the selected factor on the test results is considered to be significant if it is greater than the critical value, and vice versa.

$$SS = \sum_{k=1}^{n}(W_k - w) \quad (5\text{-}3)$$

$$V = SS/df \quad (5\text{-}4)$$

Where SS is the sum of the squared deviation; W_k is the results of each trial (k,k=1,2,3, ….., n); w is the arithmetic average of W_k; df is the degree of freedom; V is the variance of the factor.

5.2.4 Statistical analysis

In this study, the research process begins with the orthogonal experimental design, then conducts the simulation of the trails in orthogonal experiments, finally analyzes the optimization result in the aspect of thermal comfort. As the simulation in FlowDesigner only outputs the values of air temperature, surface temperature, relative humidity and air velocity, a further calculation should be conducted to obtain the PTS value.

The PTS equation, as shown in Equation (4-2), contains five parameters: operative temperature (T_{op}), humidity ratio (x), air velocity (v), metabolic rate (M) and clothing insulation (I_{cl}). The operative temperature (T_{op}) can be calculated as Equation (5-5) and the mean radiant temperature is calculated as Equation (5-6)[22]. The humidity ratio (x) is calculated by the relative humidity (φ), as shown in Equation (5-7). The metabolic rate is calculated by the formula of heart rate following the ISO8996[23]. Since the exercising state in gymnasium is the premise of the study, the average value of 300W/m^2 collected from the previous field survey is applied in this paper. The clothing insulation, calculated from ASHRAE Standard 55-2017[5], is 0.22clo for the subjects exercising in gymnasium at hot and humid climate.

$$T_{op} = AT_a + (1 - A)T_r \tag{5-5}$$

$$T_r = \sum_{N=1}^{n}(T_N F_{P-N}) \tag{5-6}$$

$$x = 0.622\frac{\varphi f_s}{P - \varphi f_s} \tag{5-7}$$

Where T_{op} is the operative temperature in °C; A is a coefficient as a function of the average air velocity[5]; T_a is the air temperature in °C; T_r is the mean radiant temperature in °C; T_N is the surface temperature of surface (N) in °C; F_{P-N} is the angle factor between a person (p) and surface (N); x is humidity ratio in g/kg'; φ is relative humidity in %; f_s is saturated water vapor pressure in Pa; P is atmospheric pressure in Pa.

5.3 The initial model of gymnasium in hot-humid region of China

5.3.1 The conditions of gymnasium in Guangzhou City

The basic for optimizing the gymnasium form is first to realize the conditons of gymnasiums exhaustively. To obtain the architectural parameters of gymnasiums, investigation was carried out around 15 naturally ventilated gymnasiums in Guangzhou. The investigation includes the building size, audience capacity, auditorium layout, building material and the characteristics of the architectural forms. Table 5-2 gives the building conditions of investigated gymnasiums, presenting that the gymnasium sizes are medium in major with around 3000~6000 seats and two-sided auditorium. Most of the gymnasiums are built by the material of reinforced concrete. In terms of the window position, most of the windows in investigated gymnasiums are at the height of the walls. As the window-to-wall ratio (WWR) stipulating less than 0.7 in public buildings according to the relevant regulations of China[24)], the WWR in most investigated gymnasiums achieve this standard and 10 of them even less than 0.3. In the aspect of roof slope, 8 gymnasiums are horizontal roofs and 7 are slope roofs. Since the shading is important in southern China, overhanging eaves are built in most of the gymnasiums with different depths.

5.3.2 Plan layout of the initial model

Abstracting the main parameters from the investigated gymnasiums in Guangzhou, an initial model of gymnasium is built up and the plan layout are shown in Fig.5-3. The gymnasium model is settled in medium size with a total area of 3150m^2. There are two sides auditorium in it, with 3688 seats. The building material is reinforced concrete and the external walls are 0.3m in thickness. Windows are built on the high position of the south wall and north wall. Although the WWR of the investigated gymnasiums are around 0.3, the openable and transparent windows are few. Thus, the WWR of initial model is set in 0.1 as the windows are all openable and transparent. In addition, the roof of initial model is horizontal, while the depth of overhanging eave is 1 meter.

Table 5-2 The conditions of naturally ventilated gymnasium in Guangzhou City

Parameter	Situation	Percentage
Size	Medium	8/15
	Small	7/15
Audience capacity (seat)	3000~6000	8/15
	≤3000	7/15
Auditorium layout (side)	≤2	9/15
	>2	6/15
Building material	Reinforced concrete	14/15
	steel	1/15
Building height (meter)	≤15	10/15
	>15	5/15
Main window position	Height of the walls	8/15
	Bottom of the walls	2/15
	Both height and bottom of the walls	2/15
	On the roof	3/15
window-to-wall ratio (WWR)	≤0.3	10/15
	0.3~0.7	5/15
Roof slope	Horizontal roof	8/15
	Single slope	3/15
	Multi-slope	4/15
Overhanging eave	Without overhanging eave	2/15
	With overhanging eave	13/15

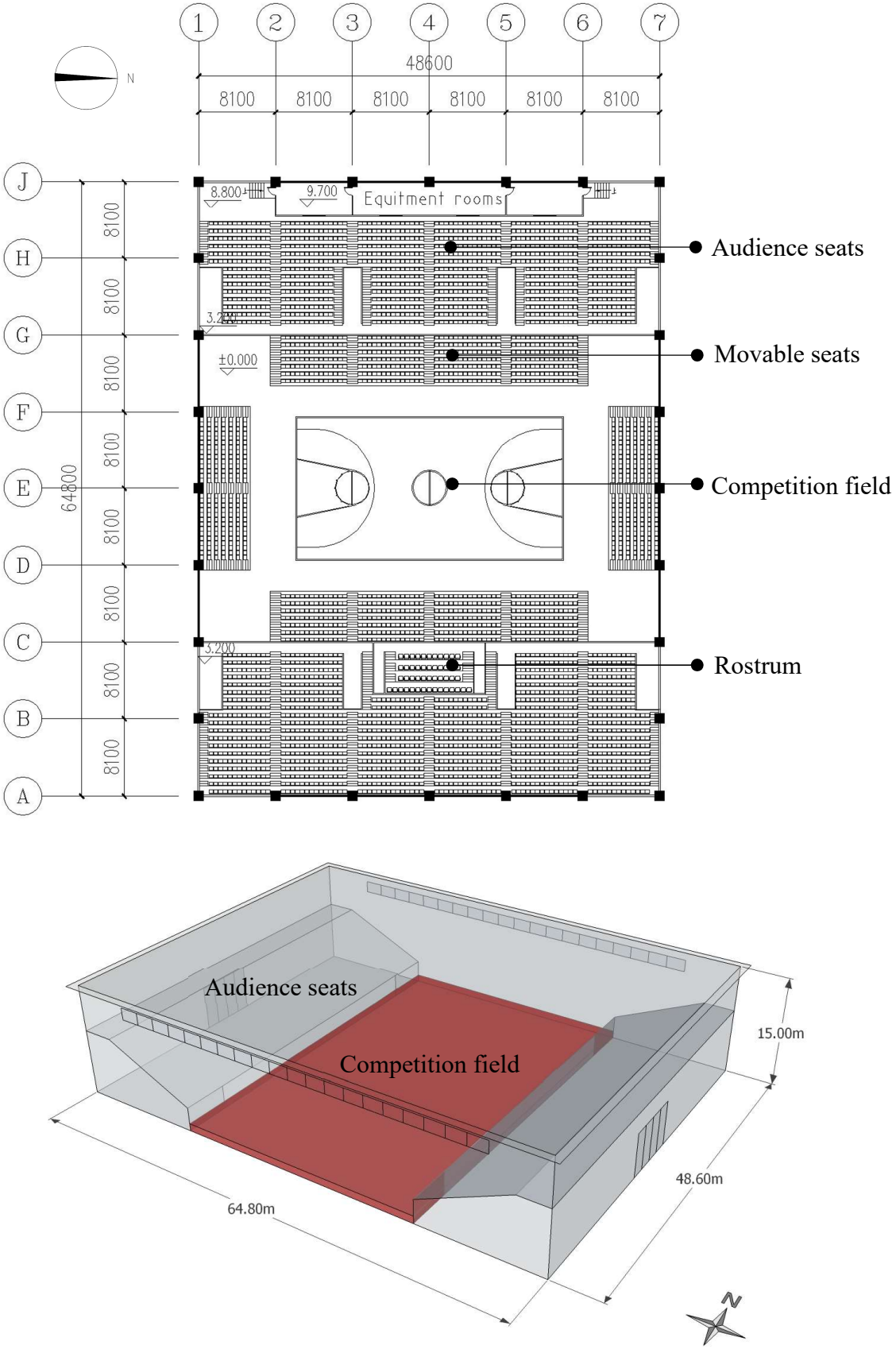

Fig.5-3 Plan layout of the initial gymnasium model

5.3.3 Simulation of the initial model

The FlowDesigner is used to simulate the thermal parameters of the initial model over a month (August) period on an hourly basis. The weather data for simulation is obtained from the Energy Plus[25]. As the gymnasium is a place for sport, the simulation zone of initial model is the competition field, rather than the audience area. The simulated and calculated results of operative temperature, humidity ratio, air velocity and the PTS values are shown in Fig.5-4. The settings in initial model simulation are used for further simulations of optimization.

Fig.5-4 presents that the indoor operative temperature of initial model ranges from 27.02ºC to 32.27ºC in August, with an average value of 29.29ºC and the humidity ratio changes from 19.08g/kg' to 21.16g/kg', with an average value of 20.16g/kg', which is consistent with the features of the hot-humid climate. In addition, the average air velocity is 0.21m/s, meeting the requirement of wind speed for sports. In the aspect of PTS value, the average PTS is 1.11, which represents "slightly hot" in thermal sensation. Furthermore, the maximum value reaches 1.71, which close to "hot" in thermal sensation, indicating that the indoor thermal comfort of initial model is not effective, and the measures should be taken to improve the thermal comfort in summer days.

5.4 Parameter analyses and optimization

In order to propose an optimal strategy of architectural form for indoor thermal comfort of gymnasiums, the factors and corresponding levels of architectural form that affecting thermal comfort of gymnasium are selected based on the initial model in this section. Later, the simulations are conducted in FlowDesigner followed by the trails generated from the orthogonal experimental design. After obtains the thermal environment data from simulations, the PTS values can be calculated. Through the range analysis and variance analysis of PTS values, the optimized architectural form of gymnasium is suggested.

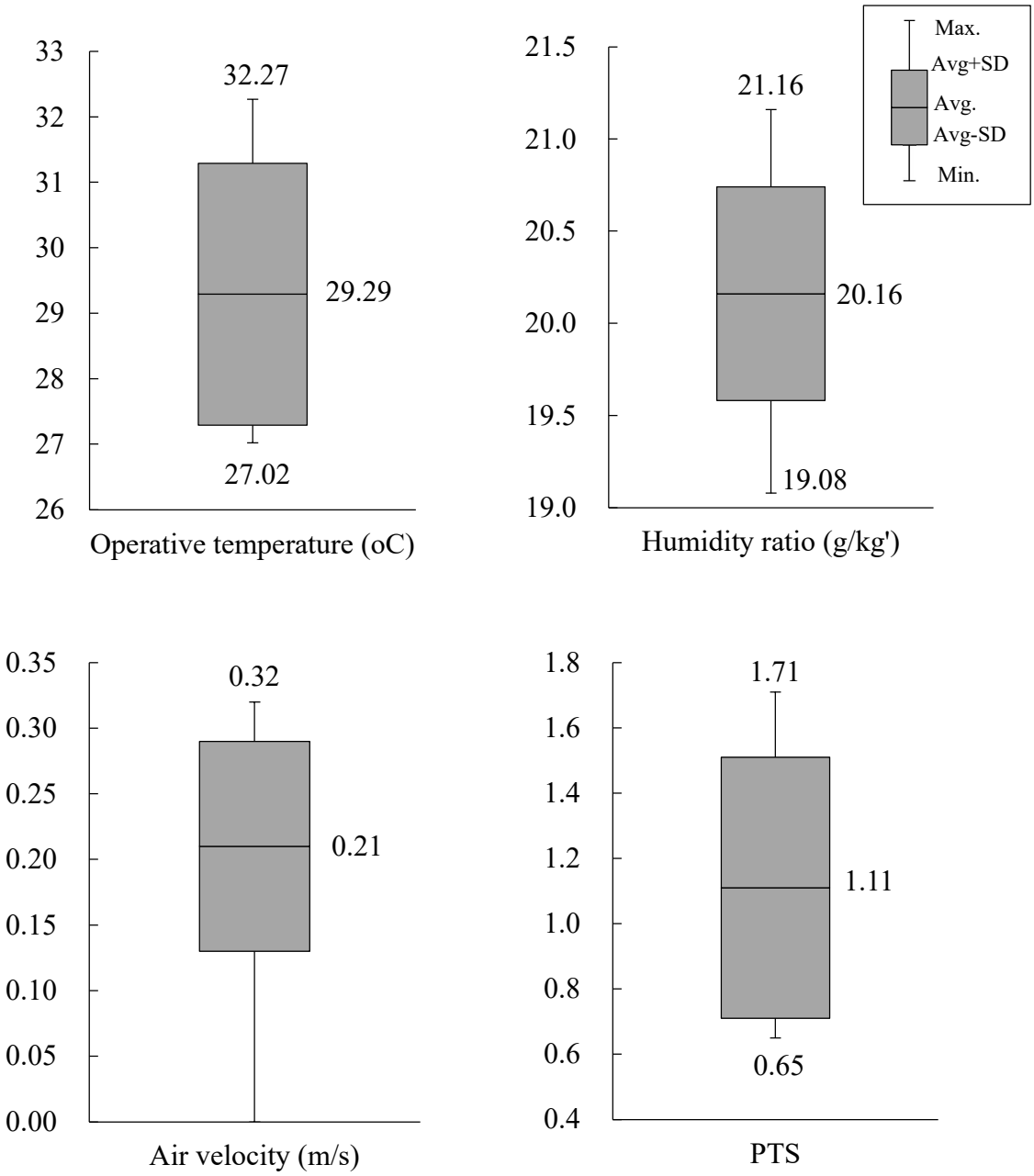

Fig.5-4 Simulated and calculated results of initial model of gymnasium

5.4.1 Simulation factors and levels of orthogonal experiment

There are many factors of architectural form that influence indoor thermal comfort of gymnasium. According to the initial model and the previous researches, six parameters of gymnasium form are addressed in this study. Factor A is main window position, Factor B is south WWR, Factor C is north WWR, Fator D is roof insulation type, Factor E is roof slope and Factor F is depth of overhanging eave. These six parameters are taken as

the factors of orthogonal experiment and three levels are chosen for each factor. The orthogonal experiment is shown in Table 5-3.

Table 5-3 Factors and corresponding levels of orthogonal experiment

Factor	Level 1	Level 2	Level 3
A: Main window position	High at the south and north wall	Low at the south wall and high at the north wall	High at the south wall and low at the north wall
B: South WWR	10%	20%	30%
C: North WWR	10%	20%	30%
D: Roof insulation type	Single reinforced concrete roof	Double reinforced concrete roof	Single insulated roof
E: Roof slope	Horizontal roof	Rise from south to north	Rise from north to south
F: Depth of overhanging eave	1m	5m	9m

(1) Factor A: The window position affects the natural ventilation, thermal comfort as well as even energy consumption. In previous researches, Prakash[26] identified a new set of strategies to locate the window openings which could reduce the PMV by 0.12%. Kim et al.[27] demonstrated that the buildings achieve the lowest energy consumption when the windows located in the middle height in all orientations. As the wind direction in Guangzhou is mainly from southeast to northwest, the window position on south and north is more valuable to study than that on east and west. The three levels in factor A in this study are different positions of main windows that selected from the result of investigation and the relevant researches.

(2) Factor B and C: As a significant factor affecting on indoor thermal environment, the WWR plays an important role in architectural design. There are extensive researches and efforts focused on the WWR up to now. Goia et al.[28] conducted simulation to

analyse the indoor thermal performances of office buildings and the results indicated that the optimal WWR is from 30% to 45%. Wen et al.[29] took the indoor air temperature as the parameter to evaluate the optimal WWR and proposed a WWR maps for the architectural design in the early stages. According to the relevant researches and regulations of China, as well as the investigation in Guangzhou, the WWR in the study are chosen in three levels, 10%, 20% and 30%.

(3) Factor D: The heat gain from the solar radiation is a key problem in the buildings in south of China. Since the roof surfaces are the main positions absorbing radiant heat, the insulation measures of roofs are critical. Zingre et al.[30] compared the thermal performances between the double skin roof and the insulated roof in Singapore, found that the double roof performs better in reducing heat gain into the building during daytimes. Susanti et al.[31] analysed the influences of cavity ventilation on the operative temperature in Japanese climate and found that the naturally ventilated cavity roof was superior to the single roof in decreasing the operative temperature. In this study, three types of roof are selected to discuss the optimum for the gymnasiums in hot and humid climate. The single skin roof is the ordinary reinforced concrete roof without any passive cooling; the double skin roof is with an air cavity of 500mm thickness inside; the insulated roof composes of reinforced concrete and an insulation board of 20 mm thickness.

(4) Factor E: Roof slope can regular the natural ventilation and cooling effect. Li et al.[32] investigated effect of different influencing parameters on thermal performance of naturally ventilated roofs and found that the roof slope plays an important role in the thermal performance of ventilated roof. Since the wind direction in Guangzhou is southeast-to-northwest, the three levels of roof slope in this study are mainly consider the south-north direction.

(5) Factor F: The overhanging eave influences natural ventilation and shading, as well as heat insulation. Li[10] simulated the symmetrical and unsymmetrical models of a gymnasium in Guangzhou, recommended adjusting the width and angle of the

overhanging eaves of the gymnasiums to improve the thermal performance. Due to most of the investigated gymnasiums in Guangzhou own overhanging eaves on the roofs, the three levels of factor F are different in the depth of overhanging eave.

5.4.2 Range analysis

Since the six factors (A~F) and three levels (1~3) for each factor are selected for the orthogonal experiment, the orthogonal table L18 (3^6) is adopted according to the principle of orthogonal experiment. Then the 18 tests are generated and simulated in FlowDesigner to obtain the thermal environment data and the PTS data. Table 5-4 illustrates the range analysis results for the influence of different factors on the thermal comfort (PTS). By comparing the R_j values of each factor, the influence of the six factors on PTS are ranked as follow: D>A=E>F>C>B. The most influential factor on thermal comfort in gymnasium is the roof insulation type. Then follow by the main window position, roof slope, depth of overhanging eave, north WWR and south WWR.

5.4.3 Correlation between factors and the PTS

The correlations between the six factors (A~F) and the PTS are presented in Fig.5-5. It illustrates the influence rules of factors levels on the PTS in the process of optimization of architectural form. Taking factor A as an example, the PTS value in Level 1, 2 and 3 is 1.031, 0.994 and 1.084 respectively. As the value in Level 2 achieves the lowest, Level 2 is the optimum for Factor A. In the same way, Factor B, C, D, E and F achieve the lowest PTS values in Level 3, Level 3, Level 2, Level 1 and Level 3 respectively. Thus, combining the optimal level of each factors, the optimum combination of gymnasium form is $A_2B_2C_3D_2E_1F_3$, which means the main windows are at the low position of the south wall and at the high position of the north wall; the south WWR is 20% and the north WWR is 30%; the roof is horizontal in double reinforced concrete and the overhanging eave is deep in 9m.

Table 5-4 Results and range analysis of the orthogonal experiments

Test number	Factor						Result of PTS
	A	B	C	D	E	F	
1	1	1	1	1	1	1	1.110
2	1	2	2	2	2	2	0.924
3	1	3	3	3	3	3	0.984
4	2	1	3	1	2	2	1.119
5	2	2	1	2	3	3	0.892
6	2	3	2	3	1	1	0.965
7	3	1	2	2	1	3	0.913
8	3	2	3	3	2	1	1.065
9	3	3	1	1	3	2	1.299
10	1	1	2	3	3	2	1.182
11	1	2	3	1	1	3	1.022
12	1	3	1	2	2	1	0.961
13	2	1	3	2	3	1	0.907
14	2	2	1	3	1	2	1.030
15	2	3	2	1	2	3	1.053
16	3	1	1	3	2	3	1.087
17	3	2	2	1	3	1	1.227
18	3	3	3	2	1	2	0.912
K_1	6.183	6.318	6.379	6.830	5.952	6.235	
K_2	5.966	6.160	6.264	5.509	6.209	6.466	
K_3	6.503	6.174	6.009	6.313	6.491	5.951	
k_1	1.031	1.053	1.063	1.138	0.992	1.039	
k_2	0.994	1.027	1.044	0.918	1.035	1.078	
k_3	1.084	1.029	1.002	1.052	1.082	0.992	
R	0.090	0.026	0.062	0.220	0.090	0.086	
Factor ranking	D>A = E>F>C>B						

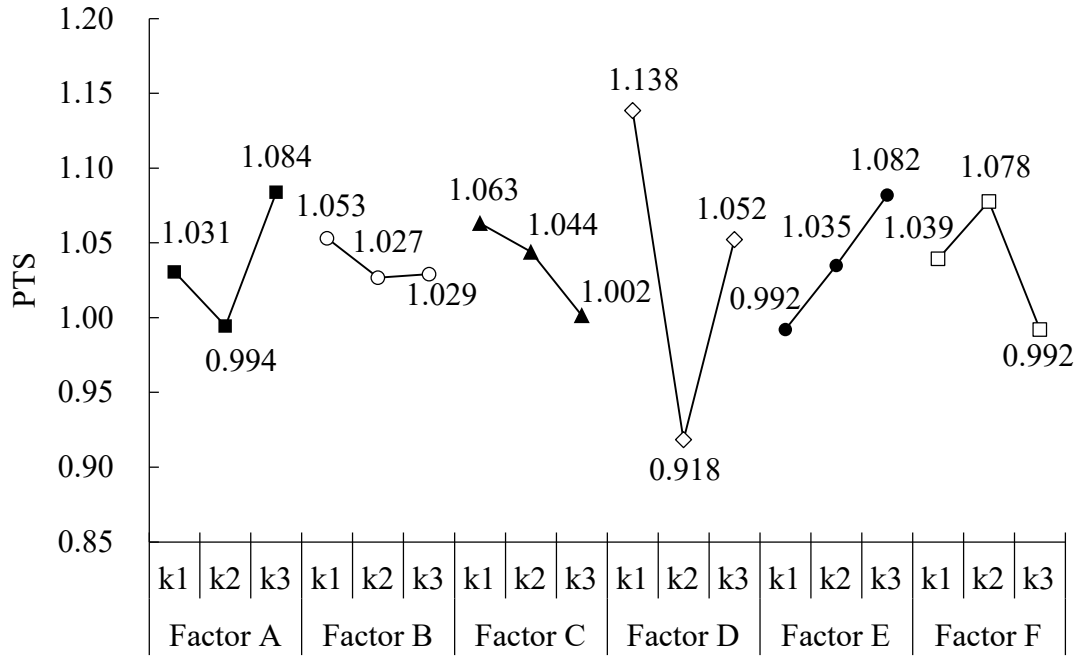

Fig.5-5 Correlations between the factors and the PTS

5.4.4 Variance analysis

Table 5-5 presents the results of the variance analysis. The sum of the squared deviation (SS), the degree of freedom (df), the variance of the factor (V) and F value (F) have been calculated according to the regulation of variance analysis in orthogonal experiment. By comparing the F values of each factor to the critical value $F_{(0.05)}$, Roof insulation type is the most significant factor influencing the thermal comfort. The factors of main window position, roof slope, depth of overhanging eave, north WWR and south WWR are less significant than the factor of roof insulation type.

5.5 Discussion on the optimization effects

5.5.1 Optimized model versus initial model

Comparing with the initial model of gymnasium, the optimized model of gymnasium improves a lot, as list in Table 5-6. The change of window position as well as WWR improve the natural ventilation as the indoor average air velocity increases from 0.21m/s

Table 5-5 variance analysis of the PTS

Factor	SS	df	V	F	$F_{(0.05)}$	Significance
A	0.024	2	0.012	0.721	3.74	
B	0.003	2	0.002	0.090	3.74	
C	0.012	2	0.006	0.361	3.74	
D	0.148	2	0.074	4.446	3.74	*
E	0.024	2	0.012	0.721	3.74	
F	0.022	2	0.011	0.661	3.74	
Deviation	0.231	14	0.016			

Table 5-6 Comparison of gymnasium form and indoor thermal performance between initial model and optimized model

Parameters	Initial model	Optimized model
Window position	High at the south and north walls	Low at the south wall and high at the north wall
WWR	South and north for 10%	South for 20% north for 30%
Roof insulation type	Single reinforced concrete roof	Double reinforced concrete roof
Roof slope	Horizontal roof	Horizontal roof
Depth of overhanging eave	1m	9m
Indoor avg. operative temperature	29.30ºC	28.21ºC
Indoor avg. humidity ratio	20.16 g/kg’	20.15 g/kg’
Indoor avg. air velocity	0.21m/s	0.77m/s
Indoor avg. PTS	1.11 (Slightly hot)	0.86 (Comfortable)

to 0.77m/s in summer days. As a significant factor, the double skin roof in optimal model improve the thermal performances, the indoor average operative temperature decreases from 29.3°C to 28.21°C and the PTS drops from 1.11 (slightly hot) to 0.86 (comfortable). Fig.5-6 shows the variation of indoor average PTS values in initial model and optimized model during a day in August. The average PTS values in optimized model are slight lower than that in initial model before 11am, then the gap between them is growing to around 0.7 until midnight. It indicates that the optimized architectural form of gymnasium would improve the indoor thermal comfort to some extent, and such optimized gymnasiums would be beneficial for the people and cities.

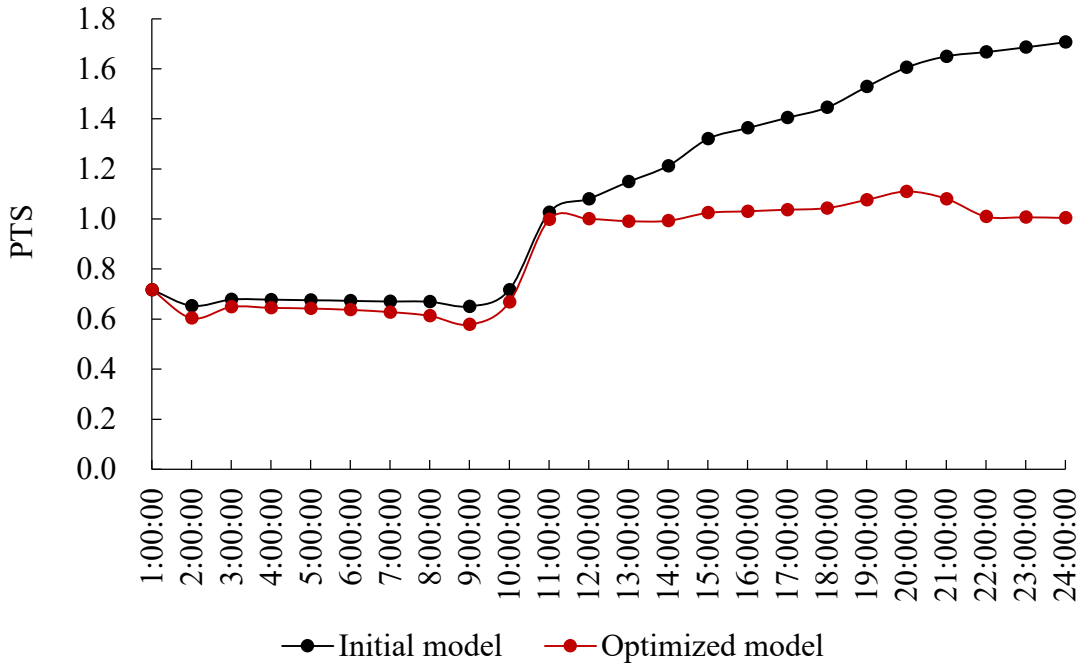

Fig.5-6 Variation of the average PTS values in initial model and optimized model

5.5.2 Practical implication

The analyses in this study indicate that the roof insulation is the most influential factor on thermal comfort in gymnasiums at hot and humid climate. Furthermore, the optimized architectural form of gymnasium has been achieved by the orthogonal experiment. This study expands the application of orthogonal experiment to multi-factor research on gymnasium design. By conducting a limited number of experiments in the

orthogonal array, full information of factors is effective obtained. This method, as minimizing the effort and time during analyze, can be an alternative approach for integrated architectural design. The results in this study, can provide as a technical reference for the gymnasium design, as well as a guideline for the research of similar type of architecture located in regions with climates.

5.6 Summary

This chapter has conducted an orthogonal design to provide an optimization analysis of the gymnasium form on indoor thermal comfort at hot-humid climate. The orthogonal experiments are applied assisted by field investigation and simulations with the FlowDesigner. The results are analyzed using range analysis and variance analysis, and the main conclusions are summarized.

1) 729 experiments have been dramatically decreased to 18 tests by the method of orthogonal experiment.

2) The range analysis and variance analysis demonstrate that the roof insulation type influents the most significantly on the thermal comfort in gymnasiums.

3) In terms of thermal comfort of gymnasium, the optimized architectural form turns out to be the combination of the windows at the low position of south wall and at the high position of north wall; 20% for south WWR and 30% for north WWR; horizontal roof with double reinforced concrete and the overhanging eave with the depth of 9m.

4) The findings benefit building designers and researchers to determine the key parameters in the gymnasium design and to improve the indoor thermal comfort as well as energy efficiency.

Chapter 6

Conclusions and suggestions

6.1 Conclusions of this study

6.1.1 From the perspective of thermal comfort models

In Chapter 2, the correlation between the PMV model and the SET* model and the effect of thermal parameters on them are preformed. Firstly, the relationship between PMV and SET* in the case of 0.5clo (summer), 1clo (winter) and total (a whole year) have been obtained by the regression of 3360 samples in the imaginary standard condition. Secondly, the frequency distribution of PMV and SET* are presented and the correspondence between PMV and SET* shows that it only meaningful to the calculation results, instead of the thermal parameters involved in the calculation. In addition, the effect of thermal parameters on PMV and SET* indicate that the values of PMV and SET* are principally affected by the air velocity at low operative temperatures and affected by the relative humidity at high operative temperatures in the sedentary condition. However, with the increase of the metabolic rate, the values of SET* are only affected by relative humidity. Furthermore, the values of PMV and SET* increase with the increase of clothing insulation while the increasing rates lower and the difference between PMV and SET* gets smaller with the increasing clothing insulation. Finally, the thermal comfort zones are analyzed by two different methods. Compared with the comfort zones by Graphic Comfort Zone Method, the comfort zones by Analytical Comfort Zone Method are more extensive and mainly extend to the left and above thanks to the increase of the metabolic rate and relative humidity.

6.1.2 From the perspective of field survey in gymnasiums

In Chapter 3, a field survey on the thermal sensation under basketball game was carried out in three naturally ventilated gymnasiums in Guangzhou, China. A total of 372 valid data regarding indoor thermal environments, human physiology and thermal sensation of subjects has been collected. During the survey, the thermal environment parameters ranged from 24.97°C~35.65°C in outdoor air temperature, 25.04°C~35.53°C in indoor air temperature, 23.86°C~36.84°C in mean radiant temperature, 12.32g/kg'~23.67g/kg'

in humidity ratio and 0m/s~1.64m/s in air velocity. In addition, the clothing insulations were 0.22clo and 0.22clo / 0.29clo for males and females. In terms of human physiology, the metabolic rate of subjects during basketball play (the average is 334.24W/m^2 for males and 274.01W/m^2 for females) was higher than that during the preparation and rest state. The blood pressure of subjects during basketball play (the average is 124mmHg for males and 123mmHg for females) was slightly higher than that during preparation and rest, which is consistent with the trend in the metabolic rate of subjects. Moreover, the mean skin temperature was 37.13°C in the stage of preparation, then declined slightly during basketball game, which lies mainly in the cooling by evaporation of sweat and the cutaneous vasoconstriction response to exercise. Besides, the skin temperatures were different in terms of gender. Finally, the TSV of subjects during basketball play highly differed to that during preparation and rest.

6.1.3 From the perspective of PTS model

In Chapter 4, the influences of thermal environment and human physiology on thermal sensation under exercise state have been analyzed. The thermal sensation vote (TSV) rose with the rise in the air temperature, mean radiant temperature and humidity ratio, while decreases with an increase in the air velocity. When considering the physiological parameters, the average values of the metabolic rate, systolic blood pressure and skin temperature are positively correlated with the TSV.

Besides, basing on the field survey in Chapter 3, the Predicted Thermal Sensation (PTS) model has been developed, as shown below. Furthermore, the rationality and accuracy of this model were validated by conducting a field survey by the same method in other two naturally ventilated gymnasiums in Guangzhou from summer to winter. This model can provide a theoretical reference for the study of thermal comfort under high-intensive sport activities in gymnasiums in hot-humid regions of China.

$$\mathrm{PTS} = -5.127 + 0.201\mathrm{T_{op}} + 0.001\mathrm{x} - 0.045\mathrm{v} + 0.002\mathrm{M} - 1.184\mathrm{I_{cl}}$$

where PTS is the Predicted Thermal Sensation whose values range from -3 to 3; T_{op} is the operative temperature in °C; x is the humidity ratio in g/kg'; v is the air velocity in m/s; M is the metabolic rate in W/m^2; I_{cl} is the clothing insulation in clo.

6.1.4 From the perspective of optimal gymnasium form

In Chpater 5, an orthogonal design has been conducted to provide an optimization analysis of the gymnasium form of the indoor thermal comfort at hot and humid climate. The orthogonal experiments are applied assisted by field investigation and simulations with the FlowDesigner. By using the method of orthogonal design, 729 experiments have been dramatically decreased to 18 tests. The results are analyzed using range analysis and variance analysis, which demonstrate that the roof insulation type influents the most significantly on the thermal comfort in gymnasiums. Finally, the optimized architectural form turns out to be the combination of the windows at the low position of south wall and at the high position of north wall; 20% for south WWR and 30% for north WWR; horizontal roof with double reinforced concrete and the overhanging eave with the depth of 9m. The findings benefit designers and researchers to determine the key parameters in the gymnasium architectural design at hot and humid climate and to improve the indoor thermal comfort as well as energy efficiency.

6.2 Suggestions for the future study

Although this study investigated and analysed the thermal environment, human phosiology and thermal sensation of athletes partaking in high-intensive exercise in gymnasium, and optimized the gymnasium form for thermal comfort at hot-humid climate by the method of orthogonal experiment and simulation, there are still some limitations.

In the case of field survey on thermal comfort, the small sample size of the study may affect the reliability of results and only basketball players were investigated in this study, whose personal performances and thermal sensation are concerned with the

characteristics of this sport. Nevertheless, subjects for other sports are not measured, so that the results in this study are limited to the scope of application. Besides, the survey plan should be more rigorous for the impact of different sport intensities on subjects' physiology and subjective perception. Therefore, further precise studies on the field survey of thermal comfort in gymnasiums should be done, focusing on different locations and the discussion on the types of sports, as well as the detailed survey plan, so as to validate the scope of the model developed in this study.

In the case of analysis on gymnasium form, six factors and three levels has been considered in this study. For the sake of comprehensive analysis between architectural form and thermal comfort, more related factors and levels of architectural form of gymnasim should be considered in the further studies. Furthermore, the correlations between the factors should also be assessed in the future, to improve the feasibility of the optimization for the thermal comfort in gymnasiums at hot and humid climate. In addition, as the roof insulation type is an important factor in gymnasiums, more details related to it (such as the thermal conductivity, capacity and green roof) could be analyzed as well.

References

Chapter 1

1) Zhang Q and Yang H. Typical meteorological database handbook for buildings. China Architecture & Building Press, 2012, p.202.
2) Fanger PO. Thermal comfort--analysis and application in environmental engineering. Copenhagen: Danish Technology Press, 1970, pp.142-155.
3) Gagga AP, Fobelets AP and Berglund LG. A standard predictive index of human response to the thermal environment. ASHRAE Transactions 1986; 92: 709-731.
4) ISO 7243:2017. Ergonomics of the thermal environment-Assessment of heat stress using the WBGT (wet bulb globe temperature) index. Geneva: International Organization for Standardization, 2017.
5) Webb CG. An analysis of some observations of thermal comfort in an equatorial climate. Brit J of Industrial Medicine 1959; 16: 297-310.
6) Bedford T. Equivalent temperature, what it is, how it's measured. Heating, Piping and Air conditioning 1951; 23: 87-91.
7) Zhang Z, Zhang Y and Jin L. Thermal comfort in interior and semi-open spaces of rural folk houses in hot-humid areas. Building and Environment 2018; 128: 336-347.
8) Djamila H, Chu CM and Kumaresan S. Field study of thermal comfort in residential buildings in the equatorial hot-humid climate of Malaysia. Building and Environment 2013; 62: 133-142.
9) Buonocore C, De Vecchi R, Scalco V, et al. Thermal preference and comfort assessment in air-conditioned and naturally ventilated university classrooms under hot and humid conditions in Brazil. Energy and Buildings 2020; 211: 1-13.
10) Damiati SA, Zaki SA, Rijal HB, et al. Field study on adaptive thermal comfort in office buildings in Malaysia, Indonesia, Singapore, and Japan during hot and humid season. Building and Environment 2016; 109: 208-223.
11) Wu Y, Liu H, Li B, et al. Thermal adaptation of the elderly during summer in a hot humid area: Psychological, behavioral, and physiological responses. Energy and Buildings 2019; 203: 1-14.
12) Li B, Li W, Liu H, et al. Physiological expression of human thermal comfort to indoor operative temperature in the non-HVAC environment. Indoor and Built Environment 2010; 19: 221-229.
13) Thapa S. Thermal comfort in high altitude Himalayan residential houses in Darjeeling, India–An adaptive approach. Indoor and Built Environment 2020; 29: 84-100.

14) Yu J, Hassan MT, Bai Y, et al. A pilot study monitoring the thermal comfort of the elderly living in nursing homes in Hefei, China, using wireless sensor networks, site measurements and a survey. Indoor and Built Environment 2020; 29: 449-464.
15) Dufton AF. The Equivalent Temperature of a Room and its Measurement. Building Res. Technical Paper No. 13. HMSO.
16) Houghten FC and Yagloglou CP. Determination of comfort zone. Journal of ASHVE 1923; 29: 361-384.
17) Yaglou CP. A method for improving the effective temperature index. Heating, Piping and Air Conditioning 1947; 19(9): 131-133.
18) ANSI/ASHRAE 55-2017. Thermal environmental conditions for human occupancy. Atlanta: American Society of Heating, Refrigerating and Air Conditioning Engineers, 2017.
19) ASHRAE Handbook-Fundamentals 2017. Chapter 9: Thermal Comfort. Atlanta: American Society of Heating, Refrigerating and Air Conditioning Engineers, 2017.
20) ISO. International Standard 7730. Moderate Thermal Environment-Determination of the PMV and PPD Indices and Specification of the Conditions for Thermal Comfort. Geneva: International Standard Organization. 1984.
21) DeDear RJ and Brager GS. Developing in adaptive model of thermal comfort and preference. *ASHRAE Trans* 1998; 104(1): 145-167.
22) Bouyer J, Vinet J, Delpech P, et al. Thermal comfort assessment in semi-outdoor environments Application to comfort study in stadia. Journal of Wind Engineering and Industrial Aerodynamics 2007; 10(95):963-976.
23) Ucuncu M, Woolf D and Zikri M. Thermal comfort of spectators in stadia built in hot climates. Adapting to Change: New Thinking on Comfort, Windsor, UK, 2010: 8.
24) Szucs A, Moreau S and Allard F. Spectators' aerothermal comfort assessment method in stadia. Building and Environment 2007; 42(6):2227-2240.
25) Ji T, Yuan W, Yang J, et al. Improved Model and Experimental study on Human Thermal Comfort of Sports in Gymnasium. Building Energy and Environment 2017; 36:11-15.
26) Qian F. Numerical simulation and study on gymnasium indoor thermal environment based on Airpak. Journal of Architecture 2012; S2:1-4.
27) Li J. Effect of form asymmetry of gymnasium on natural ventilation and thermal comfort of exercise site. Journal of South China University of Technology 2013; 41(3): 83-89.
28) Yaglou CP and Minard D. Control of Heat Casualties at Military Training Centers. *Archives of Industrial Health* 1957; 16:302-316.

29) Fanger PO. Calculation of thermal comfort: Introduction of a Basic Comfort Equation. *ASHRAE Transactions* 1967; 73: III.4.1-III.4.20.
30) Gagge AP, Stolwijk JAJ and Saltin B. Comfort and thermal sensations and associated physiological responses during exercise at various ambient temperatures. *Environmental Research* 1969; 2:209-229.
31) Gonzalez RR. Exercise physiology and sensory responses. *Studies in Environmental Science* 1981; 10: 123-144.
32) Humphreys MA and Nicol JF. The validity of ISO-PMV for predicting comfort votes in every-day thermal environments. *Energy and buildings* 2002; 34:667-684.
33) Ji W, Luo M, Cao B, Zhu Y, Geng Y and Lin B. A new method to study human metabolic rate changes and thermal comfort in physical exercise by CO2 measurement in an airtight chamber. Energy and Buildings 2018; 177: 402-412.
34) Li W, Zhang J, Zhao T and Liang R. Experimental research of online monitoring and evaluation method of human thermal sensation in different active states based on wristband device. Energy and Buildings 2018; 173: 613-622.
35) Xiao Y, Gao Y and Wang Y. Study on subjective sensation and physiological reaction with high physical activity influenced by air temperature of stadium. Indoor and Built Environment. Epub ahead of print 18 September 2019. DOI: 10.1177/ 1420326X19876071.

Chapter 2

1) Fanger PO. Thermal comfort--analysis and application in environmental engineering. Copenhagen: Danish Technology Press, 1970, pp.142-155.
2) Gagga AP, Fobelets AP and Berglund LG. A standard predictive index of human response to the thermal environment. ASHRAE Transactions 1986; 92: 709-731.
3) ANSI/ASHRAE 55-2017. Thermal environmental conditions for human occupancy. Atlanta: American Society of Heating, Refrigerating and Air Conditioning Engineers, 2017.
4) ASHRAE Handbook-Fundamentals 2017. Chapter 9: Thermal Comfort. Atlanta: American Society of Heating, Refrigerating and Air Conditioning Engineers, 2017.
5) ISO. International Standard 7730. Moderate Thermal Environment-Determination of the PMV and PPD Indices and Specification of the Conditions for Thermal Comfort. Geneva: International Standard Organization. 1984.
6) Cheung T, Schiavon S, Parkinson T, et al. Analysis of the accuracy on PMV-PPD model using the ASHRAE Global Thermal Comfort Database II. Building and Environment 2019; 153:205-217.
7) Broday EE, Moreto JA, de Paula Xavier AA, et al. The approximation between

thermal sensation votes (TSV) and predicted mean vote (PMV): A comparative analysis. International Journal of Industrial Ergonomics2019; 69:1-8.
8) Kim JT, Lim JH, Cho SH, et al. Development of the adaptive PMV model for improving prediction performances. Energy and Buildings 2015; 98:100-105.
9) Fang Z, Feng X, Liu J, et al. Investigation into the differences among several outdoor thermal comfort indices against field survey in subtropics. Sustainable cities and society 2019; 44:676-690.
10) Li B, Du C, Tan M, et al. A modified method of evaluating the impact of air humidity on human acceptable air temperatures in hot-humid environments. Energy and Buildings 2018; 158:393-405.
11) Ji W, Luo M, Cao B, et al. A new method to study human metabolic rate changes and thermal comfort in physical exercise by CO2 measurement in an airtight chamber. Energy and Buildings 2018; 177:402-412.
12) Gao J, Wang Y and Wargocki P. Comparative analysis of modified PMV models and SET models to predict human thermal sensation in naturally ventilated buildings. Building and Environment 2015; 92:200-208.
13) Ye G, Yan, C, Chen Y, et al. A new approach for measuring predicted mean vote (PMV) and standard effective temperature (SET*). Building and environment 2003; 38(1):33-44.
14) Berglund LG. Comfort criteria: Humidity and standards. Proceedings of Pan Pacific Symposium on Building and Urban Environmental Conditioning in Asia 1995; 2:369-382.
15) Blagden C. Experiments and Observations in an Heated Room By Charles Blagden, M. D. F. R. S. Philosophical Transactions 1775; 65:111-123.
16) Du H and Yang C. Re-visitation of the thermal environment evaluation index standard effective temperature (SET*) based on the two-node model. Sustainable Cities and Society 2020; 53:1-11. https://doi.org/10.1016/j.scs.2019.101899
17) Fanger PO. Calculation of thermal comfort-introduction of a basic comfort equation. ASHRAE Transactions 1967; 73(2):1-20.
18) Schellen L, Loomans MGLC, Kingma BRM, et al. The use of a thermo-physiological model in the built environment to predict thermal sensation: coupling with the indoor environment and thermal sensation. Building and Environment 2013; 59:10-22.
19) Howell WC and Stramler CS. The contribution of psychological variables to the prediction of thermal comfort judgments in real world settings. ASHRAE Transactions 1981; 87:609-621.
20) Parsons KC. The effects of gender, acclimation state, the opportunity to adjust

clothing and physical disability on requirements for thermal comfort. Energy and Buildings 2002; 34:593-599.
21) Gonzalez RR, Nishi Y and Gagge AP. Experimental evaluation of standard effective temperature a new biometeorological index of man's thermal discomfort. International journal of biometeorology 1974; 18(1):1-15.
22) Gagge AP, Fobelets AP and Berglund LG. A standard predictive index of human response to the thermal environment. ASHRAE Transactions 1986; 92:709-731.
23) Auliciem A and Szokolay SV. PLEA Note3: Thermal Comfort. Passive and Low Energy Architecture International with Department of Architecture, The University of Queensland. 2007.

Chapter 3

1) Fanger PO. Thermal comfort--analysis and application in environmental engineering. Copenhagen: Danish Technology Press, 1970, pp.142-155.
2) Gagga AP, Fobelets AP and Berglund LG. A standard predictive index of human response to the thermal environment. ASHRAE Transactions 1986; 92: 709-731.
3) ISO 7243:2017. Ergonomics of the thermal environment-Assessment of heat stress using the WBGT (wet bulb globe temperature) index. Geneva: International Organization for Standardization, 2017.
4) Webb CG. An analysis of some observations of thermal comfort in an equatorial climate. Brit J of Industrial Medicine 1959; 16: 297-310.
5) Bedford T. Equivalent temperature, what it is, how it’s measured. Heating, Piping and Air conditioning 1951; 23: 87-91.
6) Zhang Z, Zhang Y and Jin L. Thermal comfort in interior and semi-open spaces of rural folk houses in hot-humid areas. Building and Environment 2018; 128: 336-347.
7) Djamila H, Chu CM and Kumaresan S. Field study of thermal comfort in residential buildings in the equatorial hot-humid climate of Malaysia. Building and Environment 2013; 62: 133-142.
8) Buonocore C, De Vecchi R, Scalco V, et al. Thermal preference and comfort assessment in air-conditioned and naturally ventilated university classrooms under hot and humid conditions in Brazil. Energy and Buildings 2020; 211: 1-13.
9) Damiati SA, Zaki SA, Rijal HB, et al. Field study on adaptive thermal comfort in office buildings in Malaysia, Indonesia, Singapore, and Japan during hot and humid season. Building and Environment 2016; 109: 208-223.
10) Wu Y, Liu H, Li B, et al. Thermal adaptation of the elderly during summer in a hot humid area: Psychological, behavioral, and physiological responses. Energy and

Buildings 2019; 203: 1-14.
11) Li B, Li W, Liu H, et al. Physiological expression of human thermal comfort to indoor operative temperature in the non-HVAC environment. Indoor and Built Environment 2010; 19: 221-229.
12) Yaglou CP and Minard D. Control of Heat Casualties at Military Training Centers. Archives of Industrial Health 1957; 16:302-316.
13) Fanger PO. Calculation of thermal comfort: Introduction of a Basic Comfort Equation. ASHRAE Transactions 1967; 73: III.4.1-III.4.20.
14) Gagge AP, Stolwijk JAJ and Saltin B. Comfort and thermal sensations and associated physiological responses during exercise at various ambient temperatures. Environmental Research 1969; 2:209-229.
15) Gonzalez RR. Exercise physiology and sensory responses. Studies in Environmental Science 1981; 10: 123-144.
16) Humphreys MA and Nicol JF. The validity of ISO-PMV for predicting comfort votes in every-day thermal environments. Energy and buildings 2002; 34:667-684.
17) Ji W, Luo M, Cao B, et al. A new method to study human metabolic rate changes and thermal comfort in physical exercise by CO2 measurement in an airtight chamber. Energy and Buildings 2018; 177: 402-412.
18) Li W, Zhang J, Zhao T, et al. Experimental research of online monitoring and evaluation method of human thermal sensation in different active states based on wristband device. Energy and Buildings 2018; 173: 613-622.
19) Henriques IB, Mady CEK and de Oliveira Junior S. Assessment of thermal comfort conditions during physical exercise by means of exergy analysis. Energy 2017; 128: 609-617.
20) Guéritée J and Tipton MJ. The relationship between radiant heat, air temperature and thermal comfort at rest and exercise. Physiology & behavior 2015; 139: 378-385.
21) Zhai Y, Elsworth C, Arens E, et al. Using air movement for comfort during moderate exercise. Building and Environment 2015; 94: 344-352.
22) ISO 8996:2004. Ergonomics of the thermal environment-Determination of metabolic rate. Geneva. International Organization for Standardization, 2004.
23) Zhang Q and Yang H. Typical meteorological database handbook for buildings. China Architecture & Building Press, 2012, p.202.
24) JGJ/T347:2014. Standard of test methods for thermal environment of building. China Architecture & Building Press, 2014.
25) Bedford T and Warner CG. The globe thermometer in studies of heating and ventilation. Epidemiology & Infection 1934; 34: 458-473.

26) Ramanathan NL. A new weighting system for mean surface temperature of the human body. Journal of Applied Physiology 1964; 19: 531-533.
27) ISO 9886:2004. Ergonomics-Evaluation of thermal strain by physiological measurements. Geneva: The International Organization for Standardization, 2004.
28) National health commission of the People's Republic of China. Ethical review of biomedical research involving human beings, 2016.
29) JGJ31:2003. Design code for sports building. China Architecture & Building Press, 2003.
30) ANSI/ASHRAE 55-2017. Thermal environmental conditions for human occupancy. Atlanta: American Society of Heating, Refrigerating and Air Conditioning Engineers, 2017.
31) Cruz AB. Abnormal blood pressure response to exercise in badminton athletes. Science & Sports 2016; 31: 342-346.
32) Caselli S, Segui AV, Quattrini F, et al. Upper normal values of blood pressure response to exercise in Olympic athletes. American heart journal 2016; 177: 120-128.
33) Fitzgerald BT, Ballard EL and Scalia GM. Estimation of the Blood Pressure Response with Exercise Stress Testing. Heart, Lung and Circulation 2019; 28: 742-751.
34) Torii M, Yamasaki M, Sasaki T, et al. Fall in skin temperature of exercising man. British journal of sports medicine 1992; 26: 29-32.
35) ASHRAE Handbook-Fundamentals 2017. Chapter 9: Thermal Comfort. Atlanta: American Society of Heating, Refrigerating and Air Conditioning Engineers, 2017.
36) Nakayama T, Ohnuki Y and Niwa KI. Fall in skin temperature during exercise. The Japanese journal of physiology 1977; 27:423-437.
37) Christensen EH, Nielsen M and Hannisdahl B. Investigations of the circulation in the skin at the beginning of muscular work. Acta Physiologica Scandinavica 1942; 4:162-170.
38) Johnson JM, Rowell LB and Brengelmann GL. Modification of the skin blood flow-body temperature relationship by upright exercise. Journal of applied physiology 1974; 37:880-886.

Chapter 4

1) Fanger PO. Thermal comfort-analysis and application in environmental engineering. Copenhagen: Danish Technology Press, 1970.
2) Gagga AP, Fobelets AP and Berglund LG. A standard predictive index of human response to the thermal environment. ASHRAE Transactions 1986; 92: 709-731.

3) Yaglou CP and Minaed D. Control of heat casualties at military training centers. Arch Indust Health 1957; 16: 302-316.
4) Zhao J, Zhu N and Lu S. Productivity model in hot and humid environment based on heat tolerance time analysis. Building and environment 2009; 44: 2202-2207.
5) Kajiwara Y, Ono S, Nakai S, et al. Environmental temperature during summertime athletic competitions in Japan. Elsevier Ergonomics Book Series 2005; 3: 71-77.
6) Glass SC, Knowlton RG and Becque MD. Perception of effort during high-intensity exercise at low, moderate and high wet bulb globe temperatures. European journal of applied physiology and occupational physiology 1994; 68: 519-524.
7) ASHRAE Handbook-Fundamentals 2017. Chapter 9: Thermal Comfort. Atlanta: American Society of Heating, Refrigerating and Air Conditioning Engineers, 2017.
8) 2020 Frontline Systems, Inc. Excel Solver Help, https://www.solver.com/excel-solver-online-help (accessed 19 April 2020).
9) ISO 7243:2017. Ergonomics of the thermal environment-Assessment of heat stress using the WBGT (wet bulb globe temperature) index. Geneva: International Organization for Standardization, 2017.
10) Sharma MR and Ali S. Tropical summer index-a study of thermal comfort of Indian subjects. Building and Environment 1986; 21: 11-24.
11) Belding HS and Hatch TF. Index for evaluating heat stress in terms of resulting physiological strains. Heating, Piping and Air conditioning 1955; 27: 129-136.
12) Bedford T. Equivalent temperature, what it is, how it's measured. Heating, Piping and Air conditioning 1951; 23: 87-91.
13) JGJ31:2003. Design code for sports building. China Architecture & Building Press, 2003.

Chapter 5

1) Chen L and Ng E. Outdoor thermal comfort and outdoor activities: A review of research in the past decade. Cities 2012; 29(2):118-125.
2) Yao JW, Yang F, Zhuang Z, et al. The effect of personal and microclimatic variables on outdoor thermal comfort: A field study in a cold season in Lujiazui CBD, Shanghai. Sustainable Cities and Society 2018; 39:181-188.
3) deDear R and Brager GS. Towards an adaptive model of thermal comfort and preference. ASHRAE Transactions 1998; 104:145-167.
4) Humphreys MA and Nicol JF. Outdoor temperature and indoor thermal comfort: raising the precision of the relationship for the 1998 ASHRAE database of field studies, ASHRAE Transactions 2000; 106: 485-492.
5) ASHRAE Standard 55-2017. Thermal environmental conditions for human

occupancy. Atlanta GA: American Society of Heating, Refrigerating and Air-Conditioning Engineers, Inc. 2017.
6) ASHRAE Handbook-Fundamentals 2017. Chapter 9: Thermal Comfort. Atlanta: American Society of Heating, Refrigerating and Air Conditioning Engineers, 2017.
7) Fanger PO. Thermal comfort-analysis and application in environmental engineering, Copenhagen: Danish Technology Press. 1970.
8) Barbosa S and Ip K. Predicted thermal acceptance in naturally ventilated office buildings with double skin façades under Brazilian climates. Journal of Building Engineering 2016; 7: 92-102.
9) Yang L, Fu R, He WF, et al. Adaptive thermal comfort and climate responsive building design strategies in dry-hot and dry-cold areas: Case study in Turpan, China. Energy and Buildings 2020; 209:1-16.
10) Li J. Effect of Form Asymmetry of Gymnasium on Natural Ventilation and Thermal Comfort of Exercise Site. Journal of South China University of Technology 2013; 41:83-89.
11) Huang X, Ma X and Zhang Q. Effect of building interface form on thermal comfort in gymnasiums in hot and humid climates. Frontiers of Architectural Research 2019; 8:32-43.
12) Hazbei M, Nematollahi O, Behnia M, et al. Reduction of energy consumption using passive architecture in hot and humid climates. Tunnelling and Underground Space Technology 2015; 47:16-27.
13) Mazraeh HM and Pazhouhanfar M. Effects of vernacular architecture structure on urban sustainability case study: Qeshm Island, Iran. Frontiers of Architectural Research 2018; 7:11-24.
14) Manzano-Agugliaro F, Montoya FG, Sabio-Ortega A, et al. Review of bioclimatic architecture strategies for achieving thermal comfort. Journal of Physical Education 2015; 49:736-755.231
15) Zhang Q and Yang H. Typical meteorological database handbook for buildings. China Architecture & Building Press. 2012.
16) Xu Z and Han L. The Historical Changes of Winds above Open Spaces and the Surroundings of Nanjing. Urban Planning Forum 2018; 2:81-88.
17) Rowe PG, Forsyth A and Kan HY. China's urban communities: concepts, contexts, and well-being. Birkhäuser Boston. 2016.
18) Advanced Knowledge Laboratory, Inc. CFD Simulation for Architectural Design, http://www.akl.co.jp/en/ (accessed 19 April 2020).
19) NCEI. Integrated Surface Database (ISD), https://www.ncdc.noaa.gov/isd (accessed 19 April 2020).

20) ISO 7243:2017. Ergonomics of the thermal environment-Assessment of heat stress using the WBGT (wet bulb globe temperature) index. Geneva: International Organization for Standardization, 2017.
21) Li H, Li Y, Jiang B, et al. Energy performance optimization of building envelope retrofit through integrated orthogonal arrays with data envelopment analysis. Renewable Energy 2020; 149:1414-1423.
22) Bedford T and Warner CG. The globe thermometer in studies of heating and ventilation. Journal of Hygiene 1934; 34: 458-473.
23) ISO 8996:2004. Ergonomics of the thermal environment-Determination of metabolic rate. Geneva. International Organization for Standardization, 2004.
24) GB50189:2015. Design standard for energy efficiency of public buildings. China Architecture & Building Press, 2015.
25) EnergyPlus. Weather Data by Region, https://energyplus.net/weather-region/asia_wmo_region_2 (accessed 19 April 2020).
26) Prakash D and Ravikumar P. Analysis of thermal comfort and indoor air flow characteristics for a residential building room under generalized window opening position at the adjacent walls. International Journal of Sustainable Built Environment 2015; 4: 42-57.
27) Kim S, Zadeh PA, Staub-French S, et al. Assessment of the Impact of Window Size, Position and Orientation on Building Energy Load Using BIM. Procedia Engineering 2016; 145: 1424-1431.
28) Goia F. Search for the optimal window-to-wall ratio in office buildings in different European climates and the implications on total energy saving potential. Solar Energy 2016; 132:467-492.
29) Wen L, Hiyama K and Koganei M. A method for creating maps of recommended window-to-wall ratios to assign appropriate default values in design performance modeling: A case study of a typical office building in Japan. Energy and Buildings 2017; 145: 304-317.
30) Zingre KT, Yang EH and Wan MP. Dynamic thermal performance of inclined double-skin roof: Modeling and experimental investigation. Energy 2017; 133: 900-912.
31) Susanti L, Homma H and Matsumoto H. A naturally ventilated cavity roof as potential benefits for improving thermal environment and cooling load of a factory building. Energy and Buildings 2011; 43: 211-218.
32) Li D, Zheng Y, Liu C, et al. Numerical analysis on thermal performance of naturally ventilated roofs with different influencing parameters. Sustainable Cities and Society 2016; 22: 86-93.

Appendixes

A. Questionnaire of the field survey

(Translated into English)

Thank you for your cooperation. Please note that this survey is conducted following the guidelines of human-research ethics in China and approved by the management departments of measured gymnasiums. Before the survey, we will evaluate whether you are suitable to participate in. Once the evaluation is passed, please confirm that you are willing to participate in the survey voluntarily. Personal injury and property loss caused by personal body and other personal reasons shall be borne by the individual.

□ Agree □ Disagree

Date_____ **Location**_____

1) Personal information

Gender_____ Age_____

Height (cm)_____ Weight (kg)_____

Time of local living (year)_____

Exercise time per week (hour)_____

2) Personal situation

Current clothing (photograph) top:_____ bottom:_____

Diseases not suitable for strenuous exercise (such as heart disease, hypertension, etc.):

No_____ Yes, I have_____

Alcohol intake within 24 hours: No_____ Yes_____

3) Thermal sensation vote

Start time_____ End time_____

	Preparation	Basketball play				Rest
	00:10	00:20	00:30	00:40	00:50	00:60
-3, Extremely cold						
-2, Cold						
-1, Slightly cold						
0, Comfortable						
+1, Slightly hot						
+2, Hot						
+3, Extremely hot						

B. Data of field survey during basketball exercise

Date	Gender	Outdoor air temp.	Indoor air temp.	Mean radiant temp.	Humidity ratio	Air velocity	Metabolic rate	Clothing insulation	Mean skin temp.	SBP	DBP	TSV
Y/M		ºC	ºC	ºC	g/kg'	m/s	W/m^2	clo	ºC	mmHg	mmHg	
2019/8	female	31.84	33.31	33.07	20.35	0.06	265	0.22	37.33	125	80	1.25
2019/8	female	32.46	34.49	34.16	23.55	0.04	269	0.22	37.39	122	78	2
2019/8	female	34.93	34.13	35.23	23.86	0.20	271	0.22	37.24	124	75	2.25
2019/8	female	34.49	35.05	35.83	25.32	0.06	295	0.22	37.38	127	82	2.75
2019/8	female	31.91	33.13	32.45	23.67	0.10	256	0.22	37.57	126	82	1.75
2019/8	female	31.98	33.16	32.46	22.72	0.05	242	0.22	37.51	125	80	1.25
2019/8	female	35.65	35.53	34.73	22.71	0.32	272	0.22	37.67	126	81	2.25
2019/8	female	35.41	35.34	34.33	22.69	0.72	260	0.22	37.47	124	86	2.25
2019/8	female	29.30	31.02	31.16	17.74	1.05	272	0.22	37.23	127	86	1
2019/8	female	29.80	31.36	31.41	20.16	0.73	264	0.22	37.29	126	82	1.25
2019/8	female	30.73	32.04	31.14	20.14	1.05	250	0.29	37.29	125	80	1.25
2019/8	female	31.11	32.59	31.30	20.28	1.02	262	0.29	37.17	126	81	1.5
2019/8	female	29.79	31.06	30.55	20.40	0.03	289	0.22	37.44	121	76	1.25
2019/8	female	29.60	31.15	30.57	20.65	0.02	307	0.22	37.64	119	74	1.25
2019/8	female	29.13	30.38	31.03	16.82	0.03	229	0.22	37.10	121	75	1
2019/8	female	30.95	31.45	32.34	18.18	0.10	244	0.22	37.24	119	83	1.25
2019/8	female	31.87	33.68	31.05	21.42	0.07	275	0.22	37.33	120	80	1.75
2019/8	female	29.76	31.03	30.70	17.46	0.02	228	0.22	37.07	122	86	1
2019/8	female	31.66	32.54	32.20	19.02	0.08	307	0.22	37.57	118	85	1.5
2019/8	female	32.43	33.05	32.78	20.84	0.02	295	0.22	37.27	125	84	1.75

2019/9	female	32.59	33.16	32.82	21.20	0.04	259	0.22	37.58	123	85	1.75
2019/9	female	33.40	33.51	33.12	20.95	0.03	260	0.22	37.63	123	85	1.75
2019/9	female	33.80	33.80	33.31	23.11	0.01	254	0.22	37.67	121	84	2
2019/9	female	34.00	34.25	33.86	23.49	0.02	313	0.22	37.69	123	81	2
2019/9	female	30.98	31.31	31.51	21.01	0.20	198	0.22	37.33	122	84	1.25
2019/9	female	31.23	31.40	31.27	20.79	0.28	192	0.22	37.36	122	84	1.25
2019/9	female	33.79	33.36	32.93	18.18	0.23	296	0.22	37.51	124	86	1.5
2019/9	female	34.13	34.19	33.08	17.66	0.75	289	0.22	37.30	127	86	1.5
2019/9	female	29.80	31.55	31.54	18.45	0.02	237	0.22	37.07	126	82	1.25
2019/9	female	29.80	31.88	31.27	19.35	0.03	263	0.22	37.24	125	80	1.25
2019/9	female	32.80	33.25	32.72	21.91	0.24	234	0.22	37.63	126	81	1.75
2019/9	female	32.70	33.32	33.16	21.20	0.35	263	0.22	37.58	124	86	1.75
2019/9	female	29.00	28.75	28.61	16.26	0.64	267	0.29	36.54	127	86	0.75
2019/9	female	29.83	29.70	29.39	16.12	0.27	265	0.29	36.74	126	82	0.5
2019/9	female	30.97	30.52	29.97	18.21	0.93	227	0.22	37.32	125	80	0.75
2019/9	female	29.77	29.45	29.13	17.58	1.01	220	0.22	37.20	126	81	0.75
2019/9	female	27.46	26.89	26.93	18.26	0.14	211	0.22	36.18	121	76	0.5
2019/9	female	27.39	27.20	27.18	18.30	0.31	231	0.22	36.66	119	74	0.5
2019/9	female	28.16	28.65	28.31	19.92	0.11	209	0.22	36.57	121	75	0.5
2019/9	female	27.90	28.23	27.67	20.04	0.10	203	0.22	36.60	122	74	0.5
2019/10	female	29.70	29.38	28.96	17.75	0.47	313	0.22	36.90	121	74	0.75
2019/10	female	29.79	29.76	29.05	17.54	0.30	297	0.22	36.90	121	75	1
2019/10	female	28.54	28.54	28.36	14.73	0.44	355	0.22	36.62	119	77	1.25
2019/10	female	28.89	28.89	28.85	14.67	0.28	345	0.22	36.26	122	76	1.25
2019/10	female	29.15	30.93	30.65	14.91	0.05	261	0.22	37.00	123	81	1
2019/10	female	29.21	30.59	30.41	14.79	0.18	268	0.22	36.87	125	80	0.75

2019/10	female	26.35	27.31	27.88	17.97	0.58	210	0.22	36.84	119	83	0.5
2019/10	female	25.79	26.98	27.18	18.83	0.42	227	0.22	36.53	120	80	0.25
2019/10	female	28.71	29.71	29.84	13.00	0.20	297	0.29	36.89	118	86	1.25
2019/10	female	28.61	29.61	29.72	13.21	0.21	285	0.29	36.89	118	85	0.75
2019/10	female	26.26	26.60	25.96	13.34	0.33	325	0.22	36.23	125	84	1
2019/10	female	27.40	27.40	26.64	13.51	0.54	313	0.22	36.50	123	85	1.25
2019/10	female	28.14	29.76	29.41	13.60	0.12	295	0.22	37.20	123	85	1.25
2019/10	female	28.83	30.01	29.62	13.59	0.04	268	0.22	37.16	121	84	1.5
2019/10	female	25.90	25.77	24.47	12.76	0.77	259	0.22	36.62	122	82	0.5
2019/10	female	25.53	25.25	24.70	12.10	0.50	291	0.22	36.40	123	82	0.25
2019/10	female	26.95	27.43	28.12	14.60	0.22	280	0.22	36.70	121	84	0.75
2019/10	female	28.06	28.46	28.64	16.47	0.21	230	0.22	36.80	119	85	1
2019/10	female	27.13	28.12	27.76	15.68	0.07	261	0.22	36.68	121	81	0.5
2019/10	female	27.67	28.88	28.42	15.89	0.03	276	0.22	36.83	120	84	0.75
2019/8	male	31.19	32.39	31.97	21.50	0.04	292	0.22	37.49	128	82	1.25
2019/8	male	31.85	33.33	33.10	20.38	0.11	273	0.22	37.40	127	80	1.25
2019/8	male	31.74	33.60	33.09	22.10	0.02	318	0.22	37.76	123	83	1.5
2019/8	male	31.50	33.04	32.37	23.39	0.05	330	0.22	37.56	124	80	1.5
2019/8	male	31.19	31.93	31.95	19.75	0.40	355	0.22	37.25	122	84	1.5
2019/8	male	31.85	32.99	33.24	19.65	0.13	314	0.22	37.40	123	80	1.5
2019/8	male	31.59	32.41	31.46	19.71	0.47	253	0.22	36.49	127	81	0.75
2019/8	male	32.10	32.94	32.31	19.36	0.50	264	0.22	36.80	128	82	1
2019/8	male	32.67	33.56	32.78	19.68	0.35	329	0.22	37.25	127	82	1.5
2019/8	male	33.55	34.01	33.91	19.37	0.26	296	0.22	37.22	125	80	1.75
2019/8	male	30.25	31.08	30.68	21.02	0.11	325	0.22	37.10	126	77	1
2019/8	male	30.76	31.90	31.53	19.78	0.15	295	0.22	37.31	127	79	1.25

2019/8	male	29.99	29.91	29.69	20.62	0.36	338	0.22	37.02	128	80	1
2019/8	male	30.23	30.48	30.04	20.43	0.64	335	0.22	37.18	127	81	1
2019/8	male	31.36	32.50	31.97	19.87	0.02	316	0.22	37.46	124	82	1.5
2019/8	male	33.74	35.10	33.75	19.81	0.01	398	0.22	37.42	123	85	2.25
2019/8	male	33.25	34.55	33.84	20.47	0.03	385	0.22	37.35	122	86	2
2019/8	male	32.89	33.75	33.10	20.40	0.07	358	0.22	37.30	124	86	1.5
2019/8	male	33.01	33.41	33.04	17.29	0.13	394	0.22	37.39	123	83	1.75
2019/8	male	32.54	32.86	32.51	17.72	0.09	380	0.22	37.36	124	79	1.75
2019/9	male	31.56	32.21	31.74	19.92	0.02	309	0.22	37.26	128	82	1
2019/9	male	30.73	31.24	30.87	19.44	0.02	281	0.22	37.24	128	80	1
2019/9	male	33.80	33.60	33.18	20.79	0.03	330	0.22	37.64	127	81	1.75
2019/9	male	32.59	33.16	32.31	21.20	0.04	309	0.22	37.46	124	82	1.5
2019/9	male	34.36	33.97	33.11	18.16	0.36	372	0.22	37.51	123	85	1.75
2019/9	male	33.92	33.65	33.15	17.87	0.23	339	0.22	37.25	122	86	1.75
2019/9	male	33.93	34.53	33.85	20.09	0.10	310	0.22	37.34	124	86	2
2019/9	male	32.54	33.37	32.91	19.41	0.04	331	0.22	37.51	123	83	1.75
2019/9	male	32.84	33.41	33.07	19.24	0.07	384	0.22	37.32	117	85	1.75
2019/9	male	33.46	33.68	33.34	18.91	0.04	380	0.22	37.21	121	86	1.75
2019/9	male	28.69	29.66	29.50	19.00	0.04	341	0.22	37.21	126	84	1
2019/9	male	29.28	30.60	30.56	19.03	0.03	314	0.22	36.69	124	79	0.75
2019/9	male	33.00	33.31	32.71	16.44	1.22	316	0.22	38.13	128	82	1.25
2019/9	male	32.96	33.28	32.28	16.39	1.24	258	0.22	37.80	127	80	1.25
2019/9	male	26.13	27.51	26.83	15.36	0.06	374	0.22	36.72	123	83	0.75
2019/9	male	26.64	28.44	28.15	13.89	0.36	403	0.22	36.93	124	80	1
2019/9	male	27.12	29.11	28.84	14.98	0.14	342	0.22	36.78	122	84	1
2019/9	male	27.25	30.15	29.67	15.40	0.06	298	0.22	37.04	123	80	1

2019/9	male	30.25	30.65	29.81	18.72	0.43	318	0.22	37.08	127	81	1.5
2019/9	male	30.52	30.97	30.24	18.55	0.31	313	0.22	37.20	128	82	1.25
2019/10	male	29.63	29.60	29.20	16.65	0.41	310	0.22	36.84	127	82	0.75
2019/10	male	29.92	29.80	28.82	16.15	0.38	301	0.22	36.95	125	80	1
2019/10	male	26.90	27.00	26.34	13.60	0.51	323	0.22	36.89	126	77	0.5
2019/10	male	26.70	26.80	26.39	13.99	0.46	323	0.22	36.66	127	79	0.25
2019/10	male	26.81	26.60	26.30	13.93	0.67	423	0.22	36.54	123	75	1
2019/10	male	27.69	27.21	26.78	14.01	1.26	387	0.22	36.17	122	77	0.75
2019/10	male	27.50	28.80	28.79	13.08	0.34	399	0.22	36.71	121	83	1
2019/10	male	26.25	27.95	27.78	13.00	0.37	312	0.22	36.49	124	83	0.75
2019/10	male	25.65	25.65	25.72	12.98	0.42	339	0.22	36.40	123	85	0.25
2019/10	male	26.59	26.59	26.25	14.46	0.28	326	0.22	36.65	123	84	0.5
2019/10	male	28.05	29.60	29.33	12.91	0.06	303	0.22	36.75	124	83	1.25
2019/10	male	28.40	29.70	29.49	12.93	0.14	259	0.22	36.80	124	82	0.75
2019/10	male	25.76	26.36	26.30	12.30	1.64	289	0.22	36.91	120	82	0.5
2019/10	male	25.65	26.01	25.64	10.99	1.39	280	0.22	36.60	123	83	0.25
2019/10	male	27.88	27.85	27.49	13.11	0.69	412	0.22	36.63	123	86	1
2019/10	male	27.90	28.04	27.61	13.20	0.68	375	0.22	36.69	123	85	1
2019/10	male	28.71	29.22	30.29	16.82	0.15	329	0.22	36.92	124	86	1
2019/10	male	28.61	29.91	29.38	15.87	0.22	322	0.22	36.91	123	85	1
2019/10	male	25.24	25.14	24.14	12.18	1.11	309	0.22	36.63	121	82	0.25
2019/10	male	24.97	25.04	23.86	11.18	0.67	317	0.22	36.65	120	81	0.25
2019/10	male	29.75	30.00	29.11	21.03	0.08	400	0.22	36.84	122	77	1.25
2019/10	male	29.63	30.00	29.37	21.23	0.12	430	0.22	36.95	124	85	1
2019/10	male	29.45	29.75	28.79	21.41	0.13	405	0.22	36.89	125	82	1
2019/10	male	29.25	29.55	28.59	21.04	0.09	371	0.22	36.66	123	84	1

C. Gymnasium models by the orthogonal design

Factor / Level / Model	Main window position	South WWR	North WWR	Roof insulation type	Roof slope	Depth of overhanging eave
Model 1 (Initial model)	High at the south and north walls	10%	10%	Single reinforced concrete roof	Horizontal	1m
Model 2	High at the south and north walls	20%	20%	Double reinforced concrete roof	Rise from south to north	5m
Model 3	High at the south and north walls	30%	30%	Single insulated roof	Rise from north to south	9m
Model 4	Low at the south wall and high at the north wall	10%	30%	Single reinforced concrete roof	Rise from south to north	5m
Model 5	Low at the south wall and high at the north wall	20%	10%	Double reinforced concrete roof	Rise from north to south	9m
Model 6	Low at the south wall and high at the north wall	30%	20%	Single insulated roof	Horizontal	1m
Model 7	High at the south wall and low at the north wall	10%	20%	Double reinforced concrete roof	Horizontal	9m
Model 8	High at the south wall and low at the north wall	20%	30%	Single insulated roof	Rise from south to north	1m
Model 9	High at the south wall and low at the north wall	30%	10%	Single reinforced concrete roof	Rise from north to south	5m

Model 10	High at the south and north walls	10%	20%	Insulated roof in single skin	Rise from north to south	5m
Model 11	High at the south and north walls	20%	30%	Single reinforced concrete roof	Horizontal	9m
Model 12	High at the south and north walls	30%	10%	Double reinforced concrete roof	Rise from south to north	1m
Model 13	Low at the south wall and high at the north wall	10%	30%	Double reinforced concrete roof	Rise from north to south	1m
Model 14	Low at the south wall and high at the north wall	20%	10%	Single insulated roof	Horizontal	5m
Model 15	Low at the south wall and high at the north wall	30%	20%	Single reinforced concrete roof	Rise from south to north	9m
Model 16	High at the south wall and low at the north wall	10%	10%	Single insulated roof	Rise from south to north	9m
Model 17	High at the south wall and low at the north wall	20%	20%	Single reinforced concrete roof	Rise from north to south	1m
Model 18	High at the south wall and low at the north wall	30%	30%	Double reinforced concrete roof	Horizontal	5m
Optimized model	Low at the south wall and high at the north wall	20%	30%	Double reinforced concrete roof	Horizontal	9m

Model 1 (Initial model)

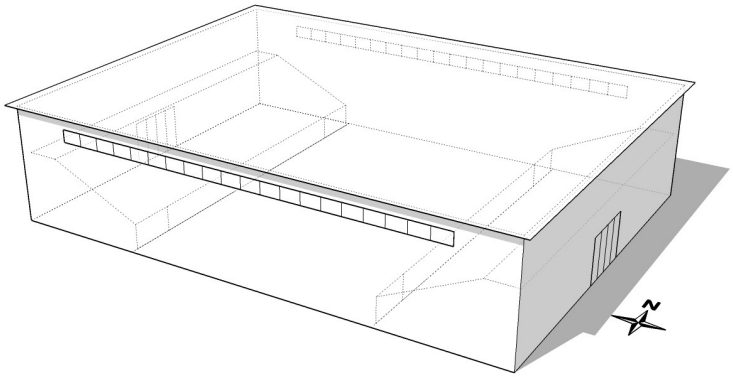

Model 2

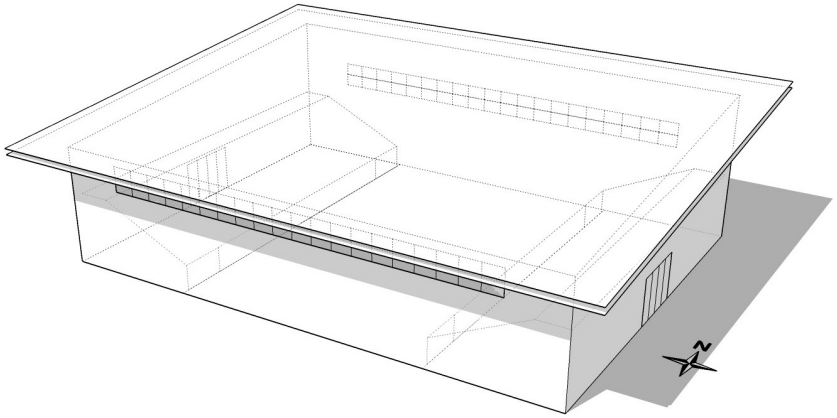

Model 3

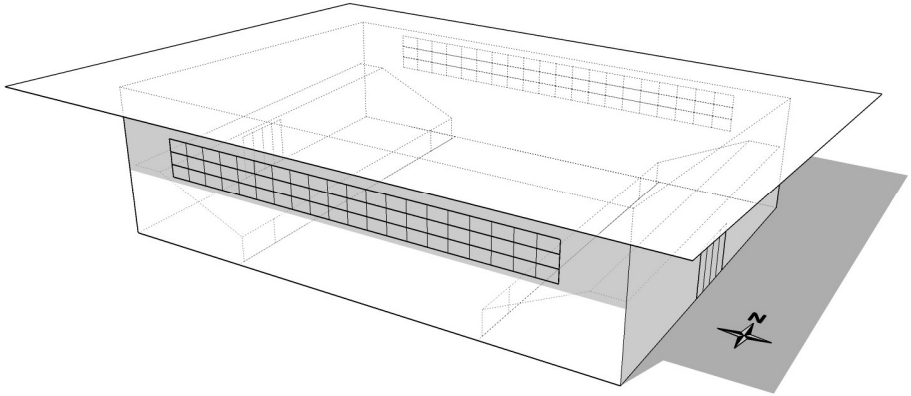

Model 4

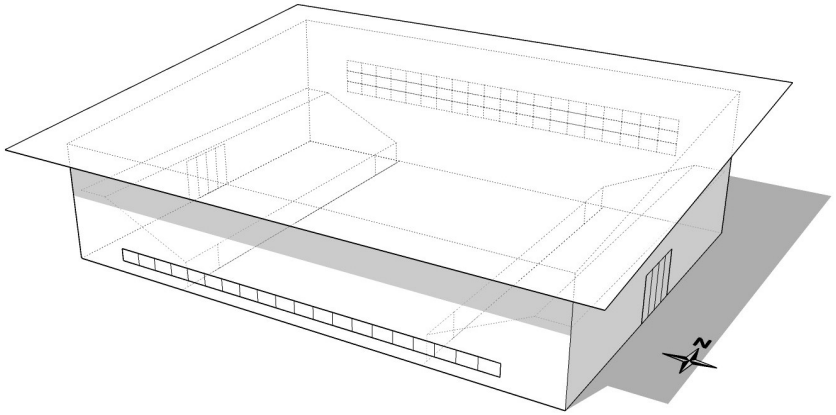

Model 5

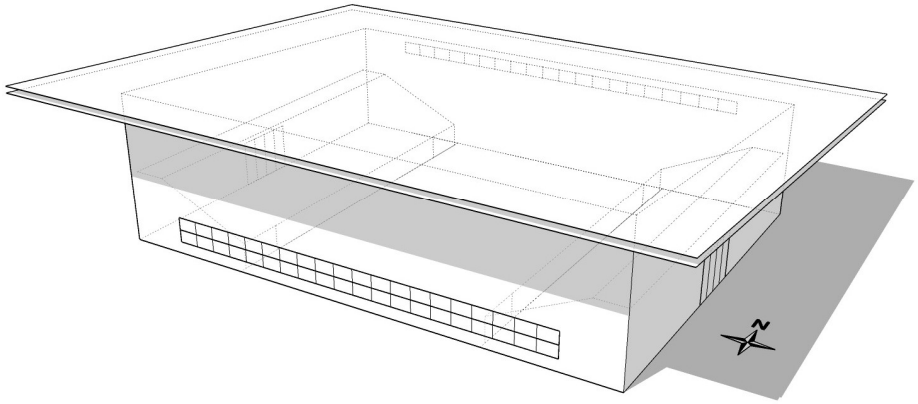

Model 6

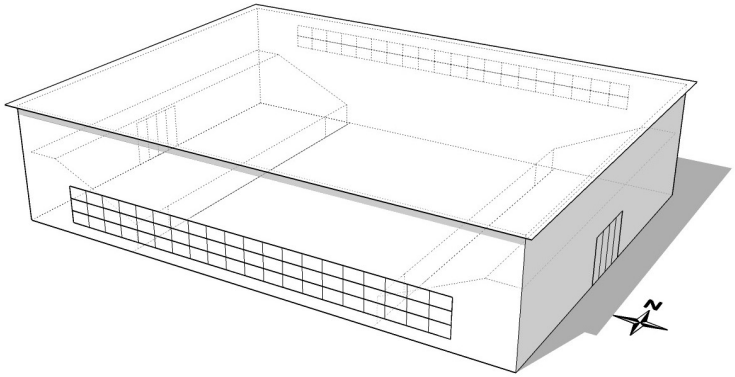

Model 7

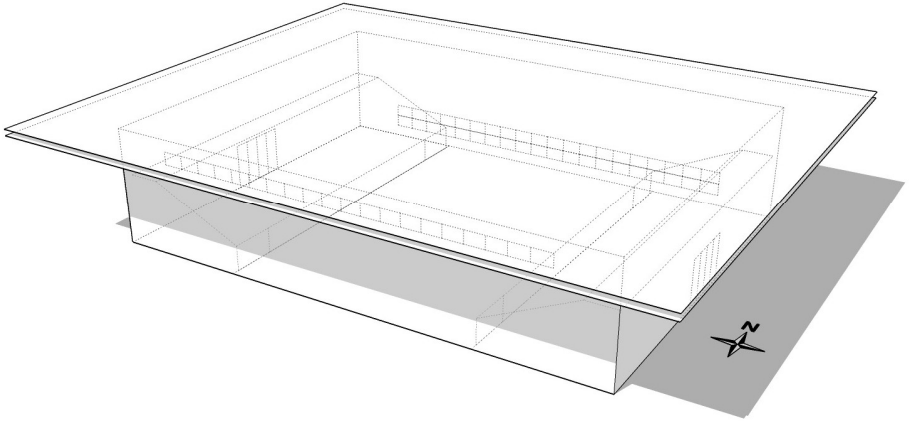

Model 8

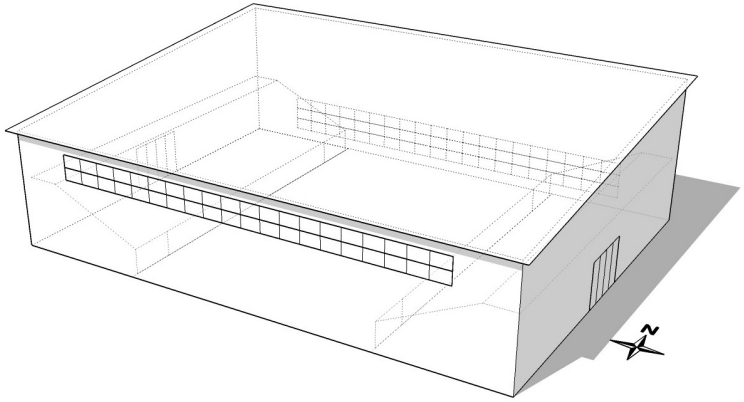

Model 9

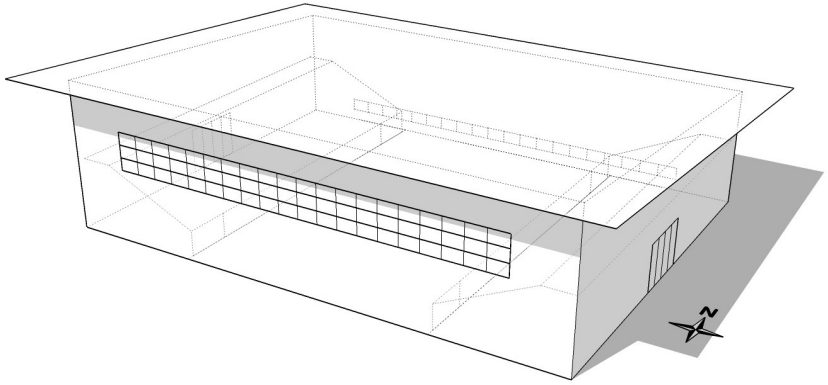

Model 10

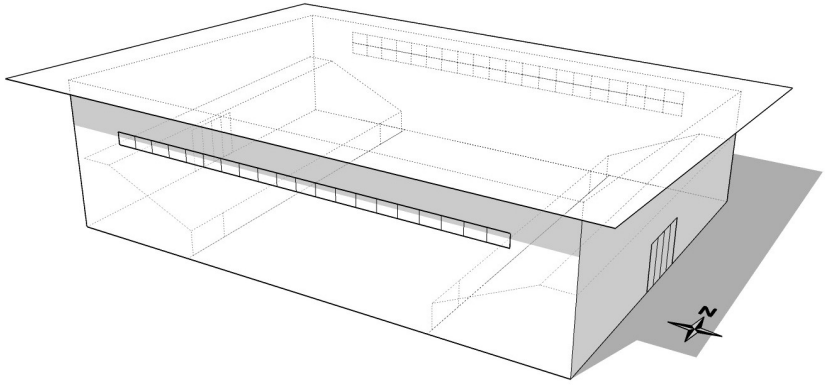

Model 11

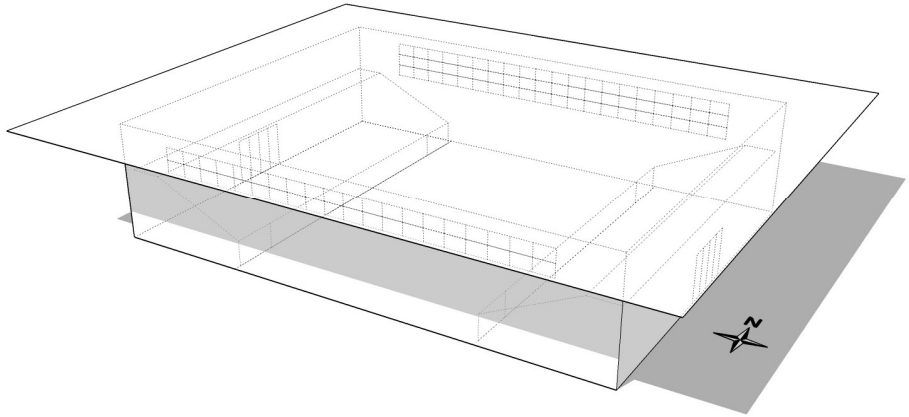

Model 12

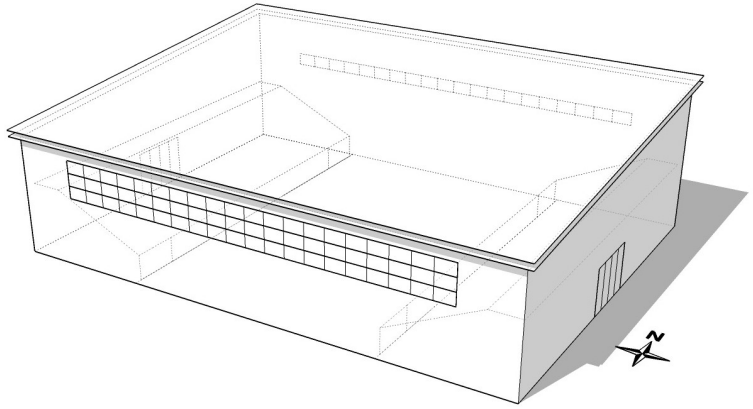

Model 13

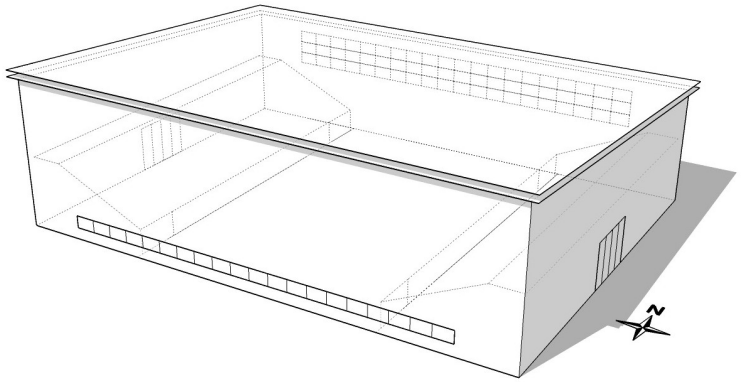

Model 14

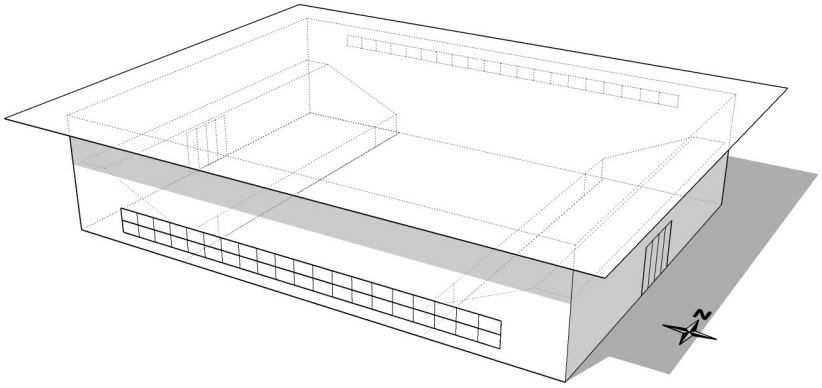

Model 15

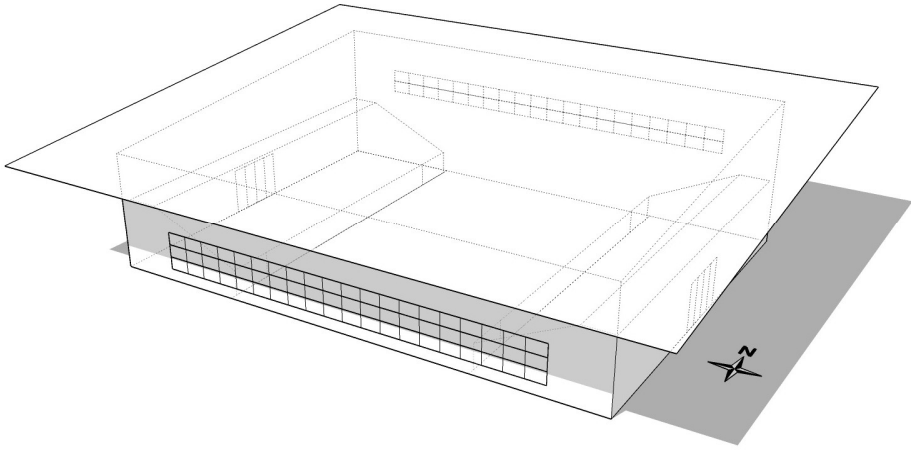

Model 16

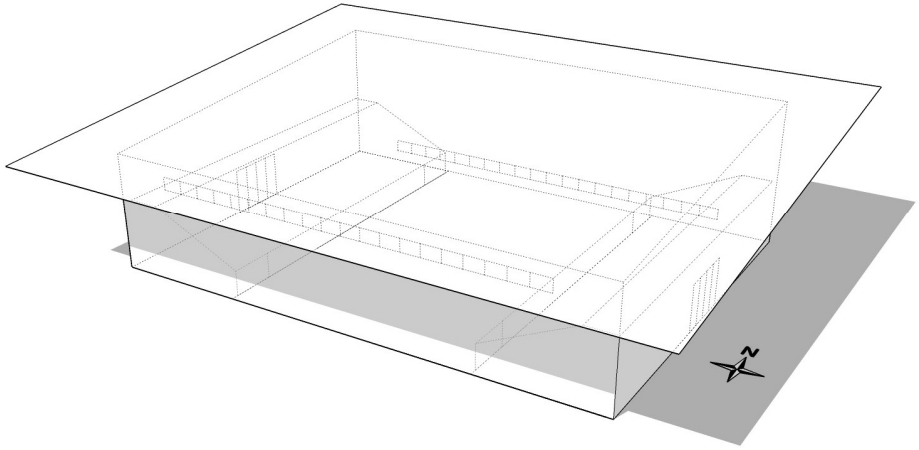

Model 17

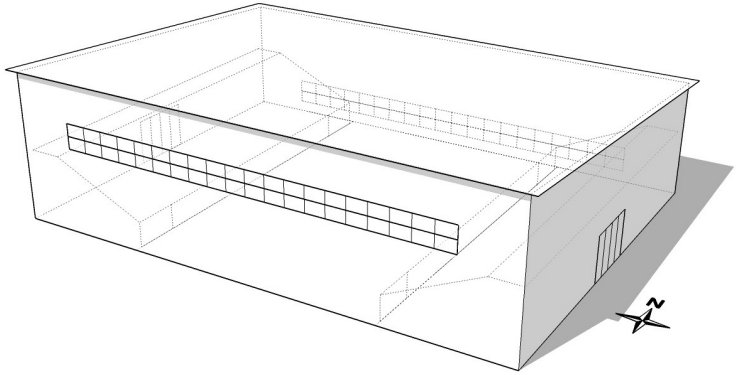

Model 18

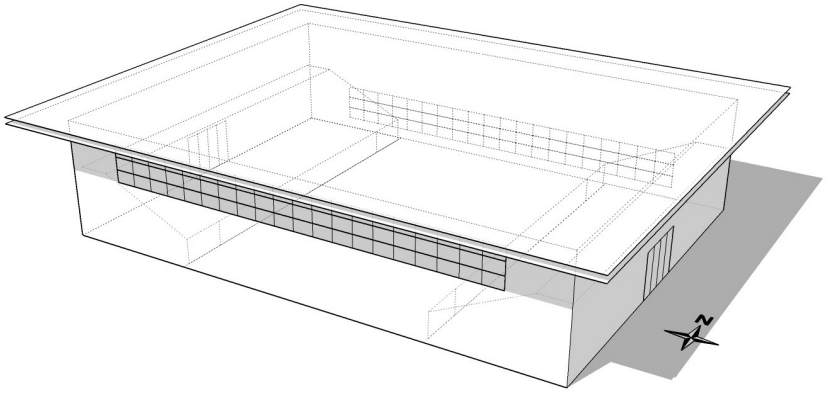

Optimized model

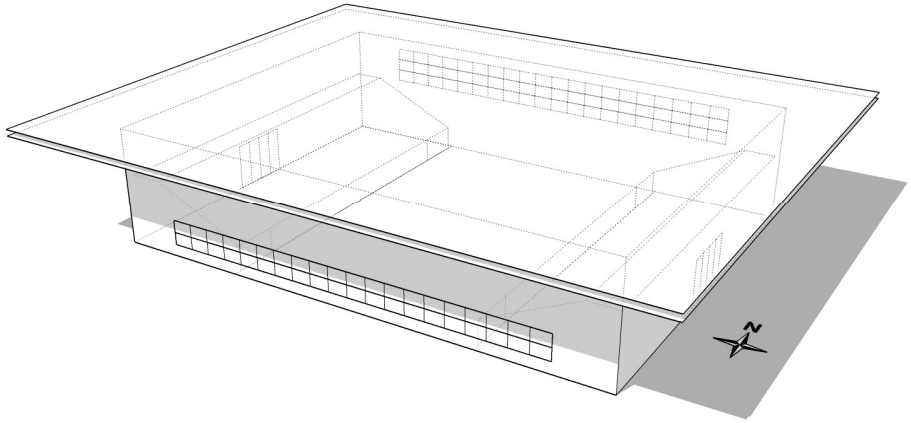

D. Simulated data of gymnasium models

Model 1 (Initial model)						
Time	Air temp.	Humidity ratio	Air velocity	Mean radiant temp.	Operative temp.	PTS
	°C	g/kg'	m/s	°C	°C	
1:00	26.59	19.81	0.00	27.99	27.29	0.72
2:00	26.88	19.83	0.32	27.29	27.04	0.65
3:00	27.01	19.78	0.29	27.39	27.16	0.68
4:00	27.01	19.66	0.28	27.38	27.16	0.68
5:00	27.00	19.45	0.27	27.37	27.15	0.68
6:00	26.99	19.24	0.26	27.34	27.13	0.67
7:00	26.98	19.08	0.25	27.32	27.12	0.67
8:00	26.98	19.31	0.24	27.31	27.11	0.67
9:00	26.87	19.90	0.28	27.25	27.02	0.65
10:00	27.10	20.39	0.27	27.71	27.35	0.72
11:00	28.74	20.63	0.15	28.98	28.86	1.03
12:00	28.78	20.67	0.13	29.47	29.12	1.08
13:00	28.85	20.52	0.12	30.08	29.46	1.15
14:00	28.84	20.35	0.11	30.71	29.78	1.21
15:00	29.15	20.49	0.19	31.51	30.33	1.32
16:00	29.18	20.92	0.18	31.91	30.54	1.36
17:00	29.20	21.16	0.17	32.28	30.74	1.41
18:00	29.23	21.13	0.16	32.66	30.94	1.45
19:00	29.53	20.91	0.15	33.18	31.36	1.53
20:00	30.00	20.56	0.14	33.47	31.74	1.61
21:00	30.23	20.23	0.31	34.66	32.00	1.65
22:00	30.17	20.03	0.27	34.93	32.08	1.67
23:00	30.11	19.92	0.25	35.24	32.17	1.69
0:00	30.06	19.89	0.25	35.58	32.27	1.71
Avg.	28.39	20.16	0.21	30.38	29.29	1.11
Model 2						
Time	Air temp.	Humidity ratio	Air velocity	Mean radiant temp.	Operative temp.	PTS
	°C	g/kg'	m/s	°C	°C	
1:00	26.59	19.81	0.00	27.99	27.29	0.72
2:00	26.73	19.84	0.54	27.21	26.92	0.62
3:00	26.80	19.78	0.44	27.20	26.96	0.63
4:00	26.81	19.65	0.40	27.20	26.97	0.63
5:00	26.82	19.43	0.37	27.20	26.97	0.64
6:00	26.84	19.23	0.34	27.19	26.98	0.64
7:00	26.84	19.07	0.32	27.18	26.98	0.64
8:00	26.85	19.32	0.30	27.18	26.98	0.64
9:00	26.73	19.94	0.32	27.11	26.88	0.62

10:00	27.13	20.41	0.32	27.51	27.28	0.70
11:00	29.04	20.66	0.28	28.60	28.86	1.02
12:00	29.15	20.68	0.27	28.61	28.94	1.04
13:00	29.06	20.50	0.27	28.54	28.86	1.02
14:00	29.04	20.33	0.27	28.57	28.85	1.02
15:00	29.95	20.50	0.54	29.32	29.70	1.18
16:00	29.97	20.95	0.54	29.41	29.74	1.19
17:00	29.98	21.19	0.54	29.49	29.78	1.20
18:00	29.99	21.12	0.54	29.57	29.83	1.20
19:00	30.10	20.89	0.54	29.72	29.95	1.23
20:00	30.05	20.54	0.54	29.67	29.90	1.22
21:00	29.39	20.19	0.55	29.24	29.33	1.10
22:00	29.36	20.00	0.53	29.23	29.30	1.10
23:00	29.32	19.90	0.52	29.21	29.28	1.09
0:00	29.27	19.88	0.51	29.20	29.24	1.09
Avg.	28.41	20.16	0.41	28.39	28.41	0.92
Model 3						
Time	Air temp.	Humidity ratio	Air velocity	Mean radiant temp.	Operative temp.	PTS
	°C	g/kg'	m/s	°C	°C	
1:00	26.59	19.81	0.00	27.94	27.26	0.71
2:00	26.65	19.84	0.55	26.93	26.76	0.59
3:00	26.71	19.78	0.41	27.07	26.86	0.61
4:00	26.72	19.64	0.37	27.09	26.87	0.62
5:00	26.73	19.42	0.34	27.09	26.88	0.62
6:00	26.74	19.22	0.32	27.09	26.88	0.62
7:00	26.75	19.06	0.30	27.08	26.88	0.62
8:00	26.74	19.33	0.28	27.07	26.87	0.62
9:00	26.65	19.95	0.26	27.03	26.80	0.61
10:00	27.31	20.43	0.25	27.97	27.58	0.76
11:00	28.49	20.67	0.20	28.84	28.63	0.98
12:00	28.53	20.68	0.20	29.24	28.88	1.03
13:00	29.29	20.49	0.19	30.18	29.74	1.20
14:00	29.29	20.32	0.17	30.62	29.95	1.25
15:00	29.57	20.50	0.46	31.17	30.21	1.28
16:00	29.59	20.96	0.45	31.35	30.30	1.30
17:00	29.62	21.19	0.45	31.36	30.31	1.31
18:00	29.64	21.12	0.45	31.30	30.31	1.31
19:00	29.85	20.88	0.45	31.40	30.47	1.34
20:00	30.10	20.53	0.44	31.42	30.63	1.37
21:00	29.51	20.18	0.48	30.76	30.01	1.24
22:00	29.47	20.00	0.46	30.62	29.93	1.23
23:00	29.43	19.90	0.45	30.48	29.85	1.21

0:00	29.39	19.88	0.44	30.37	29.78	1.20
Avg.	28.31	20.16	0.35	29.23	28.69	0.98
Model 4						
Time	Air temp.	Humidity ratio	Air velocity	Mean radiant temp.	Operative temp.	PTS
	°C	g/kg'	m/s	°C	°C	
1:00	26.59	19.81	0.00	27.99	27.29	0.72
2:00	26.79	19.84	0.94	27.29	26.94	0.60
3:00	26.83	19.77	0.48	27.48	27.09	0.66
4:00	26.82	19.63	0.50	27.48	27.09	0.65
5:00	26.81	19.42	0.53	27.45	27.06	0.65
6:00	26.79	19.21	0.55	27.38	27.03	0.64
7:00	26.78	19.06	0.57	27.31	26.99	0.63
8:00	26.77	19.34	0.59	27.28	26.97	0.63
9:00	26.67	19.94	0.74	27.29	26.86	0.60
10:00	27.21	20.41	0.72	27.83	27.40	0.71
11:00	28.92	20.64	0.64	29.35	29.05	1.04
12:00	28.95	20.68	0.62	30.22	29.33	1.10
13:00	29.01	20.51	0.59	31.34	29.94	1.22
14:00	29.21	20.34	0.56	32.92	30.70	1.38
15:00	30.00	20.49	0.92	32.94	30.88	1.40
16:00	30.02	20.93	0.86	33.46	31.05	1.44
17:00	30.04	21.18	0.80	33.98	31.22	1.47
18:00	30.06	21.12	0.74	34.56	31.41	1.51
19:00	30.34	20.90	0.70	35.44	31.87	1.61
20:00	30.55	20.56	0.66	36.52	32.34	1.70
21:00	29.61	20.21	0.59	37.73	32.86	1.81
22:00	29.39	20.02	0.65	37.44	31.81	1.60
23:00	29.23	19.91	0.69	37.23	31.63	1.56
0:00	29.11	19.89	0.73	37.14	31.52	1.53
Avg.	28.44	20.16	0.64	31.46	29.43	1.12
Model 5						
Time	Air temp.	Humidity ratio	Air velocity	Mean radiant temp.	Operative temp.	PTS
	°C	g/kg'	m/s	°C	°C	
1:00	26.59	19.81	0.00	27.99	27.29	0.72
2:00	26.71	19.84	1.10	27.14	26.84	0.58
3:00	26.82	19.78	0.44	27.49	27.09	0.66
4:00	26.81	19.64	0.44	27.45	27.07	0.65
5:00	26.80	19.42	0.46	27.43	27.05	0.65
6:00	26.76	19.21	0.49	27.41	27.02	0.64
7:00	26.73	19.05	0.53	27.39	27.00	0.63
8:00	26.70	19.35	0.56	27.38	26.97	0.63

9:00	26.55	19.96	0.75	27.27	26.77	0.58
10:00	27.09	20.43	0.75	27.48	27.21	0.67
11:00	28.55	20.65	0.75	28.28	28.47	0.92
12:00	28.65	20.68	0.73	28.36	28.56	0.94
13:00	28.73	20.50	0.72	28.44	28.64	0.96
14:00	28.75	20.33	0.70	28.48	28.67	0.96
15:00	29.75	20.49	1.15	29.29	29.61	1.13
16:00	29.75	20.95	1.10	29.32	29.62	1.14
17:00	29.76	21.18	1.06	29.37	29.64	1.14
18:00	29.76	21.12	1.02	29.41	29.66	1.15
19:00	29.81	20.90	0.98	29.50	29.71	1.16
20:00	29.93	20.55	0.95	29.65	29.85	1.19
21:00	29.25	20.19	0.80	29.32	29.27	1.08
22:00	29.20	20.00	0.80	29.38	29.26	1.08
23:00	29.16	19.90	0.80	29.46	29.25	1.08
0:00	29.12	19.88	0.80	29.53	29.24	1.07
Avg.	28.24	20.16	0.75	28.43	28.32	0.89
Model 6						
Time	Air temp.	Humidity ratio	Air velocity	Mean radiant temp.	Operative temp.	PTS
	°C	g/kg'	m/s	°C	°C	
1:00	26.59	19.81	0.00	27.93	27.26	0.71
2:00	26.67	19.84	1.05	26.99	26.76	0.56
3:00	26.76	19.77	0.41	27.23	26.95	0.63
4:00	26.77	19.64	0.41	27.26	26.97	0.63
5:00	26.79	19.42	0.42	27.25	26.98	0.64
6:00	26.77	19.22	0.45	27.17	26.93	0.62
7:00	26.73	19.05	0.49	27.10	26.88	0.61
8:00	26.71	19.35	0.52	27.06	26.85	0.61
9:00	26.50	19.98	0.71	26.89	26.62	0.55
10:00	28.02	20.45	0.72	28.17	28.06	0.84
11:00	28.12	20.67	0.70	30.64	28.88	1.01
12:00	29.17	20.68	0.69	31.21	29.78	1.19
13:00	29.06	20.49	0.64	30.84	29.60	1.15
14:00	29.05	20.32	0.63	31.40	29.76	1.19
15:00	29.25	20.50	1.26	30.99	29.77	1.16
16:00	29.27	20.96	1.20	31.12	29.82	1.17
17:00	29.29	21.19	1.14	31.10	29.83	1.18
18:00	29.31	21.12	1.09	31.09	29.85	1.18
19:00	29.55	20.88	1.05	31.26	30.06	1.23
20:00	29.84	20.53	1.02	31.56	30.36	1.29
21:00	29.68	20.19	0.86	31.56	30.24	1.27
22:00	29.59	20.00	0.87	31.54	30.17	1.26

23:00	29.51	19.90	0.88	31.48	30.10	1.24
0:00	29.45	19.88	0.90	31.37	30.02	1.23
Avg.	28.27	20.16	0.76	29.59	28.69	0.96
Model 7						
Time	Air temp.	Humidity ratio	Air velocity	Mean radiant temp.	Operative temp.	PTS
	°C	g/kg'	m/s	°C	°C	
1:00	26.59	19.81	0.00	27.99	27.29	0.72
2:00	26.81	19.84	0.47	27.17	26.95	0.63
3:00	26.94	19.78	0.47	27.27	27.08	0.65
4:00	26.94	19.64	0.43	27.27	27.07	0.65
5:00	26.94	19.43	0.39	27.25	27.06	0.65
6:00	26.93	19.23	0.37	27.24	27.05	0.65
7:00	26.92	19.06	0.35	27.22	27.04	0.65
8:00	26.91	19.33	0.33	27.20	27.03	0.65
9:00	26.73	19.93	0.35	27.11	26.88	0.62
10:00	27.11	20.41	0.35	27.43	27.24	0.69
11:00	28.37	20.65	0.27	28.25	28.32	0.91
12:00	28.40	20.68	0.26	28.27	28.35	0.92
13:00	28.48	20.50	0.25	28.32	28.41	0.93
14:00	28.48	20.33	0.25	28.35	28.43	0.94
15:00	29.80	20.49	0.47	29.46	29.67	1.17
16:00	29.81	20.94	0.47	29.49	29.68	1.18
17:00	29.81	21.18	0.46	29.53	29.70	1.18
18:00	29.82	21.12	0.46	29.57	29.72	1.19
19:00	29.85	20.89	0.46	29.64	29.76	1.19
20:00	29.99	20.55	0.46	29.76	29.90	1.22
21:00	29.56	20.20	0.47	29.35	29.48	1.14
22:00	29.53	20.01	0.45	29.31	29.45	1.13
23:00	29.49	19.90	0.44	29.30	29.41	1.12
0:00	29.45	19.88	0.43	29.30	29.39	1.12
Avg.	28.32	20.16	0.38	28.38	28.35	0.91
Model 8						
Time	Air temp.	Humidity ratio	Air velocity	Mean radiant temp.	Operative temp.	PTS
	°C	g/kg'	m/s	°C	°C	
1:00	26.59	19.81	0.00	27.94	27.26	0.71
2:00	26.70	19.84	0.50	26.99	26.82	0.60
3:00	26.76	19.78	0.56	27.05	26.88	0.61
4:00	26.77	19.65	0.50	27.06	26.88	0.61
5:00	26.77	19.43	0.45	27.06	26.89	0.62
6:00	26.78	19.23	0.41	27.05	26.89	0.62
7:00	26.78	19.06	0.38	27.03	26.88	0.62

8:00	26.77	19.33	0.35	27.03	26.87	0.62
9:00	26.59	19.95	0.34	26.97	26.74	0.59
10:00	27.62	20.42	0.33	28.22	27.86	0.82
11:00	28.05	20.66	0.28	29.08	28.47	0.94
12:00	28.82	20.68	0.27	30.73	29.59	1.17
13:00	29.75	20.50	0.23	31.68	30.52	1.36
14:00	29.79	20.32	0.22	32.47	30.86	1.43
15:00	30.07	20.50	0.49	32.53	31.05	1.45
16:00	30.09	20.95	0.49	32.66	31.12	1.47
17:00	30.11	21.19	0.49	32.71	31.15	1.47
18:00	30.13	21.12	0.50	32.63	31.13	1.47
19:00	30.23	20.89	0.50	32.68	31.21	1.48
20:00	30.50	20.54	0.50	32.78	31.41	1.52
21:00	29.96	20.20	0.51	31.99	30.77	1.39
22:00	29.91	20.01	0.51	31.63	30.60	1.36
23:00	29.86	19.91	0.50	31.27	30.43	1.33
0:00	29.82	19.88	0.50	30.96	30.27	1.30
Avg.	28.55	20.16	0.41	29.92	29.11	1.06
Model 9						
Time	Air temp.	Humidity ratio	Air velocity	Mean radiant temp.	Operative temp.	PTS
	ºC	g/kg'	m/s	ºC	ºC	
1:00	26.59	19.81	0.00	27.99	27.29	0.72
2:00	26.72	19.84	0.39	27.37	26.98	0.64
3:00	26.86	19.78	0.27	27.70	27.20	0.69
4:00	26.88	19.65	0.25	27.62	27.18	0.68
5:00	26.90	19.44	0.23	27.59	27.18	0.68
6:00	26.91	19.23	0.22	27.58	27.18	0.68
7:00	26.92	19.07	0.21	27.55	27.17	0.68
8:00	26.92	19.32	0.21	27.51	27.15	0.68
9:00	26.67	19.95	0.27	27.34	26.94	0.63
10:00	27.09	20.42	0.27	27.73	27.35	0.72
11:00	28.89	20.66	0.21	29.16	29.00	1.05
12:00	28.93	20.68	0.20	30.01	29.36	1.13
13:00	29.00	20.50	0.20	31.13	30.06	1.27
14:00	29.01	20.32	0.19	32.54	30.78	1.41
15:00	30.28	20.49	0.34	34.47	31.96	1.64
16:00	30.29	20.95	0.33	35.50	32.37	1.73
17:00	30.30	21.19	0.33	36.50	32.78	1.81
18:00	30.30	21.12	0.33	37.56	33.21	1.89
19:00	30.33	20.89	0.33	38.50	33.60	1.97
20:00	30.53	20.54	0.33	39.02	33.92	2.04
21:00	31.04	20.20	0.31	39.07	34.26	2.10

22:00	31.04	20.01	0.32	39.53	34.44	2.14
23:00	30.91	19.90	0.33	39.40	34.31	2.11
0:00	30.88	19.88	0.34	39.01	34.13	2.08
Avg.	28.76	20.16	0.27	32.39	30.24	1.30
Model 10						
Time	Air temp.	Humidity ratio	Air velocity	Mean radiant temp.	Operative temp.	PTS
	ºC	g/kg'	m/s	ºC	ºC	
1:00	26.59	19.81	0.00	27.94	27.26	0.71
2:00	26.74	19.84	0.37	27.07	26.88	0.62
3:00	26.84	19.78	0.24	27.25	27.01	0.65
4:00	26.85	19.65	0.23	27.22	27.00	0.65
5:00	26.86	19.44	0.22	27.20	26.99	0.65
6:00	26.85	19.23	0.22	27.17	26.98	0.64
7:00	26.84	19.07	0.22	27.16	26.97	0.64
8:00	26.82	19.32	0.23	27.16	26.96	0.64
9:00	26.72	19.92	0.25	27.21	26.91	0.63
10:00	27.51	20.40	0.24	28.26	27.81	0.81
11:00	28.68	20.65	0.16	33.61	31.15	1.49
12:00	28.69	20.68	0.16	33.13	30.91	1.44
13:00	28.75	20.51	0.15	33.11	30.93	1.44
14:00	29.34	20.34	0.14	33.05	31.20	1.50
15:00	30.03	20.49	0.36	31.46	30.60	1.37
16:00	30.06	20.95	0.36	31.96	30.82	1.41
17:00	30.08	21.19	0.36	32.80	31.17	1.48
18:00	30.10	21.13	0.36	34.66	31.93	1.63
19:00	30.16	20.89	0.36	38.95	33.68	1.99
20:00	30.35	20.54	0.36	37.35	33.15	1.88
21:00	30.26	20.21	0.35	36.40	32.71	1.79
22:00	29.68	20.02	0.33	33.25	31.11	1.47
23:00	29.54	19.91	0.32	32.92	30.89	1.43
0:00	29.44	19.89	0.32	32.73	30.75	1.40
Avg.	28.49	20.16	0.26	31.21	29.66	1.18
Model 11						
Time	Air temp.	Humidity ratio	Air velocity	Mean radiant temp.	Operative temp.	PTS
	ºC	g/kg'	m/s	ºC	ºC	
1:00	26.59	19.81	0.00	27.99	27.29	0.72
2:00	26.76	19.84	0.58	27.05	26.87	0.61
3:00	26.82	19.77	0.49	27.21	26.98	0.63
4:00	26.83	19.64	0.43	27.24	26.99	0.64
5:00	26.85	19.43	0.38	27.27	27.01	0.64
6:00	26.86	19.23	0.34	27.28	27.03	0.65

7:00	26.87	19.07	0.30	27.27	27.03	0.65
8:00	26.88	19.32	0.28	27.24	27.02	0.65
9:00	26.75	19.93	0.22	27.25	26.95	0.64
10:00	27.55	20.41	0.22	28.04	27.75	0.80
11:00	27.91	20.65	0.22	28.30	28.07	0.87
12:00	28.06	20.68	0.23	28.74	28.33	0.92
13:00	28.69	20.50	0.23	29.66	29.08	1.07
14:00	29.78	20.33	0.20	30.89	30.22	1.30
15:00	30.18	20.49	0.49	31.26	30.61	1.36
16:00	30.20	20.95	0.50	31.45	30.70	1.38
17:00	30.21	21.19	0.51	31.65	30.79	1.40
18:00	30.23	21.12	0.51	31.85	30.88	1.42
19:00	30.26	20.89	0.51	32.08	30.99	1.44
20:00	30.38	20.54	0.50	32.28	31.14	1.47
21:00	29.54	20.19	0.50	31.80	30.44	1.33
22:00	29.49	20.01	0.47	31.82	30.42	1.33
23:00	29.45	19.90	0.45	31.79	30.38	1.32
0:00	29.42	19.88	0.44	31.73	30.34	1.31
Avg.	28.44	20.16	0.38	29.55	28.89	1.02
Model 12						
Time	Air temp.	Humidity ratio	Air velocity	Mean radiant temp.	Operative temp.	PTS
	°C	g/kg'	m/s	°C	°C	
1:00	26.59	19.81	0.00	27.99	27.29	0.72
2:00	26.74	19.84	0.47	27.29	26.96	0.63
3:00	26.79	19.78	0.42	27.31	27.00	0.64
4:00	26.80	19.64	0.39	27.29	26.99	0.64
5:00	26.81	19.43	0.36	27.29	27.00	0.64
6:00	26.82	19.23	0.34	27.28	27.00	0.64
7:00	26.83	19.07	0.32	27.28	27.01	0.65
8:00	26.84	19.32	0.30	27.28	27.01	0.65
9:00	26.76	19.93	0.27	27.25	26.95	0.64
10:00	26.88	20.41	0.26	27.43	27.10	0.67
11:00	28.99	20.65	0.23	28.46	28.78	1.01
12:00	29.14	20.68	0.22	28.50	28.88	1.03
13:00	29.15	20.50	0.21	28.58	28.92	1.04
14:00	29.00	20.33	0.20	28.65	28.86	1.03
15:00	29.95	20.50	0.31	30.05	29.99	1.25
16:00	29.98	20.94	0.32	30.19	30.06	1.26
17:00	30.00	21.18	0.33	30.26	30.11	1.27
18:00	30.03	21.12	0.33	30.32	30.14	1.28
19:00	30.17	20.90	0.34	30.43	30.27	1.30
20:00	30.34	20.55	0.34	30.43	30.38	1.32

21:00	29.68	20.20	0.38	29.88	29.76	1.20
22:00	29.64	20.01	0.36	29.88	29.74	1.19
23:00	29.60	19.91	0.35	29.89	29.72	1.19
0:00	29.55	19.88	0.34	29.89	29.69	1.18
Avg.	28.46	20.16	0.31	28.71	28.57	0.96
Model 13						
Time	Air temp.	Humidity ratio	Air velocity	Mean radiant temp.	Operative temp.	PTS
	ºC	g/kg'	m/s	ºC	ºC	
1:00	26.59	19.81	0.00	27.99	27.29	0.72
2:00	26.76	19.84	1.00	27.23	26.90	0.59
3:00	26.77	19.77	0.55	27.52	27.07	0.65
4:00	26.76	19.63	0.56	27.48	27.05	0.64
5:00	26.75	19.42	0.58	27.43	27.02	0.64
6:00	26.74	19.21	0.61	27.40	26.94	0.62
7:00	26.73	19.05	0.63	27.37	26.92	0.61
8:00	26.72	19.34	0.64	27.35	26.91	0.61
9:00	26.64	19.94	0.80	27.28	26.84	0.59
10:00	27.32	20.41	0.79	27.62	27.41	0.71
11:00	28.65	20.65	0.72	28.30	28.55	0.94
12:00	28.68	20.68	0.69	28.33	28.58	0.95
13:00	28.70	20.51	0.67	28.39	28.61	0.95
14:00	29.01	20.34	0.65	28.53	28.86	1.01
15:00	30.01	20.49	1.02	29.42	29.83	1.18
16:00	30.01	20.93	0.97	29.45	29.84	1.19
17:00	30.01	21.18	0.92	29.49	29.85	1.19
18:00	30.02	21.12	0.88	29.52	29.87	1.20
19:00	30.08	20.90	0.85	29.61	29.94	1.21
20:00	30.17	20.55	0.82	29.79	30.06	1.24
21:00	29.32	20.20	0.69	29.49	29.37	1.11
22:00	29.19	20.01	0.72	29.47	29.27	1.08
23:00	29.08	19.91	0.75	29.55	29.22	1.07
0:00	28.99	19.88	0.79	29.68	29.20	1.07
Avg.	28.32	20.16	0.72	28.49	28.39	0.91
Model 14						
Time	Air temp.	Humidity ratio	Air velocity	Mean radiant temp.	Operative temp.	PTS
	ºC	g/kg'	m/s	ºC	ºC	
1:00	26.59	19.81	0.00	27.93	27.26	0.71
2:00	26.71	19.84	0.89	27.01	26.80	0.58
3:00	26.81	19.77	0.34	27.33	27.02	0.65
4:00	26.82	19.64	0.35	27.31	27.01	0.65
5:00	26.80	19.43	0.38	27.22	26.97	0.64

6:00	26.76	19.22	0.42	27.15	26.92	0.62
7:00	26.75	19.06	0.46	27.12	26.90	0.62
8:00	26.74	19.34	0.49	27.10	26.88	0.61
9:00	26.63	19.96	0.65	27.11	26.78	0.59
10:00	27.58	20.43	0.66	27.92	27.68	0.77
11:00	29.22	20.65	0.63	30.73	29.67	1.17
12:00	29.16	20.68	0.61	32.32	30.11	1.26
13:00	29.13	20.50	0.59	33.23	30.77	1.39
14:00	29.55	20.34	0.57	36.79	32.45	1.73
15:00	29.96	20.50	0.96	31.12	30.31	1.28
16:00	29.98	20.95	0.91	31.23	30.36	1.29
17:00	29.99	21.18	0.86	31.31	30.38	1.30
18:00	30.00	21.12	0.82	31.38	30.41	1.31
19:00	30.03	20.89	0.79	31.45	30.46	1.32
20:00	30.16	20.54	0.77	31.65	30.60	1.35
21:00	29.93	20.20	0.69	33.91	31.12	1.46
22:00	28.56	20.01	0.69	33.24	29.96	1.22
23:00	28.38	19.90	0.71	31.89	29.43	1.12
0:00	28.30	19.88	0.73	31.53	29.27	1.08
Avg.	28.36	20.16	0.62	30.21	28.98	1.03
Model 15						
Time	Air temp.	Humidity ratio	Air velocity	Mean radiant temp.	Operative temp.	PTS
	°C	g/kg'	m/s	°C	°C	
1:00	26.59	19.81	0.00	27.99	27.29	0.72
2:00	26.70	19.84	1.20	27.15	26.83	0.57
3:00	26.83	19.77	0.51	27.54	27.11	0.66
4:00	26.82	19.64	0.52	27.49	27.09	0.65
5:00	26.82	19.42	0.53	27.40	27.05	0.64
6:00	26.78	19.21	0.56	27.31	26.99	0.63
7:00	26.75	19.05	0.60	27.24	26.95	0.62
8:00	26.73	19.35	0.62	27.22	26.87	0.61
9:00	26.55	19.98	0.81	27.25	26.76	0.57
10:00	27.24	20.44	0.83	27.92	27.44	0.71
11:00	29.19	20.67	0.79	29.44	29.26	1.08
12:00	29.18	20.68	0.77	30.05	29.44	1.12
13:00	29.11	20.49	0.76	30.70	29.58	1.15
14:00	29.10	20.32	0.73	31.55	29.83	1.20
15:00	29.42	20.50	1.42	32.39	30.31	1.26
16:00	29.44	20.96	1.36	32.85	30.46	1.29
17:00	29.46	21.19	1.31	33.26	30.60	1.33
18:00	29.48	21.12	1.27	33.68	30.74	1.36
19:00	29.79	20.88	1.23	34.28	31.14	1.44

20:00	30.12	20.53	1.20	34.91	31.56	1.52
21:00	29.85	20.20	0.98	35.87	31.66	1.55
22:00	29.67	20.01	1.00	36.09	31.59	1.54
23:00	29.57	19.91	1.04	36.27	31.58	1.53
0:00	29.51	19.89	1.06	36.38	31.57	1.53
Avg.	28.36	20.16	0.88	30.93	29.15	1.05
Model 16						
Time	Air temp.	Humidity ratio	Air velocity	Mean radiant temp.	Operative temp.	PTS
	ºC	g/kg'	m/s	ºC	ºC	
1:00	26.59	19.81	0.00	27.94	27.26	0.71
2:00	26.77	19.84	0.33	27.12	26.91	0.63
3:00	26.84	19.77	0.38	27.17	26.97	0.64
4:00	26.85	19.66	0.34	27.17	26.98	0.64
5:00	26.86	19.45	0.31	27.16	26.98	0.64
6:00	26.87	19.24	0.29	27.15	26.98	0.64
7:00	26.87	19.07	0.27	27.15	26.98	0.64
8:00	26.86	19.31	0.26	27.14	26.97	0.64
9:00	26.74	19.91	0.29	27.16	26.91	0.63
10:00	27.26	20.39	0.28	28.29	27.67	0.78
11:00	28.90	20.64	0.20	29.64	29.20	1.09
12:00	28.94	20.68	0.19	30.40	29.67	1.19
13:00	29.85	20.51	0.19	31.72	30.79	1.41
14:00	29.84	20.34	0.16	32.25	31.05	1.47
15:00	30.16	20.49	0.30	32.13	30.94	1.44
16:00	30.18	20.93	0.31	32.41	31.07	1.46
17:00	30.20	21.18	0.31	32.63	31.17	1.48
18:00	30.22	21.12	0.31	32.73	31.22	1.50
19:00	30.32	20.90	0.31	32.85	31.33	1.52
20:00	30.55	20.56	0.31	33.05	31.55	1.56
21:00	30.68	20.22	0.33	32.62	31.46	1.54
22:00	30.67	20.02	0.31	32.59	31.43	1.54
23:00	28.52	19.91	0.29	30.99	29.51	1.15
0:00	28.44	19.88	0.31	30.99	29.46	1.14
Avg.	28.58	20.16	0.27	30.02	29.19	1.09
Model 17						
Time	Air temp.	Humidity ratio	Air velocity	Mean radiant temp.	Operative temp.	PTS
	ºC	g/kg'	m/s	ºC	ºC	
1:00	26.59	19.81	0.00	27.99	27.29	0.72
2:00	26.73	19.84	0.44	27.33	26.97	0.63
3:00	26.87	19.78	0.33	27.65	27.18	0.68
4:00	26.88	19.64	0.31	27.57	27.16	0.68

5:00	26.87	19.42	0.30	27.51	27.12	0.67
6:00	26.84	19.22	0.29	27.45	27.08	0.66
7:00	26.80	19.06	0.29	27.39	27.04	0.65
8:00	26.77	19.33	0.29	27.36	27.01	0.65
9:00	26.53	19.95	0.32	27.37	26.86	0.62
10:00	27.52	20.43	0.32	28.04	27.73	0.79
11:00	29.12	20.66	0.26	29.29	29.19	1.09
12:00	29.13	20.68	0.26	30.37	29.63	1.18
13:00	29.14	20.49	0.26	31.52	30.09	1.27
14:00	29.14	20.32	0.26	32.34	30.42	1.34
15:00	30.23	20.50	0.49	34.09	31.77	1.60
16:00	30.28	20.95	0.49	34.74	32.06	1.66
17:00	30.31	21.19	0.49	35.19	32.26	1.70
18:00	30.35	21.13	0.48	35.59	32.44	1.73
19:00	30.81	20.89	0.48	36.13	32.94	1.83
20:00	30.95	20.54	0.47	36.29	33.09	1.86
21:00	30.83	20.21	0.42	37.38	33.45	1.94
22:00	30.50	20.02	0.45	37.28	33.21	1.89
23:00	30.20	19.92	0.48	37.10	32.96	1.84
0:00	30.01	19.90	0.52	36.93	32.78	1.80
Avg.	28.72	20.16	0.36	31.66	29.91	1.23
Model 18						
Time	Air temp.	Humidity ratio	Air velocity	Mean radiant temp.	Operative temp.	PTS
	°C	g/kg'	m/s	°C	°C	
1:00	26.59	19.81	0.00	27.99	27.29	0.72
2:00	26.67	19.84	0.68	27.00	26.77	0.58
3:00	26.77	19.78	0.61	27.16	26.89	0.61
4:00	26.77	19.63	0.55	27.16	26.93	0.62
5:00	26.77	19.42	0.50	27.16	26.93	0.62
6:00	26.78	19.22	0.45	27.17	26.93	0.62
7:00	26.78	19.06	0.41	27.17	26.94	0.63
8:00	26.78	19.33	0.38	27.18	26.94	0.63
9:00	26.61	19.95	0.34	27.07	26.80	0.60
10:00	27.29	20.43	0.33	27.61	27.42	0.73
11:00	29.21	20.67	0.26	28.59	28.96	1.04
12:00	29.21	20.68	0.25	28.60	28.96	1.04
13:00	29.12	20.49	0.25	28.56	28.89	1.03
14:00	28.94	20.32	0.25	28.66	28.83	1.02
15:00	29.60	20.49	0.51	29.46	29.55	1.15
16:00	29.64	20.95	0.51	29.51	29.59	1.16
17:00	29.67	21.19	0.51	29.56	29.63	1.17
18:00	29.70	21.12	0.51	29.61	29.67	1.17

19:00	29.88	20.89	0.51	29.73	29.82	1.20
20:00	30.11	20.54	0.50	29.78	29.97	1.24
21:00	29.33	20.19	0.50	29.07	29.23	1.08
22:00	29.30	20.00	0.49	29.04	29.19	1.08
23:00	29.26	19.90	0.48	29.02	29.16	1.07
0:00	29.21	19.88	0.47	29.00	29.13	1.07
Avg.	28.33	20.16	0.43	28.37	28.35	0.91
Optimized model						
Time	Air temp.	Humidity ratio	Air velocity	Mean radiant temp.	Operative temp.	PTS
	ºC	g/kg'	m/s	ºC	ºC	
1:00	26.59	19.81	0.00	27.99	27.29	0.72
2:00	26.71	19.84	0.55	27.19	26.85	0.60
3:00	26.82	19.77	0.48	27.41	27.06	0.65
4:00	26.83	19.64	0.49	27.36	27.04	0.65
5:00	26.83	19.42	0.50	27.33	27.03	0.64
6:00	26.83	19.21	0.53	27.30	27.01	0.64
7:00	26.79	19.05	0.58	27.27	26.98	0.63
8:00	26.76	19.35	0.62	27.26	26.91	0.61
9:00	26.60	19.97	0.82	27.21	26.78	0.58
10:00	27.15	20.44	0.83	27.42	27.23	0.67
11:00	28.99	20.67	0.80	28.56	28.86	1.00
12:00	28.98	20.69	0.78	28.61	28.87	1.00
13:00	28.92	20.50	0.75	28.59	28.82	0.99
14:00	28.92	20.33	0.72	28.60	28.82	0.99
15:00	29.20	20.49	1.25	28.86	29.10	1.03
16:00	29.21	20.95	1.18	28.88	29.11	1.03
17:00	29.22	21.19	1.13	28.91	29.13	1.04
18:00	29.24	21.12	1.09	28.95	29.15	1.04
19:00	29.40	20.89	1.05	29.09	29.31	1.08
20:00	29.57	20.54	1.03	29.24	29.47	1.11
21:00	29.35	20.19	0.86	29.14	29.29	1.08
22:00	28.90	20.00	0.85	29.01	28.94	1.01
23:00	28.86	19.90	0.86	29.08	28.92	1.01
0:00	28.81	19.88	0.88	29.17	28.92	1.01
Avg.	28.14	20.16	0.78	28.27	28.20	0.86

Publications

Journal Paper:

1) **Xiaodan Huang**, Qingyuan Zhang, Zhangyuan Wang, et al. Thermal sensation under high-intensive exercise in naturally ventilated gymnasiums in hot-humid areas of China: Taking basketball players for example. Indoor and Built Environment, 2020. Doi: 10.1177/1420326X20978275

2) **Xiaodan Huang**, Xiaoli Ma and Qingyuan Zhang. Effect of building interface form on thermal comfort in gymnasiums in hot and humid climates. Frontiers of Architectural Research, 2019, 8(1):32-43.

3) **Xiaodan Huang**, Qingyuan Zhang and Xiaoli Ma. The Thermal Comfort Models of Venue in Hot and Humid Subtropical Regions. CCAMLR Science, 2018, 25(3):244-252.

4) **Xiaodan Huang** and Qingyuan Zhang. Comparative analysis of Predicted Mean Vote (PMV) and Standard Effective Temperature (SET*) in the imaginary standard environment. 2020. (Submitted to journal)

5) **Xiaodan Huang**, Qingyuan Zhang, Ineko Tanaka, et al. Optimization of architectural form for thermal comfort in naturally ventilated gymnasium at hot and humid climate by orthogonal experiment. 2020. (Submitted to journal)

Proceedings Paper:

1) 張晴原, **黄暁丹**. Study on the thermal comfort models of gymnasiums in hot and humid subtropical regions, Part 1. 日本建築学会大会梗概集環境工学Ⅱ, 2019:593-594

2) **黄暁丹**, 張晴原. Study on the thermal comfort models of gymnasiums in hot and humid subtropical regions, Part 2. 日本建築学会大会梗概集環境工学Ⅱ, 2019:595-596

Acknowledgements

My doctoral study will soon come to an end and, at the completion of my graduation thesis, I wish to express my sincere appreciation to all those who have offered me invaluable help during the years of doctoral study.

My deepest gratitude goes first and foremost to Professor Qingyuan Zhang, my academic advisor, for his constant encouragement and valuable guidance in the academic studies. He has walked me through all the stages of the writing of dissertation. In addition, his great knowledge and personal behavior specially kindness admired me. I learnt a lot from him not limited by the research knowledge.

I express my hearty thanks to all the examination committee members: Professor Satoru Sadohara, Professor Ineko Tanaka, Professor Satoshi Yoshida and Professor Keiko Inagaki, for their patient instructions in various subjects and precious suggestions thoughout my study.

I would like to greatly acknowledge the administration of Yokohama National University for giving me opportunity to conduct the study and scholarship for my study. I sincerely appreciate the technical supports and the assistances from the relevant organizations in Guangzhou China in the field survey and data collection of this study.

My thanks would go to my beloved family for their loving considerations and great confidence in me all through these years. I also owe my sincere gratitude to my friends and my fellow classmates who spent their time on me not only to teach Japanese, but also give me the opportunity to experience the fantastic Japanese cultue.

Finally, I would like to express my appreciation to the colleagues of Guangdong University of Technology, specially all members of School of Art and Design for their enormous encouragement.

Xiaodan Huang
Yokohama National University
February, 2021